Structural and swelling studies of normal, dried and extracted corneal stroma

Thesis

STRUCTURAL AND SWELLING STUDIES OF NORMAL, DRIED AND EXTRACTED CORNEAL STROMA

Thesis submitted for the degree of Doctor of Philosophy

in the Discipline of Biophysics

by

Susan Barbara Whitburn, B.A.

Open University June 1981.

Date of Submission: 9.6.81
Date of award: 25.8.81

ProQuest LLC
789 East Eisenhower Parkway
P.O. Box 1346
Ann Arbor, MI 48106 - 1346

Dedication

To Jacqueline and Melanie.

ABSTRACT

Corneal stroma is an unusual tissue in that normally it is transparent to visible light. Loss of transparency *in vitro* or *in vivo* is associated with an increase in water content (hydration). The structure of the stroma in normal and swollen states is of interest in understanding the process by which the tissue becomes opaque.

Several experimental techniques were used to investigate the structure and properties of specimens of cornea treated in various ways. Fresh, pre-dried and extracted specimens were used to study changes in swelling rate. Glycosaminoglycans were extracted with salt and enzyme solutions, and also precipitated *in situ*. Inorganic ions were extracted with distilled water and analysis of these carried out by flame photometry. Low-angle X-ray diffraction was used to monitor the change in interfibrillar spacing with hydration, and the high intensity synchrotron X-ray source enabled larger-angle reflections to be detected, and the change in these with hydration was also investigated. Charge properties were studied by monitoring the pH of the bathing solution, and by measuring the potential difference between the stroma and the bathing solution; from which the fixed charge concentration due to the macromolecular matrix was calculated. Frozen sections of cornea at physiological and higher hydrations were stained by a double-antibody technique and viewed with a fluorescence microscope.

Results from these experiments suggest a structure for the stroma which is less ordered than was previously thought. The X-ray reflections at higher angles did not show the expected dependence on hydration for an ordered lattice. The change in interfibrillar spacing with hydration indicated that the fibrils probably exist as bundles separated by 'lakes'; a conclusion supported by the microscopy. Predrying,and extraction of glycosaminoglycans produced a reduction in

swelling, but extraction of inorganic ions produced an increase, thus indicating that these molecules are involved in the swelling pressure, and probably, in association with inorganic ions, restrict the swelling of pre-dried cornea. That this restriction occurs between the fibrils is indicated by the higher proportion of lake water in pre-dried specimens. Matrix fixed charge concentration of fresh cornea was shown to increase with pH, and to be considerably higher for pre-dried specimens, and for fresh in a chloride-containing bathing solution; thus confirming the existence of lakes, and suggesting binding of chloride to the matrix.

ACKNOWLEDGEMENTS

I would like to thank my supervisor, Professor G. F. Elliott, for three years of help and guidance, as well as for initiating these studies. Mr. Ken Ball taught me the immunofluorescence technique and allowed me the use of his laboratory at the Canadian Red Cross Memorial Hospital. Thanks also to Dr. Michel Koch and Dr. Joan Bordas at EMBL, Hamburg, without whom the synchrotron X-ray work could not have been done. Dr. Zehra Sayers has read this thesis at its various stages, and has made many helpful comments, as well as assisting me with the synchrotron X-ray work.

I am also indebted to the many friends and colleagues who have helped with discussions, practical assistance and moral support. In particular, Mrs. Dawn Collins, Mr. Peter Finnimore and Mrs. Rosemary Hughes for technical assistance and Dr. Derek Cummings for help with the computing.

Finally, I must thank my husband, Terry, for providing moral support and encouragement when it was most needed.

LIST OF CONTENTS

TABLE OF ILLUSTRATIONS

Chapter 5.

CHAPTER 1

Introduction.

The cornea forms part of the outermost coat of the eye. The larger part of this protective tunic is the sclera, which unlike the cornea, is not transparent. In the normal eye, the cornea and the sclera are subjected to considerable pressure from the interocular fluid, which exerts a pressure of 10 - 20 mm Hg. (Leydhecker, Akiyama and Neumann, 1958). The structure of both tissues is thus required to be such as to provide the strength and elasticity necessary to withstand this pressure. Additionally, the cornea must be transparent to visible light and have a refractive index such that a considerable amount of the focusing of the eye takes place at its surface.

1.1 The structure of the corneal stroma.

The stroma is the central and larger part of the cornea. It is bounded on the anterior surface by Bowmans membrane and the epithelium, and on the posterior surface by Descemets membrane and the endothelium. (More detail of the anatomy of the cornea can be found in Davson, 1980).

The normal corneal stroma is about 78% water and 15% collagen by weight. The other 7% of the solid constituents include 5% other proteins, 0.7% keratan sulphate, 0.3% chondroitin sulphate and 1% salts. (Maurice, 1969). The collagen molecules, as in other connective tissue, are arranged as fibrils; with uniform diameters unlike those of sclera and other collagenous tissues, where the fibrils vary considerably in size. (Borcherding, Blacik, Sittig, Bizzell, Breen and Weinstein, 1975). The corneal stroma consists of layers or 'lamellae', with the fibrils within

one lammella lying roughly parallel to each other, but not to those in neighbouring lammellae. (See diagram in figure 3.1 chapter 3). The collagen fibrils, and the lammellae, lie parallel to the surface of the cornea.

1.2 The transparency of the cornea.

Under normal conditions the cornea is transparent to visible light, but swollen cornea *in vivo* or *in vitro* becomes opaque. In fact, it is surprising that the cornea, being built up of fibrils with diameters smaller than the wavelength of visible light, should be transparent at all. Maurice (1957), from an examination of the birefringence of the cornea, showed that the size of the fibrils and the difference in refractive index between them and the ground substance suggests that incident light will be scattered and the tissue appear opaque. However, he also showed that this scattering of light will not occur if the fibrils are of uniform diameter and are arranged in parallel rows. In this situation the diffracted rays will tend to cancel each other out by destructive interference, and leave the undiffracted rays unaffected. Hart and Farrell (1969) suggest that only short range ordering is required and the regularity of spacing need not extend over many wavelengths in any region.

Goldman and Benedek (1967) report that the theory of the scattering of light from random arrays shows that large amounts of scattering and consequent opacity results only if there are substantial fluctuations in the index of refraction which take place over distances comparable to or larger than the wavelength of light. Later (Goldman, Benedek, Dohlman and Kravitt, 1968) they report finding 'lakes' in swollen cornea, both within and between lammellae, with dimensions greater than $\lambda/2n$ (i.e.

$\sim$200nm), which could account for the scattering of light of wavelength λ. However, Maurice (1957) suggests that swelling between lammellae should produce irridiscence, and this is not observed.

1.3 The origin of the swelling pressure.

If exised corneal stroma is placed in an aqueous bathing solution, it will swell to many times its original size. In vivo or during in vitro experiments on viable intact cornea, the hydration of the tissue is kept constant by a 'metabolic pump' located in the endothelium. (Mishima and Kudo, 1967). The scraping of the surface removes these cells and thus there is no active transport out of the tissue to oppose the influx due to the swelling pressure. Similar swelling (with the associated opacity) can be observed in vivo when the endothelium is damaged, or when the interocular pressure increases above normal due to, for instance, blockage of the drainage channels in the trabecular meshwork.

Pieces of corneal stroma in aqueous solutions do not, however, swell equally in all directions, but increase only in thickness along the optical axis. (ie. perpendicular to the plane of the lammellae). The thickness of the cornea is linearly related to its hydration (Hedbys and Mishima, 1966), and any change at right angles to the optical axis is undetectable. It is also possible to measure the rate of flow of water through the stroma. Hedbys and Mishima (1962) found that the resistance to water flow was the same both along the optical axis and in any direction perpendicular to it, for hydrated cornea. If the specimen was dried, a much higher resistance to water flow was observed in the direction of the optical axis. This was explained by postulating channels, parallel to the fibrils, remaining open in dry tissue, whereas the fibrils themselves are generally too close to allow easy flow of water. Enzyme dig-

estion of the glycosaminoglycans greatly decreases the resistance to water flow (Hedbys, 1963), suggesting that it is these constituents of the stroma that contribute the majority of the resistance.

Although the glycosaminoglycans increase the resistance to water flow through the cornea, it seems likely that they contribute to the swelling pressure, especially as treatment with cetyl pyridinium chloride, which precipitates glycosaminoglycans, causes a reduction in the swelling rate (Hedbys, 1961). Hart and Farrell (1971) suggest that the swelling pressure of the stroma can be described as the sum of four contributions: an excluded volume effect, a negative elastic contribution deriving from the spring-like character of the glycosaminoglycan chains, short-range chain-solvent interactions and a Donnan term arising from free negatively charged sites in the tissue. The actual contribution attributed to each varies. Friedman, Kearns, Michenfelder and Green (1972) find that, in rabbit cornea, about half of the swelling pressure at normal hydration is Donnan-osmotic, and that this is sensitive to the molecular organisation of the ground substance between the fibrils (Friedman and Green, 1971). This is also the conclusion of Hedbys (1963) who measured the osmotic gradient due to ions as 1.4mM, out of a total swelling pressure of 3.5mM. Hodson (1971) concludes that the main cause of swelling is the Donnan potential, and that at physiological hydration, when swelling pressure = imbibition pressure (Hedbys, Mishima and Maurice, 1963), his theoretical treatment suggests that there is no electrostatic repulsion or radial crosslinking between the fibrils.

The macromolecular matrix of the corneal stroma carries an overall negative charge, due mainly to the glycosaminoglycans since at physiological pH the collagen is close to its isoelectric point (Pirie, 1947). Changing the pH of the bathing solution will alter the overall charge of

the matrix (Goodfellow, 1975), and thus the Donnan-osmotic contribution to the swelling pressure. Varying the sodium chloride concentration of the bathing solution changes the concentration of sodium and chloride found in the tissue at equilibrium (Green, Hastings and Friedman, 1971). Green et al concluded that the sodium binds to the macromolecular matrix and the chloride does not, but the data presented is not inconsistent with chloride binding.

The rate of swelling of corneal stroma in aqueous solutions depends on the pH and ionic strength of the bathing solution. (Goodfellow, 1975, Elliott, Goodfellow and Woolgar, 1980). The smallest swelling rate is observed at low pH ($\sim$4), and the greatest in distilled water. In distilled water the initial rate of swelling is very high and drops to about zero in several hours. However, other solutions produce a swelling rate that is initially much slower, but shows no sign of approaching zero after several days.

1.4 The corneal proteoglycans.

Although the arrangement of the collagen fibrils can be inferred, at least to some degree, from electron micrographs, it is more difficult to define the position and structure of the proteoglycans and glycoproteins. Francois, Rabaey and Vandermeersche (1954) and Hogan, Alvarado and Weddell (1971) found that the collagen fibrils in the corneal stroma appeared to be covered with a dense coat of granules; Borcherding et al (1975) supposed that these granules were proteoglycan molecules on the surface of the fibril, and that the mutual repulsion of these highly charged molecules would cause the protein cores to be oriented perpendicular to the fibril, and that the negatively charged field produced would be able to maintain the spatial relationships of the fibrils.

Granular material has also been observed by Goldman et al (1968) in the wide interlamellarspaces he found in swollen corneal stroma.

Kaye, Cremer-Bartels, Buddecke and Dische (1976) extracted the glycosaminoglycans from the cornea using sodium chloride and calcium chloride solutions. Subsequent electron microscopical examination of the specimens revealed no lakes or other interruptions to the collagen matrix when sodium chloride alone was used, except that the periodicity of the collagen fibrils became more distinct. Calcium chloride extraction, however, destroyed the structure and produced shorter fibrils. Dische, Cremer-Bartels and Kaye (1978) found much the same results, and concluded that, as sodium chloride only extracted a proportion of the proteoglycans present (~80%) and calcium chloride was able to extract the majority of the rest, the proteoglycans in the cornea were of two different types. They suggest that the proteoglycans extractable only by calcium chloride are involved in the reinforcement of the head to tail junction of the collagen molecules in the fibrils.

Hassel, Newsome and Hascall (1979) and Axelsson and Heinegard (1978) used 4M guanidine hydrochloride to extract the proteoglycans from Rhesus monkey and bovine cornea, respectively. Both groups obtained proteoglycan fractions but Hassel et al were able to separate two different proteoglycans by using dissociative conditions whereas Axelsson and Heinegard were unable to do this under associative conditions - suggesting some interaction between the two molecules involving weak bonding interactions. The two proteoglycans found proved to be very different from those extracted from cartilage. Cartilage proteoglycans contain about 10% protein with about 100 chondroitin sulphate and 50 keratan sulphate chains per molecule (Hascall,1977). Corneal proteoglycans are of two types:one containing about 70% protein with 1 or 2 chondroitin

sulphate chains (nearly twice as large as those in cartilage) and several glycoprotein-like oligosaccharide chains. The other has about 74% protein with one or two keratan sulphate chains (the same size as those in cartilage) and several glycoprotein-like oligosaccharides. (Hassel et al, 1979).

A soluble protein has been isolated from bovine cornea using low ionic strength extraction solutions. (Alexander, Silverman and Henley, 1980). It has been shown to be a single polypeptide chain of molecular weight ~54000, with no saccharide content, and no unusual amino acid composition so that it is not a collagen or actin-like molecule. An antiserum to this protein, prepared and tested for antigenic reactivity by Silverman, Alexander and Henley (1980 a) & b)), suggests that it is specific to cornea, but is not species-specific among a number of mammals including humans. The protein cores of bovine and monkey cornea proteoglycan have different amino acid contents (Hassel et al, 1979 , Axelsson and Heinegard, 1978), and the antigenic site of pig invertebral disk proteoglycan has been shown to be the binding region on the protein core (Beard, Ryvar, Brown and Muir, 1980), although no information about the antigenicity of corneal proteoglycan is available.

Mathews (1967) proposes the existence of cross-linking between the fibrils of the corneal stroma. However, although the proteoglycans may be associated with the collagen fibrils (Dische et al, 1978, Borcherding et al, 1975), it is unlikely that they actually form interfibrillar crosslinks. Hodson (1971) investigated the possible reasons for corneal swelling and could find no evidence of crosslinking, or, given the observed swelling properties, no justification for assuming them. Crosslinking has been demonstrated between the collagen molecules that make up the fibril (Harding and Crabbe, 1979), but these

do not involve glycosaminoglycans.

It has been suggested that the absence of a first order collagen reflection in the low angle X-ray diffraction pattern of cornea may be due to the occlusion of the gap between the ends of the collagen molecules in the fibril by glycoproteins or glycosaminoglycans. (Elliott, Goodfellow and Woolgar, 1978, Goodfellow, Elliott and Woolgar,1978). This is in accordance with the observation by Kaye et al (1976) that sodium chloride extracted cornea showed more distinct periodicity along the collagen fibril, and calcium chloride extraction produced shorter, disordered fibrils.

1.5 The preservation of corneal specimens.

For physical studies of the cornea it is necessary to preserve the cornea in a way that maintains the structural and swelling properties and the chemical composition as near as possible to those of fresh specimens. Dische et al (1978) found that freezing had no effect on the glycosaminoglycan content and only minimal effect on the swelling of bovine cornea. Goodfellow et al (1978) and Elliott et al (1980) used cornea preserved by drying over silica gel, but make no comment on the differences in the subsequent swelling properties or the interfibrillar spacings. Other structural studies have used electron microscopy, where the fresh (or swollen) tissue was fixed prior to drying, staining and embedding. This process, in itself, may produce structural changes that are impossible to avoid with this technique.

1.6 The purpose of this thesis.

The purpose of this thesis is to investigate the structural and

swelling properties of normal, dried and extracted specimens of bovine corneal stroma using a variety of experimental techniques. The likely forces contributing to the swelling pressure are investigated and the swelling in distilled water is monitored.

Theoretical calculations of the matrix fixed charge (Otori, 1967, Hodson, 1971) take into account the considerable negative charge provided by the glycosaminoglycans. Extraction of all or some of these macromolecules should affect the swelling and charge properties of the cornea and also, perhaps, the structure. Cetyl pyridinium chloride is used to precipitate the glycosaminoglycans in situ and extraction of both chondroitin sulphate and keratan sulphate containing proteoglycans is carried out under associative conditions using sodium chloride solution and under dissociative conditions using guanidine hydrochloride solution. The enzyme chondroitinase ABC is also used to extract the chondroitin sulphate by cleaving the glycosidic bonds and allowing the resulting dimers to diffuse out of the stroma. The effects of these extraction processes and of extraction with distilled water are investigated by studying the swelling properties of variously treated specimens and by monitoring the change in pH of the bathing solution during swelling. The matrix fixed charge is measured using a microelectrode technique, the interpretation of which makes use of the Donnan-osmotic theory. The inorganic ion concentration of the stroma after swelling in distilled water is measured using flame photometry. (We are indebted to Dr. Alison Brading of the Dept. of Pharmacology, University of Oxford, for the use of apparatus and for help with the technique).

Light microscopy, using immunofluorescence and chemical staining, together with X-ray diffraction studies, is used to study the structural changes associated with pre-drying and with swelling. In particular, the

X-ray diffraction technique allows structural information to be obtained from specimens of fresh cornea without prior fixing of the tissue. The high intensity of synchrotron X-rays allows the detection of reflections associated with fibril packing and the rapid monitoring of changes in interfibrillar spacing with hydration. An extension of this work included an investigation into the degree to which regular ordering of the collagen fibrils occurs in the corneal stroma. This work was carried out in collaboration with Dr. Z. Sayers, and the results will be reported in detail in Sayers, Whitburn, Harmsen, Koch, Meek and Elliott (in preparation). Finally, the synchrotron diffraction patterns contain a set of X-ray reflections which arise from the regular packing of the collagen molecules within the fibril. An analysis of these reflections, presented as a comparison of the electron density profiles of tendon collagen and corneal collagen, is reported elsewhere (Meek, Elliott, Sayers, Whitburn and Koch, 1981).

CHAPTER 2

Materials and Methods I - Preparation of Specimens.

Adult cows eyes were obtained from the slaughter-house within a few hours of the death of the animal. The corneas were dissected out by cutting inside the limbus, and the epithelial and endothelial cells removed by gentle scraping with a scalpel. Discs (9mm in diameter) were cut with a specially designed cutter in order to keep the specimen size as uniform as possible for the swelling experiments. Strips and squares were cut with a scalpel for other experiments. Specimens were then either used immediately, or preserved by drying or freezing.

The drying of fresh and previously extracted and swollen cornea was carried out at room temperature and pressure over silica gel. The time required for drying depended on the initial hydration, but was in the range 7 to 14 days.

The squares to be used for microscopy were quick-frozen in 2-methylbutane, in liquid nitrogen,

and stored at -20°C in airtight bags.

2.1 Extraction.

Fresh discs, strips and squares of cornea for use in swelling, X-ray diffraction, microelectrode and microscopy studies were treated with solutions of salts and enzymes, and distilled water. The salt solutions were expected to extract the proteoglycans from the cornea (Kaye et al, 1976) , whereas the enzyme was only expected to remove the chondroitin sulphate chains from the protein core of the proteo-

glycan. This is achieved by cleavage of the glycosidic bonds to produce disaccharide units which diffuse out of the tissue. (Suzuki, Saito, Yamagata,Anno, Seno, Kawai and Furuhashi,1968). Distilled water was expected to extract the inorganic ions, but very little, if any, of the macromolecular components in the time given. (Dische et al,1978). The guanidine hydrochloride in particular was expected to remove large amounts of intact proteoglycan. (Axelsson and Heinegard, 1978, Hassel et al, 1979).

2.1.1 Sodium Chloride Extraction.

Discs, strips and squares were extracted at 4°C with 0.15M sodium chloride solution for a total of 7 days, with one change of solution after 3 days. To prevent degradation by micro-organisms, chrystamycin (1%) and nystatin (0.04%) were added. The control experiment substituted water for the 0.15M sodium chloride solution. 25cm^3 of solution were used to extract 10 discs (9mm diameter), or the equivalent mass in strips and squares. This procedure was based on that used by Dische et al (1978), except that less changes of solution were used and no stirring or homogenisation took place. These modifications were thought advisable to minimise mechanical damage to the specimens, although the extraction would probably not be complete.

2.1.2 Guanidine Hydrochloride Extraction.

4M guanidine hydrochloride solution was prepared in a pH 5.8 buffer of 0.01M sodium acetate and 0.01M sodium EDTA. (Hassel et al, 1979). This was used to extract pieces of fresh cornea (10 discs or equivalent mass in 25cm^3 solution) at 4°C for 24 hours. The control used the EDTA/acetate buffer alone.

2.1.3 Enzyme Extraction.

Chondroitinase ABC, (Yamagata, Saito, Habuchi and Suzuki, 1968), obtained from Miles Laboratories Ltd., was used to digest the chondroitin sulphate in corneal stroma. 10 cornea discs (or equivalent) were digested in a solution of 2.5 units of enzyme in 10 cm^3 of phosphate buffer, pH 8. (see buffer solution table in chapter 3, table 3.1). The control experiment used 10 cm^3 of buffer alone. The specimens were incubated in these solutions for 5 hours at 37°C.

2.1.4 Cetyl Pyridinium Chloride Treatment.

Fresh specimens of cornea were treated with 0.15M cetyl pyridinium chloride solution for 24 hours at 4°C. Because of the relatively low solubility of cetyl pyridinium chloride in distilled water, a more concentrated solution was impracticable, and in this case 50 cm^3 of solution were used for 10 discs of cornea. The control experiment used 50cm^3 of distilled water under the same conditions. The object of this experiment was the precipitation of the proteoglycans *in situ*. These precipitated polysaccharides are insoluble in water, although they will dissolve in solutions of sodium chloride. (Hedbys, 1961).

All the extracted discs for use in swelling experiments were washed for 2 hours at the end of the extraction period. They were then dried over silica gel for 7 - 14 days. Specimens for use in the other experiments were also washed in distilled water, but were then used immediately, frozen or dried, as appropriate. Fresh and pre-dried pieces of cornea for microscopy were swollen for 4 hours in distilled water before freezing and sectioning.

CHAPTER 3

Materials and Methods II - Experimental Techniques.

3.1 Swelling in distilled water.

To determine the swelling rate, discs of cornea were swelled individually in $4cm^3$ distilled water over a period of 2 hours. At 5 minute intervals during the first 30 minutes and at 10 and 15 minute intervals later, the cornea were removed, blotted carefully on tissue, weighed and returned to the bathing solution. At the end of the swelling period the cornea were dried over silica gel and the dry weight determined. The cornea were weighed as rapidly as possible on a torsion balance of range 0 to 500mg, capable of weighing to within $\pm$ 1mg. The weight of one cornea disc varied from about 10mg to about 300mg, depending on hydration, so the maximum single weighing error was less than 10%.

From each set of raw swelling data the hydration (defined as mass water/dry mass) was calculated for each measurement. The results from the individual experiments were combined by calculating the mean hydrations for each time interval. The computer was also used to calculate the standard error of the mean, and to plot the results as a graph of hydration against time. (Figures 4.1 - 4.6). The number of experiments in each set (n) was approximately 25.

3.1.1 Fresh and Pre-dried cornea.

Swelling experiments were carried out on 9mm discs of fresh cornea, and on similar specimens that had been dried over silica gel for 7 days. At the end of the swelling period all the specimens were dried over silica gel and the swelling experiment repeated. Data was thus obtained

for first and second swellings of fresh and pre-dried cornea.

In order to compare the variations in swelling rate, straight lines were fitted to the first four points and the last four points (where the slope was fairly constant) of the swelling curves using the CURFIT library program on the Hewlett Packard 2000 computer. This program uses a linear regression method for curve fitting. Significance testing on the slopes of these lines was carried out using the Student t test, as described in Haber and Runyan (1973). (See table 4.3 in chapter 4).

This process was repeated for a third swelling, and, in the case of fresh cornea, again for a fourth, but the significance testing was not considered useful for this data since the change was small, and the specimens showed signs of disintegration by this stage.

3.1.2 Extracted Cornea.

Extracted cornea and the control specimens were dried after washing and then the swelling monitored as described above.

The osmotic pressure of the bathing solutions was measured with a MSE Advanced Osmometer. This was done at the end of each swelling period and used as an indication of the amount of material extracted from the specimen during the swelling process.

3.2 X-ray Diffraction.

The technique of low-angle X-ray diffraction was used to study the arrangement of the collagen fibrils in the corneal stroma; particularly to determine the centre-to-centre spacing between neighbouring fibrils for various hydrations.

3.2.1 The Apparatus.

An Elliott GX13 rotating anode generator was used with a mirror-monochromater camera of large specimen-film distance. (approximately 80cm.) The specimens were mounted in water-tight cells and exposed to the X-ray beam for 2-3 hours. The data were collected on Kodak 'NoScreen' film. The hydration of the cornea was checked by weighing before and after exposure.

Use was also made of the synchrotron X-ray facility at the EMBL outstation in Hamburg. The X13 mirror-monochromater camera on the storage ring DORIS was used with specimen-film distances of about 3.2m and about 1.5m, and exposure times of 10-30s and 5-30mins, respectively. The long camera with short exposure times was used tc detect the first order reflections from the fibril lattice, and the shorter camera used for higher orders of this and of the collagen gap-overlap repeat. The specimens were again mounted in water-tight cells, and weighed before each exposure to determine the hydration. The data were collected on film and with a position-sensitive detector.

3.2.2 Determination of the Interfibrillar Spacing.

Discs of fresh and pre-dried cornea were hydrated in distilled water. Diffraction data were collected from both types of specimen at various hydrations. Low hydrations (below physiological) of fresh cornea were obtained either by shrinking the specimen in 40% dextran (BDH) solution, or by drying in air.

These specimens produced reflections arising from the packing of the fibrils in the stroma and also from the packing of the collagen

molecules along the fibril (~67nm gap-overlap repeat). Because of the random arrangement of the lamellae (figure 3.1), reflections appear on the film as circles. In order to produce two separate sets of reflections on the film, strips of cornea were mounted in the beam so that the X-rays passed at right angles to the visual axis. In the idealised situation shown in figure 3.1 we would expect the collagen reflections to appear along one axis of the film and the interfibrillar reflections to appear mainly along the other. Because the synchrotron X-ray beam is rather better-focused in the vertical direction than the horizontal, strips of cornea were mounted to obtain the best possible resolution, i.e. horizontally for interfibrillar reflections and vertically for collagen reflections. (see figures 4.7 and 4.8 in chapter 4).

This method facilitated the detection of weak second and third interfibrillar reflections, as well as the very strong first order peak. A range of hydrations was used to determine whether these weak reflections moved with changes in interfibrillar spacing, and were therefore higher orders of the reflection produced by the packing of the fibrils. The spacings of the first order reflections obtained were compared with those obtained by passing X-rays parallel to the visual axis in an attempt to determine whether there was any difference in the separation of the fibrils in the two directions.

The real-space distances can be calculated using the Bragg equation: $n\lambda = 2\sin\theta d$ where n = order of the reflection, λ = wavelength of the X-rays and θ = the diffraction angle of the reflection.

For very small angles (θ), $\sin\theta$ approximates very closely to $\tan\theta$, which can be expressed as distance of reflection from centre of beam (a)/specimen-film distance (D).

Therefore:

$$n\lambda = 2\frac{a}{D}d$$

Schematic diagram of the arrangement of collagen fibrils in the ox cornea

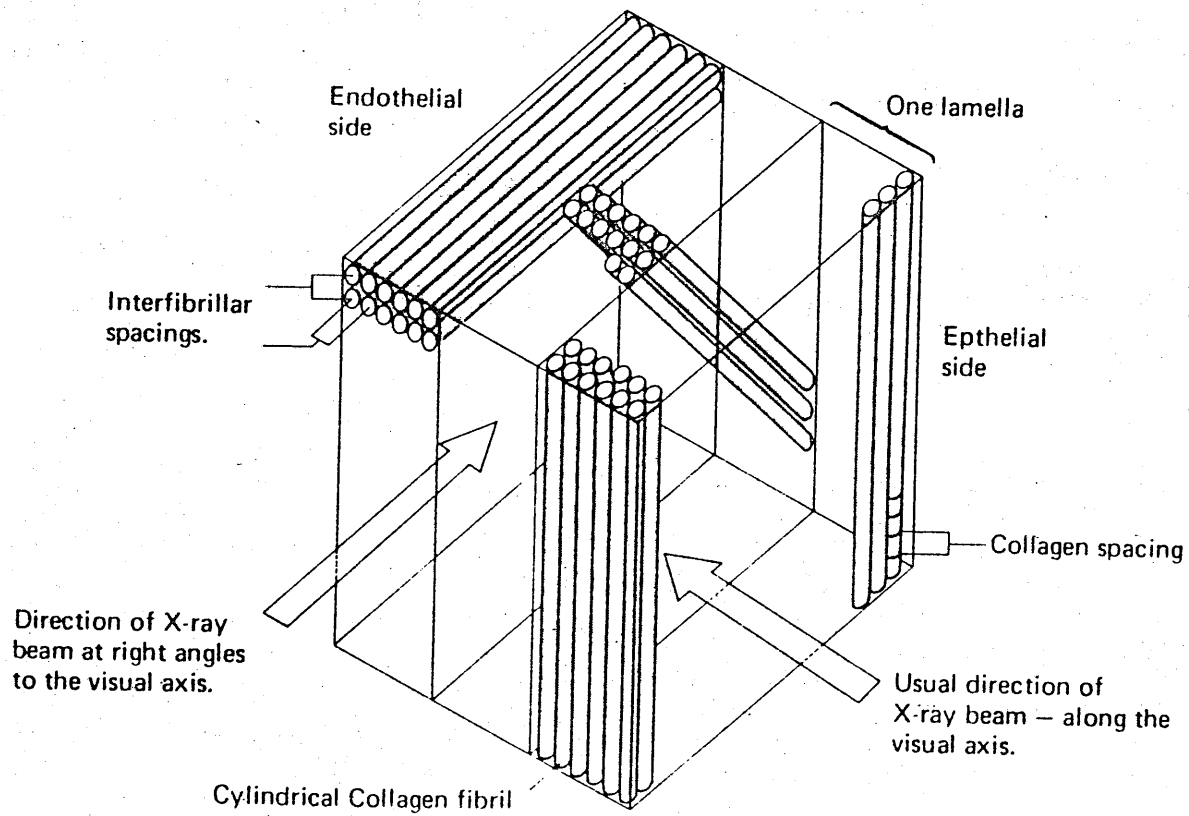

Figure 3.1

The wavelenghth of the synchrotron X-rays was not known accurately and the specimen-film distance was difficult to measure, so the collagen reflections obtained from wet rat tail tendon (where the spacing between the fibrils is known to be 67nm) were used to calibrate the camera. By rearranging the Bragg equation: $\frac{\lambda D}{2} = \frac{ad}{n}$ it is possible to obtain a value for the constant $\frac{\lambda D}{2}$ and to use this to calculate the interfibrillar spacings for cornea. This method was used both for the film and the detector data obtained using synchrotron X-rays, but was not necessary for the GX13 data since the wavelenghth of the X-rays was known accurately (copper-$K_{\alpha 1}$ radiation) and the specimen-film distance easy to measure directly.

The radii of the circular first order reflections of the interfibrillar spacings on film were located and measured both by eye and from densitometer traces obtained on a Joyce-Lobel microdensitometer. The diffraction data collected by the detector were processed on the computer at EMBL Hamburg, and a plot of log(intensity) against detector channel number produced. (examples in figures 4.11 and 4.12) The peaks were measured directly from these plots and the centre of the beam calculated using data collected from several specimens of dry cornea and rat tail tendon; using the reflections from the collagen backbone. The interfibrillar spacings for all specimens were then calculated as described above.

The CURFIT program was used to fit straight lines to the computer-produced plot of $(\text{interfibrillar spacing})^2$ against hydration; both for fresh and for pre-dried specimens. (see figure 4.13) The mean of the intercepts of these two lines was calculated and used as an estimate of the spacing for dry tissue, which does not itself give a detectable reflection. (see section 4.2.2)

3.3 Inorganic Ion Analysis.

Solutions of extractable inorganic ions were obtained by swelling 10 cornea discs (9mm diameter) in $40cm^3$ of distilled water for 2 hours. The extracted cornea were then charred, oxidised with hydrogen peroxide and the residue dissolved in $40cm^3$ of distilled water. These solutions were assayed for sodium, potassium and chloride by absorption flame photometry.

3.3.1 Absorption Flame Photometry.

Preliminary analysis showed that the ratio of sodium to potassium in the solutions was approximately 10:1.Therefore, because sodium absorbs at many wavelengths, standard solutions were prepared containing sodium and potassium chlorides in this ratio of 10:1.The concentrations of the standards ranged from 0.02 mM K^+/0.2 mM Na^+ to 0.5 mM K^+/5 mM Na^+. The solutions and standards were used neat for potassium analysis and diluted 1:2 with distilled water for sodium analysis. Absorbances were measured at wavelengths of 580nm for sodium and 760nm for potassium.

Analysis of the chloride content of the solutions required an indirect method. The chloride ion was precipitated with excess silver nitrate, the silver chloride separated by centrifugation and the absorbance of the residual silver determined. Standard solutions were obtained in two ways: solutions containing concentrations of silver ranging from 0.1mM to 1.9mM were prepared from 'AnalaR' silver nitrate. Stock solutions containing 2mM and 3mM, respectively, were prepared, and $5cm^3$ of these solutions were then used to precipitate the chloride from $5cm^3$ of the sodium and potassium standard solutions prepared earlier. This produced standard silver solutions ranging from 0.175mM to 1.225mM.

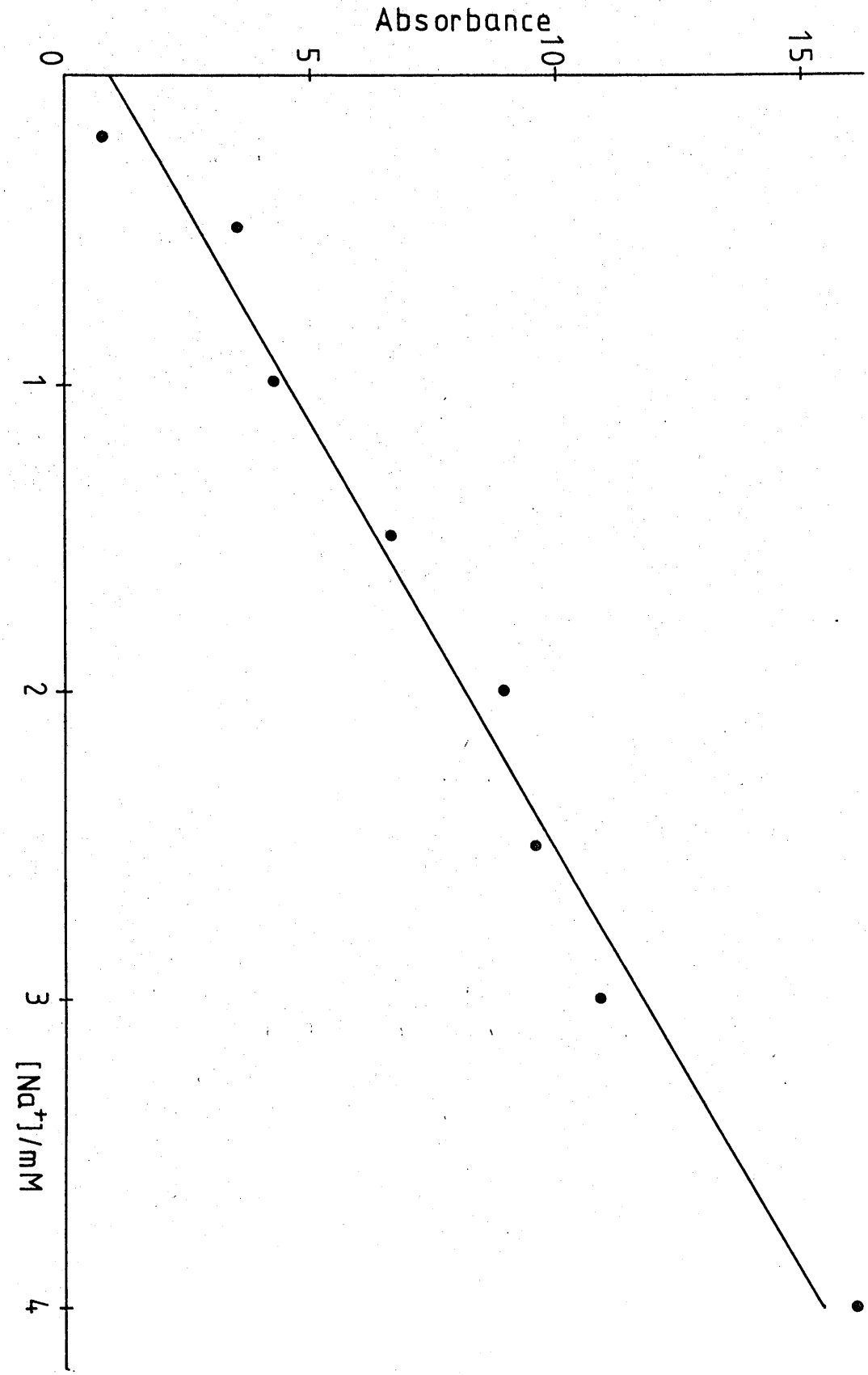

Figure 3.2 - standard curve for sodium determinations.

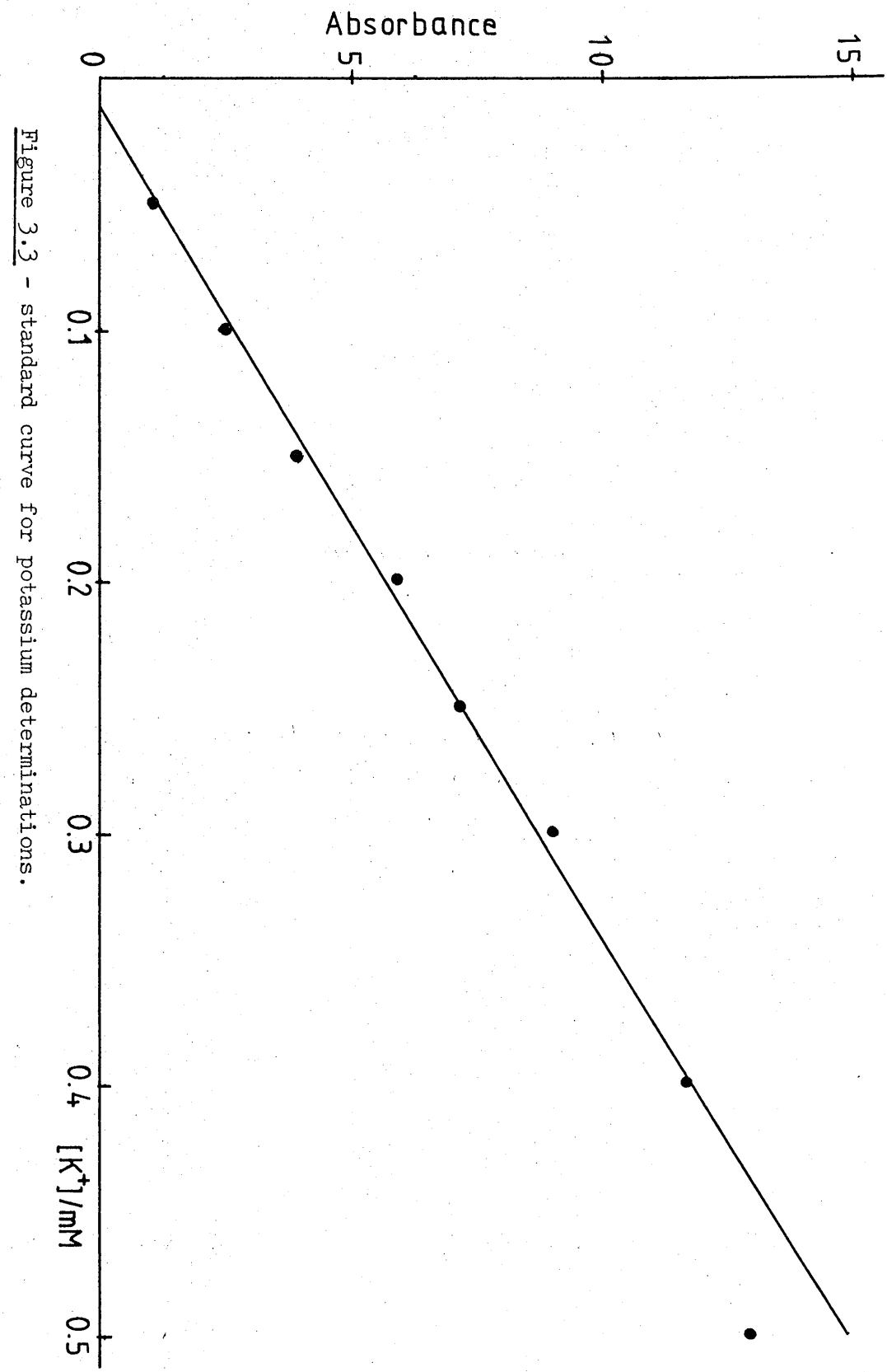

Figure 3.3 - standard curve for potassium determinations.

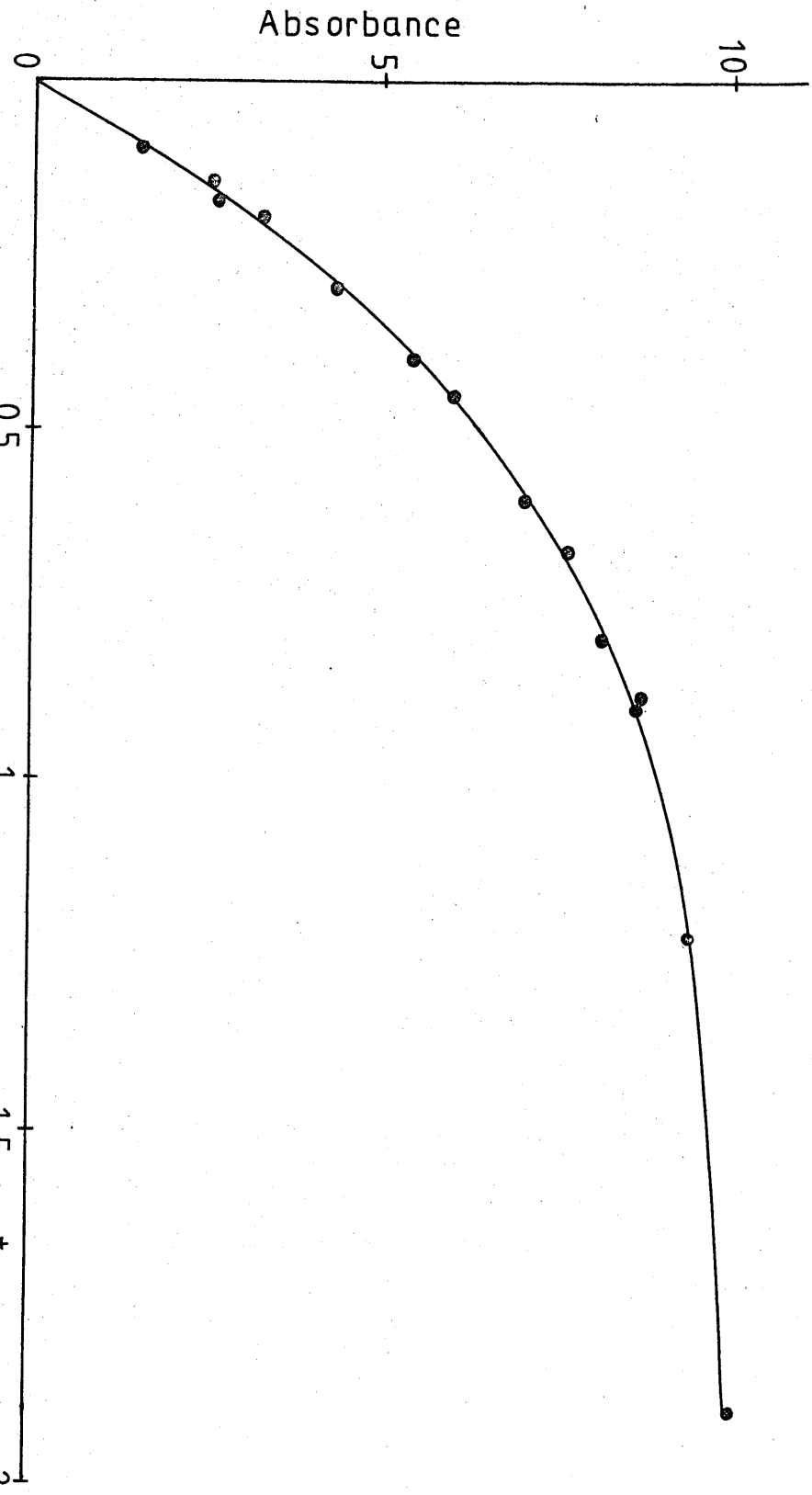

Figure 3.4 - standard curve for chloride determinations.

No significant difference was observed between the standards prepared by either method, so the results were combined to produce the standard curve. The same two silver nitrate stock solutions were used to precipitate the chloride from the test solutions as for the standards, and the absorbance of the excess silver in both standards and tests was measured at a wavelength of 338nm.

The plots of absorbance against concentration of sodium and potassium were straight lines over the range of concentrations used. (figures 3.2 and 3.3) However, the absorbance by sodium at the wavelength used for silver was considerable, and the plot obtained was not linear. Since comparable quantities of sodium were present in both standards and test solutions, a smooth curve was fitted to the data, and this used to convert the silver absorbances to concentrations. This standard curve is shown in figure 3.4.

3.4 Change in pH of Bathing Medium.

Figure 3.5 shows the apparatus that was designed and built to allow the pH change of the cornea bathing solution to be monitored under an atmosphere of nitrogen. The inert atmosphere was necessary because the carbon dioxide in the atmosphere tended to dissolve in the bathing medium even with a covering of cling-film, causing fluctuations of the pH.

Distilled water was boiled to remove dissolved gases and $40cm^3$ of the cooled water placed in the flask. 10 fresh cornea discs (9mm diameter) were carefully placed on the lip of the plunger, positioned as to be above the water level. The apparatus was assembled and nitrogen gas circulated for 10 minutes. The experiment was started by lowering the

Figure 3.5

Apparatus for measuring the change in pH of the bathing solution when cornea swells.

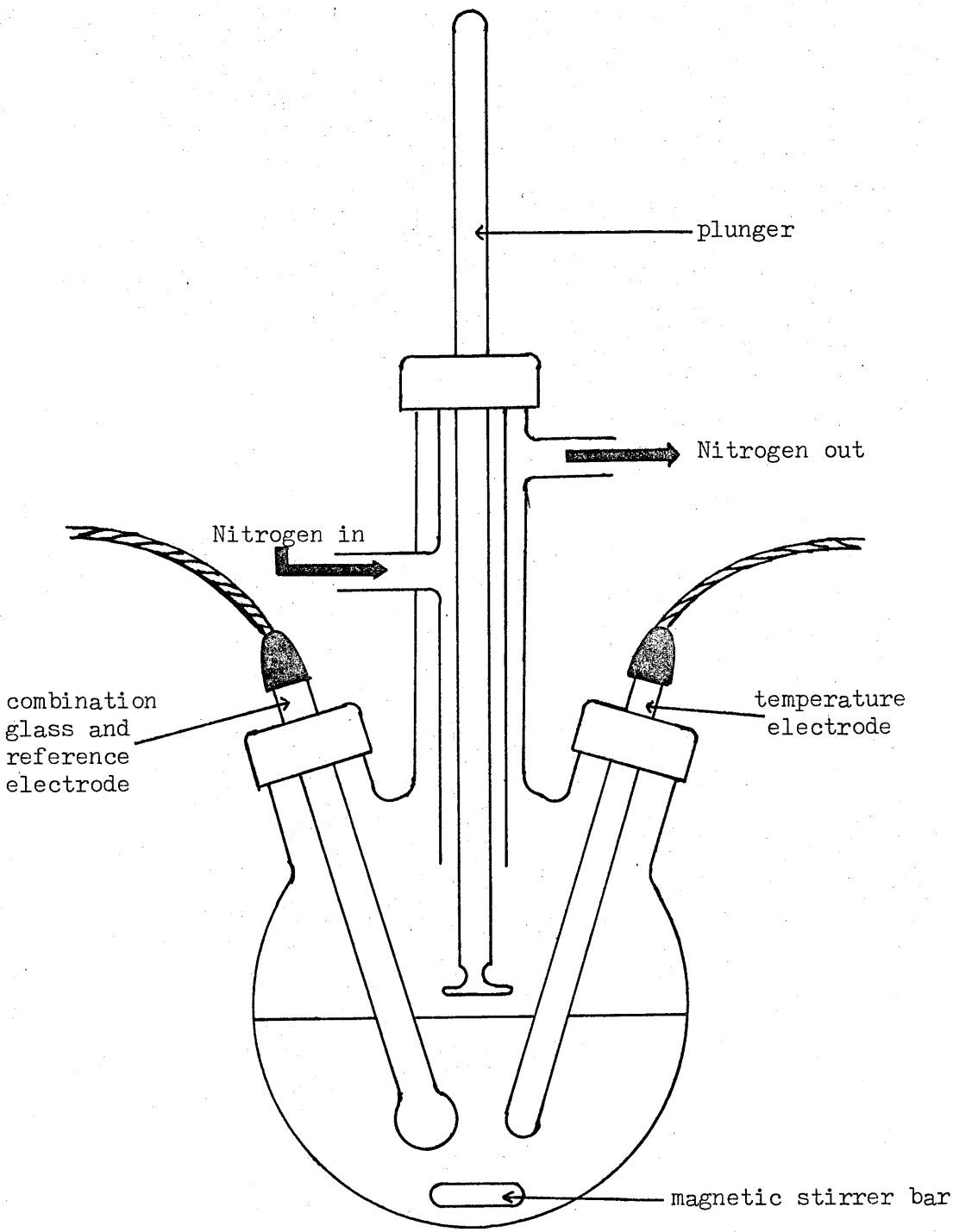

plunger into the water and twisting rapidly to dislodge the cornea. The pH was noted every minute for the first 10 minutes, and then at longer intervals, for a total of 2 hours. The osmotic pressure of the bathing solution was measured at the end of the experiment.

In a second experiment, boiled and cooled water was adjusted to pH about 8 with dilute sodium hydroxide solution, and the experiment carried out as above on 10 further fresh cornea discs.

For each point, the hydrogen ion concentration was calculated from the pH ($pH = -\log[H^+]$), and a graph of pH against time plotted for both experiments. (figure 4.14) A comparison of the quantity of hydrogen ions taken up by the cornea and the quantity of cations extracted in the same time was made. (section 4.4)

3.5 Microelectrode Measurements.

3.5.1 The Apparatus.

The apparatus used for the microelectrode measurements was that designed by Naylor (1978) and is shown in outline in figure 3.6. Microelectrodes were prepared from glass capilliary tubing using an Ealing-Beck microelectrode puller. The prepared electrodes were filled with 3M potassium chloride solution and mounted in an electrode holder with a silver/silver chloride junction and also filled with 3M potassium chloride solution.

3.5.2 Bathing Solutions.

Phosphate buffer solutions of various hydrogen ion concentrations

The Microelectrode Technique

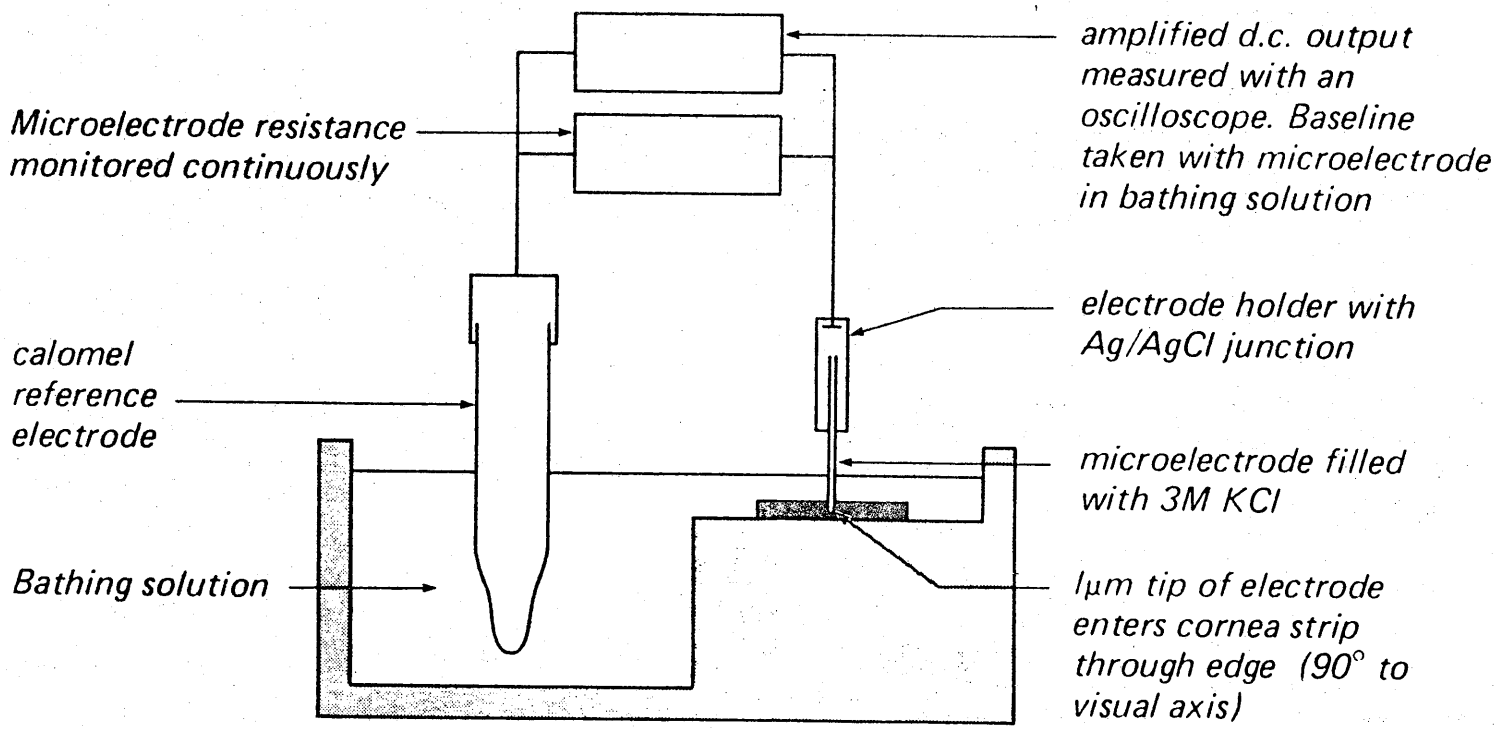

Figure 3.6

and of ionic strength 0.02 were prepared; one containing some chloride. A computer program based on the Perrin equation (Perrin and Sayce, 1967), was used to calculate the concentrations of phosphates needed to give the specific pH and ionic strength required. Table 3.1 gives the details of the composition of the bathing solutions used. The ionic strength was kept low (0.02) to reduce the possibility of extracting the macromolecular components of the cornea during the experiment.

3.5.3 The Measurements.

Thin strips of cornea (pre-weighed) were mounted edge-on in a specially designed bath, and held in position with stainless steel pins. (figure 3.6). This method of mounting was necessary because the anterior and posterior surfaces of the corneal stroma are too tough to allow penetration by the microelectrode. Sufficient bathing solution was then added to the deep part of the bath to submerge the tip of the reference electrode, but leaving the specimen unwetted. The microelectrode was then checked for resistance in this solution before positioning it above the strip of cornea. More buffer was then added to just cover the cornea, and 20 potential measurements ($\overset{e}{\wedge}$) made as quickly as possible; moving the microelectrode after each one. The specimen was then immediately removed from the bathing solution, blotted gently on tissue and re-weighed. Later, a dry weight was obtained, and the hydration of the tissue calculated, before and after the experiment. The change in hydration that occurred during the measurements was of the order of 10-20%. (see tables 4.15 - 4.18).

Several such experiments were carried out on different pieces of fresh cornea for each bathing solution. The fixed charge on the macromolecular matrix was calculated and adjusted for hydration.(tables 4.15-4.18).

Table 3.1 - Composition of buffer solutions used for microelectrode measurements. (Computer calculated using Perrin equ'n.)

pH		Concentrations of species in solution / mM							Volumes of stock solutions in cm^3, diluted to 1 dm^3.	Total ion conc./mM		
actual	calculated	$[PO_4^{3-}]$	$[HPO_4^{2-}]$	$[H_2PO_4^-]$	$[NaHPO_4^-]$	$[Cl^-]$	$[H_3PO_4]$	$[Na^+]$		$[PO_4^{3-}]$	$[Na^+]$	$[Cl^-]$
8.30	9	2.89×10^{-3}	6.62	5.90×10^{-2}	0.321	0	7.77×10^{-9}	13.7	10 0.7M Na_2HPO_4	7.00	14.00	0
7.75	8	2.69×10^{-4}	6.16	0.549	0.288	0	7.24×10^{-7}	13.2	10 0.65M Na_2HPO_4 10 0.05M NaH_2PO_4	7.00	13.50	0
6.80	7	2.24×10^{-5}	5.14	4.58	0.276	0	6.04×10^{-5}	15.1	10 0.54M Na_2HPO_4 10 0.46M NaH_2PO_4	10.00	15.40	0
5.85	6	7.35×10^{-7}	1.69	15.10	0.112	0	1.99×10^{-2}	18.6	10 0.18M Na_2HPO_4 10 1.51M NaH_2PO_4	16.90	18.70	0
4.93	5	9.88×10^{-9}	0.226	20.20	1.66×10^{-2}	0	2.66×10^{-2}	20.6	10 0.02M Na_2HPO_4 20 1.012M NaH_2PO_4	20.44	20.64	0
3.90	4	9.82×10^{-11}	2.25×10^{-2}	20.00	1.60×10^{-3}	0	0.264	20.0	20 1.0M NaH_2PO_4 10 0.03M H_3PO_4	20.30	20.00	0
2.95	3	9.80×10^{-13}	2.24×10^{-3}	20.00	1.51×10^{-4}	0	2.64	19.0	19 1.0M NaH_2PO_4 10 0.364M H_3PO_4	22.64	19.00	0
5.75	6	4.37×10^{-7}	1.00	8.93	6.75×10^{-2}	8	1.18×10^{-3}	19.0	10 0.1M Na_2HPO_4 10 0.9M NaH_2PO_4 10 0.8M NaCl	10.00	19.00	8.0

Measurements were also made on specimens rehydrated to approximately physiological hydration after being dried; both from fresh and after extraction with sodium chloride solution; and on very hydrated specimens of sodium chloride extracted cornea, used immediately after washing in distilled water.

3.6 Microscopy.

3.6.1 Raising Antibodies.

An antigen was prepared from the sodium chloride extraction solution from the first 3 days of extraction.(see section 2.1.1) This solution was dialysed against 2 changes of distilled water for 24 hours (to remove most of the sodium chloride), and concentrated approximately 10-fold in a rotary evaporator at reduced pressure.

$0.1cm^3$ of the concentrated cornea extract was emulsified with $0.1cm^3$ of Freunds Complete Adjuvant (to enhance the immune response), and $0.1cm^3$ of this emulsion injected subcutaneously into the shoulders of each of two New Zealand White rabbits. Two weeks later, a similar dose was injected into the other shoulders of the two animals. After 1 month, a booster dose of $0.05cm^3$ of extract alone was injected into the ear vein of each rabbit. After a further month, $15\text{-}20cm^3$ of blood was taken from the ear veins of the rabbits. The blood was stored at $4^{\circ}C$ overnight to allow clotting to occur, then centrifuged and the serum stored in small aliquots at $-20^{\circ}C$.

A rabbit antiserum to pig invertebral disc proteoglycan was a gift from Helen Beard of the Charles Salt Research Institute.

3.6.2 Testing the serum.

The serum from the two rabbits was tested for the presence of antibodies by the Ouchterlony double diffusion method. (Ouchterlony and Nilsson, 1973).

The centre wells of the Ouchterlony plates were filled with the antigen (from sodium chloride extract); neat and a 1:10 dilution. The outside wells were filled with the sera; neat and at dilutions of 1:2, 1:5,1:10,1:50 and 1:100. Phosphate buffered saline (PBS), pH 7.4, was used to dilute the extracts and sera. 1% agarose in PBS was used as the diffusion medium. The prepared plates were covered and left for 48-72 hours in a wet box for the precipitin lines to develop.

The same procedure was used to test the antigenic reaction of the pig invertebral disc antiserum to the concentrated sodium chloride extract.

3.6.3 Immunofluorescence staining.

Pieces of cornea, previously frozen in liquid nitrogen, were mounted in gelatin blocks on a cryostat chuck, and quick-frozen with liquid carbon dioxide. 6μm sections were cut, mounted on slides and air dried for 30 minutes. These sections were then stained in the following way:

Rabbit serum, appropriately diluted with PBS, was applied to each of the sections, which were then incubated in a wet box at room temperature for 20 minutes. The sections were rinsed with PBS and washed in a bath of PBS for 10 minutes. Optimally diluted fluorescein (FITC) labelled

anti-rabbit IgG (Wellcome Reagents Ltd.) was added, and the slides again left in the wet box for 20 minutes. They were then rinsed and washed in PBS for 1 hour, and finally mounted in buffered glycerol, pH 8.5, ready for viewing.

Initially, various concentrations of sera and fluorescein labelled conjugate were used to determine the optimum dilutions. Serum was finally used at dilutions of 1:10, 1:30 and 1:300. The fluorescein conjugate was used at a dilution of 1:32. Experiments were carried out on physiological and higher hydrations of fresh and pre-dried cornea, and on sodium chloride-extracted cornea.

3.6.4 Photomicroscopy.

The stained sections were viewed with a Leitz Dialux 20 microscope, fitted with a Ploemopak*and an HBO 50 mercury lamp. Photographs were taken with a Wild MPS 20 camera, using Ektachrome ASA 160 or ASA 400 film. Exposure times varied, but were of the order of 3-4 minutes.

3.6.5 Acridine Orange and Eosin and Haematoxylin staining.

Using sections prepared as for the immunofluorescence microscopy, chemical staining of the acid mucopolysaccharides was carried out using Acridine Orange. (Hicks and Matthaei, 1958).

Several drops of a 4% solution of ferric ammonium sulphate were applied to the slides. After 15 minutes, the slides were washed in running tap water for a further 15 minutes. 0.1% Acridine Orange solution was then applied, left for $1\frac{1}{2}$ minutes, washed off in running tap water for 15 minutes and the sections then mounted in Apathy mountant ready

*(Ploem, 1967)

for viewing.

Some frozen sections of fresh cornea were stained with Eosin and Haematoxylin (Ehrlich) in order to show the location of the keratocytes.

CHAPTER 4

Results

The computer programs used for the calculations were written for and executed on a Tektronix 4051 micro-computer, using a 4662 graph plotter and a Texas line-printer. Appendix II contains listings of these programs.

4.1 Swelling in distilled water.

4.1.1 Fresh and Pre-dried Cornea.

Tables 4.1 and 4.2 give the averaged results of the first and second swellings of fresh and pre-dried cornea respectively. Figures 4.1 and 4.2 are graphical representations of this data. Both fresh and pre-dried specimens swell more rapidly the second time. Inspection of the graphs suggests that the main difference in swelling rate occurs during the first 30 or so minutes, and that if the experiment had been continued beyond 120 minutes, the curves may well have coincided.

Figure 4.3 shows the difference between first swellings of fresh and pre-dried cornea; the fresh reaching a much higher hydration in 120 minutes. Here the difference in the swelling rates is not so marked in the early stages, but after about 60 minutes the swelling rate of the pre-dried cornea falls off rapidly, and the two curves are diverging.

The significance of these observations was tested statistically using Student's t test. Null hypotheses were set up to the effect that there was no difference in any of the initial or final swelling rates. Directional alternative hypotheses were used that stated that the second (or first fresh) swelling rates were greater than the first (or first

Table 4.1 - Swelling of fresh cornea in distilled water.

Time/mins.	Hydration	
	first swelling	second swelling
5	3.17 ± 0.13	4.71 ± 0.23
10	4.35 ± 0.11	7.64 ± 0.28
15	5.60 ± 0.11	10.06 ± 0.32
20	7.10 ± 0.12	12.07 ± 0.33
25	8.73 ± 0.17	13.79 ± 0.34
30	10.42 ± 0.21	15.26 ± 0.37
40	12.88 ± 0.31	17.73 ± 0.42
50	15.32 ± 0.34	19.63 ± 0.44
60	17.29 ± 0.39	21.37 ± 0.48
75	19.68 ± 0.43	23.36 ± 0.54
90	21.63 ± 0.51	24.96 ± 0.60
105	23.44 ± 0.53	26.38 ± 0.69
120	25.04 ± 0.54	27.71 ± 0.80

(± s.e.m., n~25)

Table 4.2 - Swelling of pre-dried cornea in distilled water.

Time/mins.	Hydration	
	first swelling	second swelling
5	1.55 ± 0.07	2.70 ± 0.14
10	2.75 ± 0.13	5.09 ± 0.24
15	4.08 ± 0.19	7.16 ± 0.30
20	5.46 ± 0.25	8.93 ± 0.34
25	6.73 ± 0.29	10.31 ± 0.37
30	7.88 ± 0.34	11.50 ± 0.40
40	9.63 ± 0.39	13.17 ± 0.46
50	10.95 ± 0.44	14.41 ± 0.49
60	11.95 ± 0.46	15.38 ± 0.53
75	13.11 ± 0.52	16.28 ± 0.57
90	14.02 ± 0.56	17.08 ± 0.61
105	14.79 ± 0.59	17.76 ± 0.64
120	15.38 ± 0.62	18.25 ± 0.66

(± s.e.m., n~25)

Figure 4.1

First and second swellings of fresh cornea in distilled water.

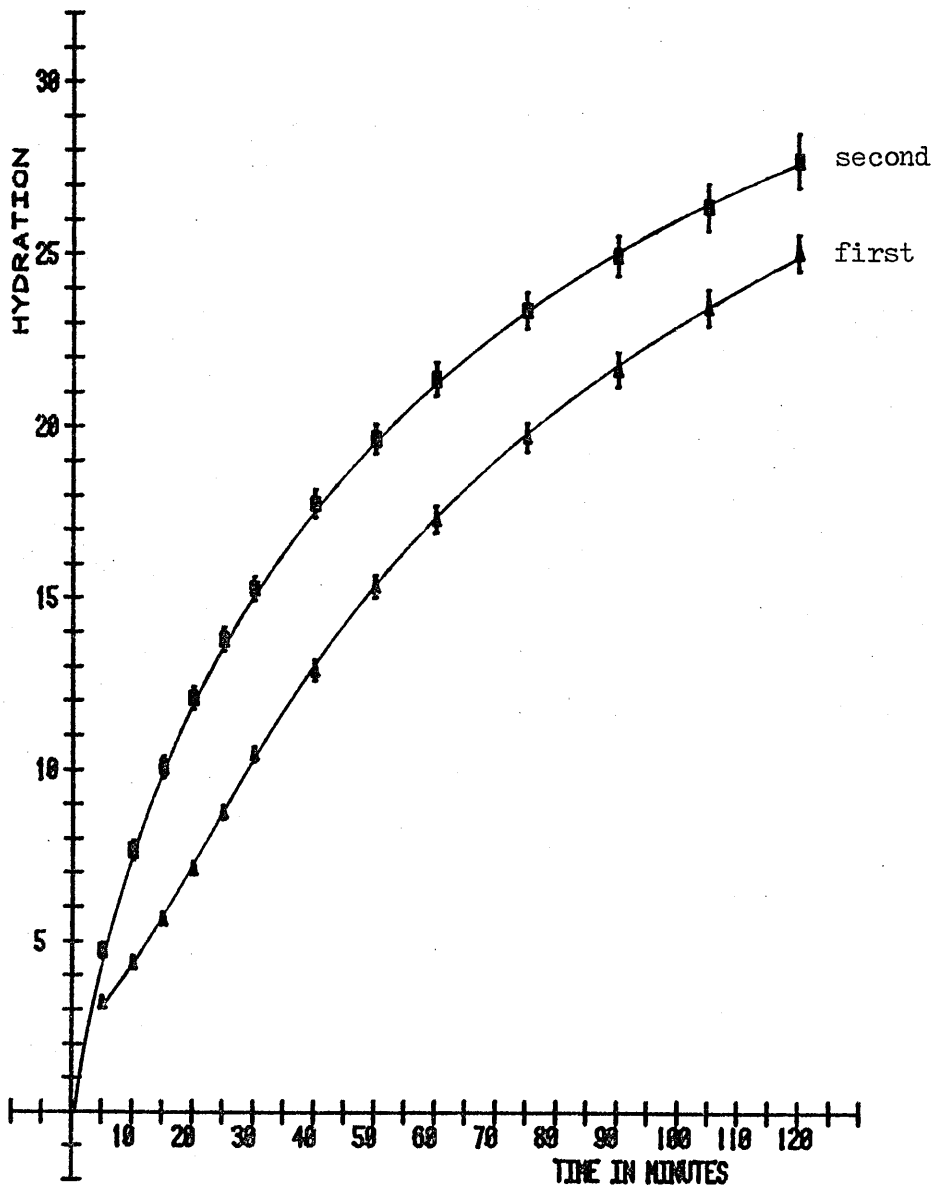

Figure 4.2

First and second swellings of pre-dried cornea in distilled water.

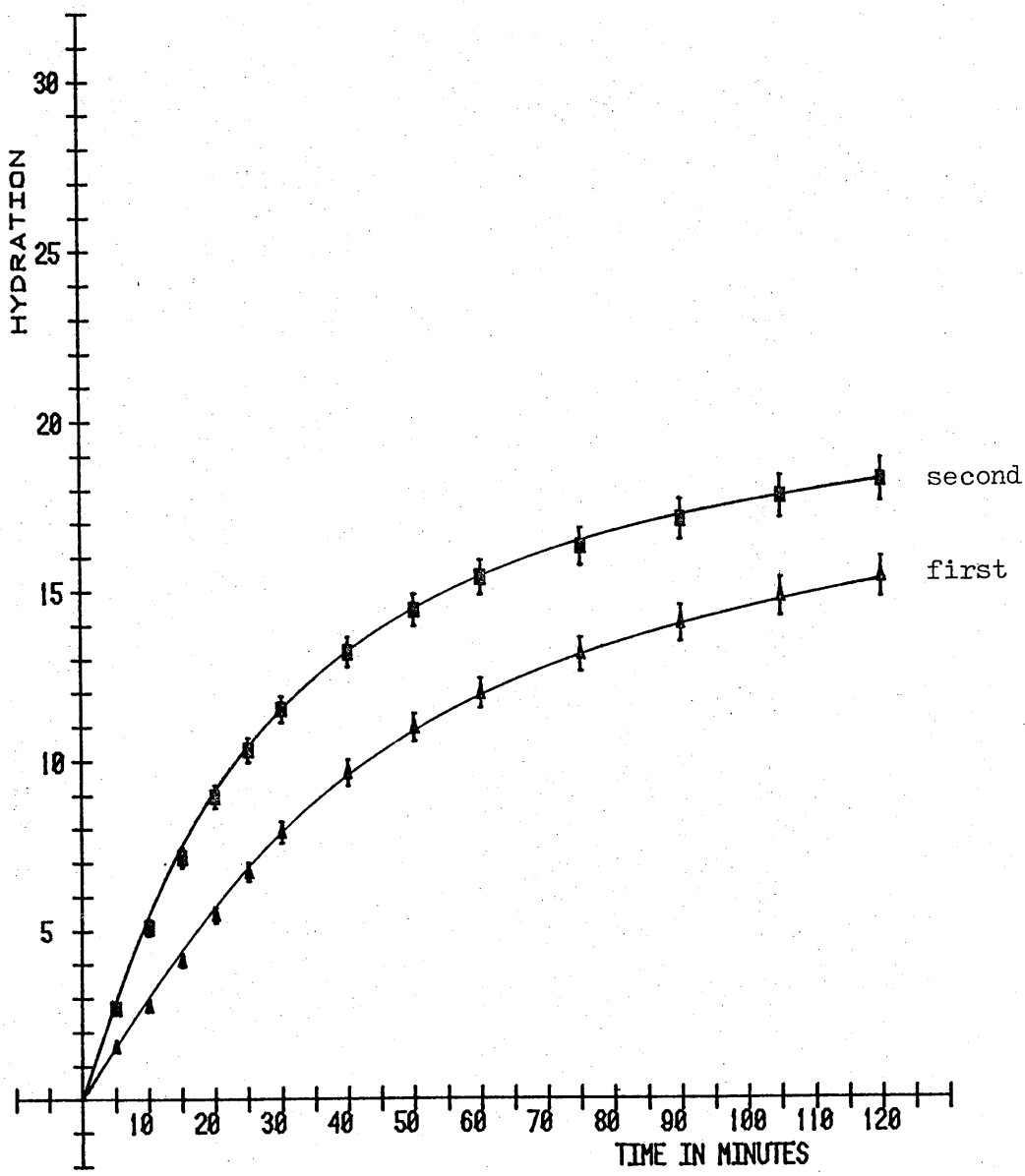

Figure 4.3

First swellings of fresh and pre-dried cornea in distilled water.

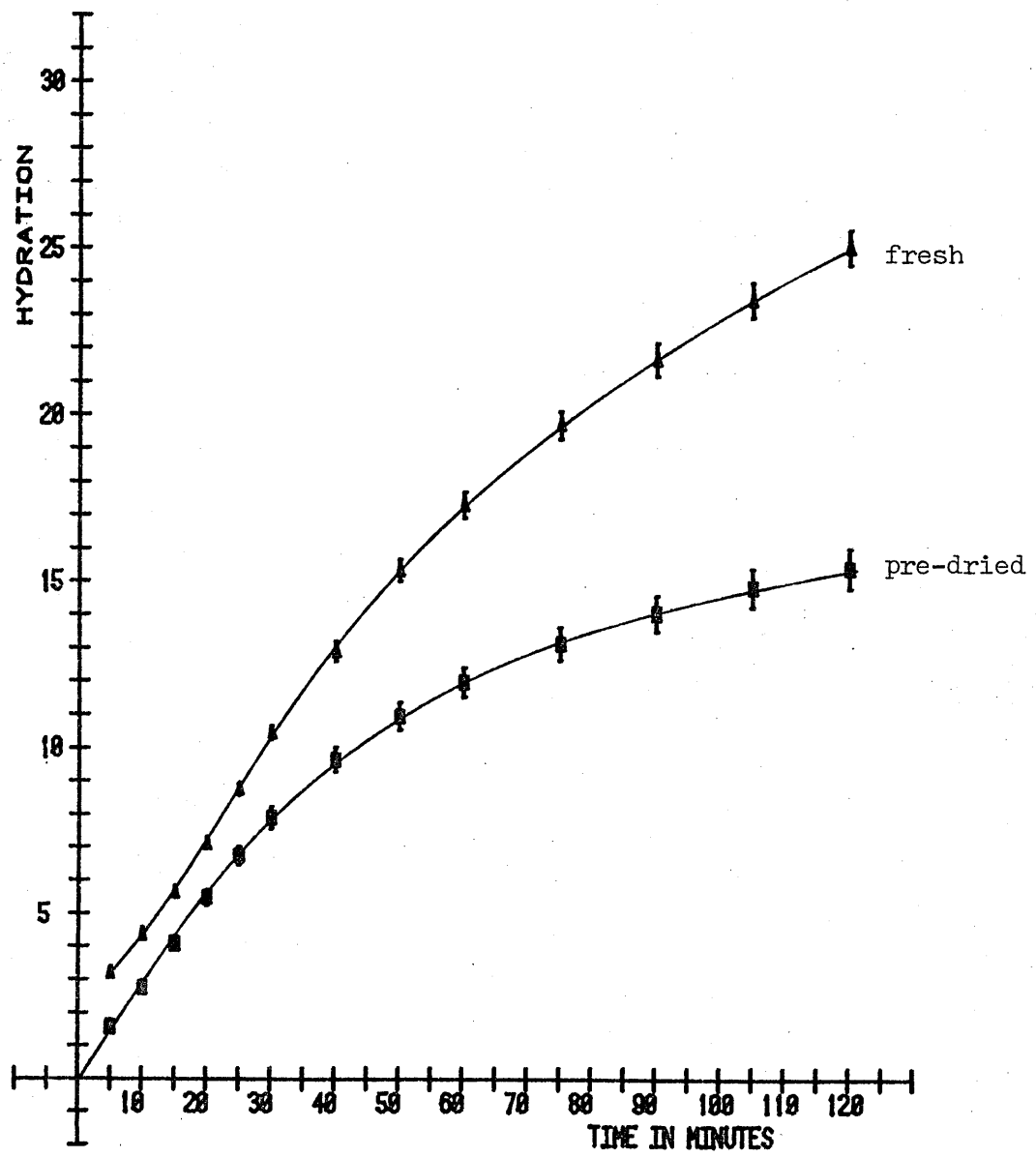

pre-dried) swelling rates. The numerical results of these tests are given in table 4.3.

Significance level: for all experiments $\alpha = 0.01$.

Sampling distribution: for all experiments is Student's t distribution with df = $n_1 + n_2 - 2$, or 25 + 25 - 2 = 48.

For a significance level of 0.01 and a one-tailed test, the critical region is $t_{0.01} = 2.423$. Since, in each case H_1 predicts that the slopes of the second swellings or fresh ($\bar{X}_1$) will be greater than those of the first swellings or pre-dried ($\bar{X}_2$), the critical region consists of all values of $t \geq 2.423$.

For the initial slopes of first and second swellings and for the final slope of fresh and pre-dried first swellings, the obtained values of t fall within the critical region so we reject the null hypotheses. For the other experiments the obtained values of t fall outside the critical region so we accept the null hypotheses.

The results of the statistical test indicate that the initial swelling rates of second swellings of both fresh and pre-dried cornea are significantly greater than those of the first swellings. The final rates do not show this property. For the comparison between fresh and pre-dried first swellings the reverse is true with the significant difference occurring in the final swelling rates.

4.1.2 Extracted Cornea.

Tables 4.4 and 4.5 contain data on swelling of extracted cornea

Table 4.3a - initial and final rates of hydration for first and second swellings of fresh and pre-dried cornea, with t values.

	second swelling		first swelling		t
	slope($\bar{X}_1$)	s.e.($S_{\bar{x}_1}$)	slope($\bar{X}_2$)	s.e.($S_{\bar{x}_2}$)	
Fresh-initial rate hydn.	0.4184	0.0265	0.2909	0.0109	4.450
Dried-initial rate hydn.	0.3509	0.0228	0.2569	0.0033	4.080
Fresh-final rate hydn.	0.0965	0.0029	0.1192	0.0037	-4.829
Dried-final rate hydn.	0.0439	0.0033	0.0506	0.0034	-1.414

Table 4.3b - initial and final rates of hydration for first swellings of fresh and pre-dried cornea, with t values.

	fresh		pre-dried		t
	slope($\bar{X}_1$)	s.e.($S_{\bar{x}_1}$)	slope($\bar{X}_2$)	s.e.($S_{\bar{x}_2}$)	
1st swelling initial rate.	0.2909	0.0109	0.3509	0.0228	-2.374
1st swelling final rate.	0.1192	0.0037	0.0506	0.0034	13.652

in distilled water. Figure 4.4 shows the swelling curves of cornea discs dried after extraction with chondroitinase and 0.15M sodium chloride solutions. Chondroitinase would only be expected to extract the chondroitin sulphate which is less than half the total glycosaminoglycan content of the cornea (Payrau,Pouliquin,Faure, and Offret,1967). We should therefore expect a finite residual swelling pressure, but less than that in untreated cornea.

The effect of extraction with 0.15M sodium chloride is much more marked, and the specimens do not even reach physiological hydration in the 120 minute experimental period. Dische et al (1978) shows that extraction with this sodium chloride solution should extract a large proportion of both glycosaminoglycans. However, a faster method (Hassel et al, 1979) is to use 4M guanadine hydrochloride. Figure 4.5 shows the effect of this extraction on the subsequent swelling of the cornea.

Cetyl pyridinium chloride precipitates the glycosaminoglycans in situ (Hedbys,1961) and the effect of treating the cornea with this solution is very similar to that of the guanadine hydrochloride extraction, as can be seen in figure 4.5.

4.1.3 Further Swelling of Fresh and Pre-dried Cornea.

Table 4.6 and figure 4.6 show the effect of further swelling of fresh and pre-dried cornea. The third swellings show the same pattern of swelling as the first and second, ie. pre-dried swelling more slowly and to a lower 120 minute-hydration than fresh. However, the swelling rate of both specimens this third time is considerably less than the respective first or second swellings, (compare with figures 4.1 and 4.2), and the cornea discs were showing distinct signs of mechanical damage

Table 4·4 - Swelling of chondroitinase and sodium chloride extracted cornea in distilled water.

Time/ mins.	Hydration		
	chondroitinase extracted	sodium chloride extracted	control
5	3.09 ± 0.11	1.04 ± 0.06	5.03 ± 0.14
10	4.91 ± 0.15	1.25 ± 0.04	7.97 ± 0.18
15	6.52 ± 0.17	1.34 ± 0.04	10.60 ± 0.19
20	7.87 ± 0.20	1.38 ± 0.05	12.70 ± 0.25
25	9.06 ± 0.24	1.43 ± 0.05	14.71 ± 0.31
30	10.04 ± 0.26	1.44 ± 0.04	16.36 ± 0.35
40	11.72 ± 0.38	1.54 ± 0.05	19.31 ± 0.43
50	12.73 ± 0.41	1.57 ± 0.04	21.55 ± 0.47
60	13.72 ± 0.45	1.62 ± 0.05	23.68 ± 0.57
75	15.02 ± 0.56	1.69 ± 0.06	26.28 ± 0.65
90	15.99 ± 0.59	1.77 ± 0.07	28.28 ± 0.87
105	16.84 ± 0.66	1.84 ± 0.07	29.82 ± 0.87
120	17.52 ± 0.70	1.90 ± 0.07	31.22 ± 0.96

(± s.e.m., n~10)

Table 4·5 - Swelling of guanidine hydrochloride extracted and cetyl pyridinium chloride treated cornea in distilled water.

Time/ mins.	Hydration		
	guanidine HCl extracted	C.P.C. treated	control
5	0.47 ± 0.04	0.83 ± 0.08	3.01 ± 0.13
10	0.71 ± 0.04	1.19 ± 0.14	4.87 ± 0.23
15	0.91 ± 0.04	1.51 ± 0.20	6.27 ± 0.30
20	1.12 ± 0.06	1.72 ± 0.26	7.36 ± 0.36
25	1.29 ± 0.04	1.90 ± 0.33	8.50 ± 0.44
30	1.44 ± 0.05	2.09 ± 0.39	9.42 ± 0.48
40	1.71 ± 0.06	2.41 ± 0.53	11.14 ± 0.64
50	1.78 ± 0.15	2.65 ± 0.65	12.57 ± 0.77
60	2.15 ± 0.07	2.84 ± 0.71	13.92 ± 0.89
75	2.48 ± 0.09	3.04 ± 0.84	15.65 ± 1.07
90	2.78 ± 0.10	3.21 ± 0.91	16.97 ± 1.21
105	3.02 ± 0.10	3.32 ± 0.96	18.31 ± 1.33
120	3.32 ± 0.09	3.39 ± 1.03	19.57 ± 1.41

(± s.e.m., n~10)

Figure 4.4

Swelling of sodium chloride and chondroitinase extracted cornea in distilled water.

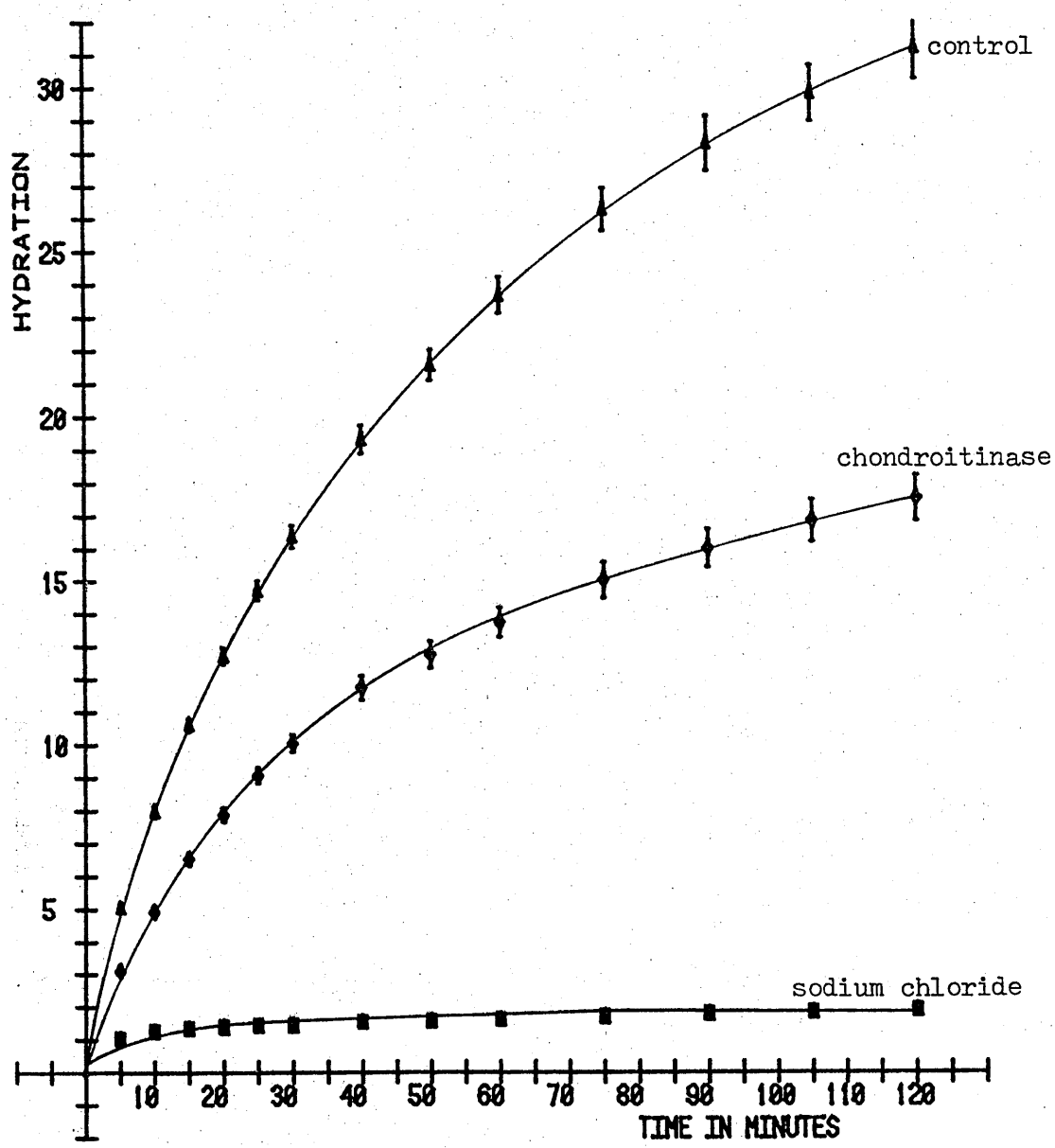

Figure 4·5

Swelling of guanidine hydrochloride and cetyl pyridinium chloride extracted cornea in distilled water.

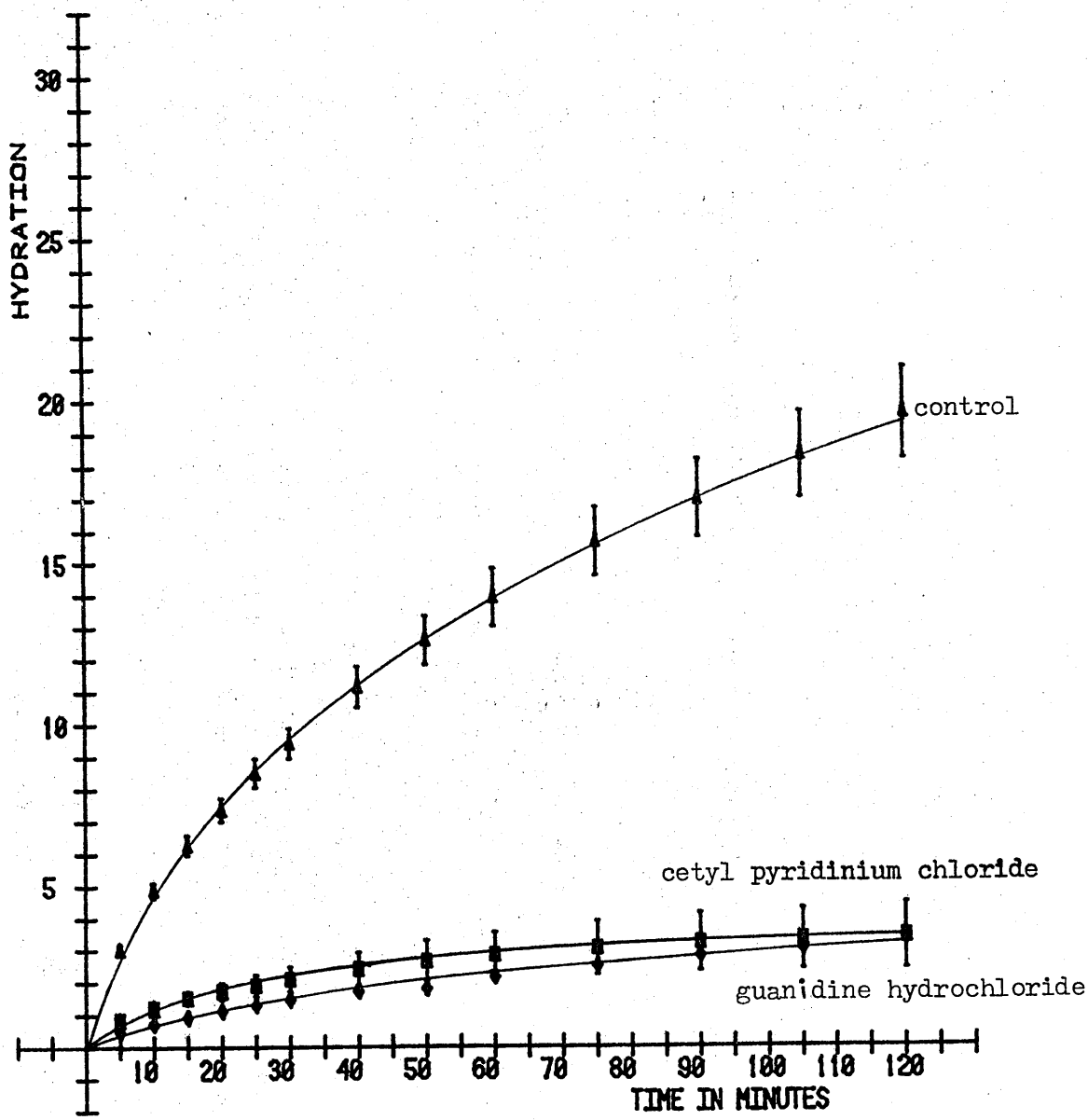

Table 4·6 - Third and fourth swellings of fresh and pre-dried cornea in distilled water.

Time/ mins.	Hydration		
	Fresh (3rd)	Fresh (4th)	Pre-dried (3rd)
5	3.83 ± 0.19	3.39 ± 0.13	2.13 ± 0.09
10	6.02 ± 0.26	5.56 ± 0.26	3.59 ± 0.14
15	7.73 ± 0.34	7.23 ± 0.34	4.90 ± 0.18
20	9.09 ± 0.44	8.63 ± 0.41	6.07 ± 0.22
25	10.20 ± 0.52	9.84 ± 0.49	6.94 ± 0.25
30	11.23 ± 0.61	11.10 ± 0.64	7.76 ± 0.29
40	12.89 ± 0.78	12.74 ± 0.70	8.93 ± 0.33
50	14.27 ± 0.93	14.12 ± 0.84	9.81 ± 0.37
60	15.30 ± 1.02	15.27 ± 0.95	10.43 ± 0.40
75	16.61 ± 1.18	16.72 ± 1.14	11.15 ± 0.43
90	17.66 ± 1.31	17.89 ± 1.30	11.67 ± 0.46
105	18.51 ± 1.41	18.73 ± 1.42	12.07 ± 0.48
120	19.23 ± 1.49	19.62 ± 1.57	12.39 ± 0.50

(± s.e.m., n~25)

Figure 4·6

Third and fourth swellings of fresh and pre-dried cornea in distilled water.

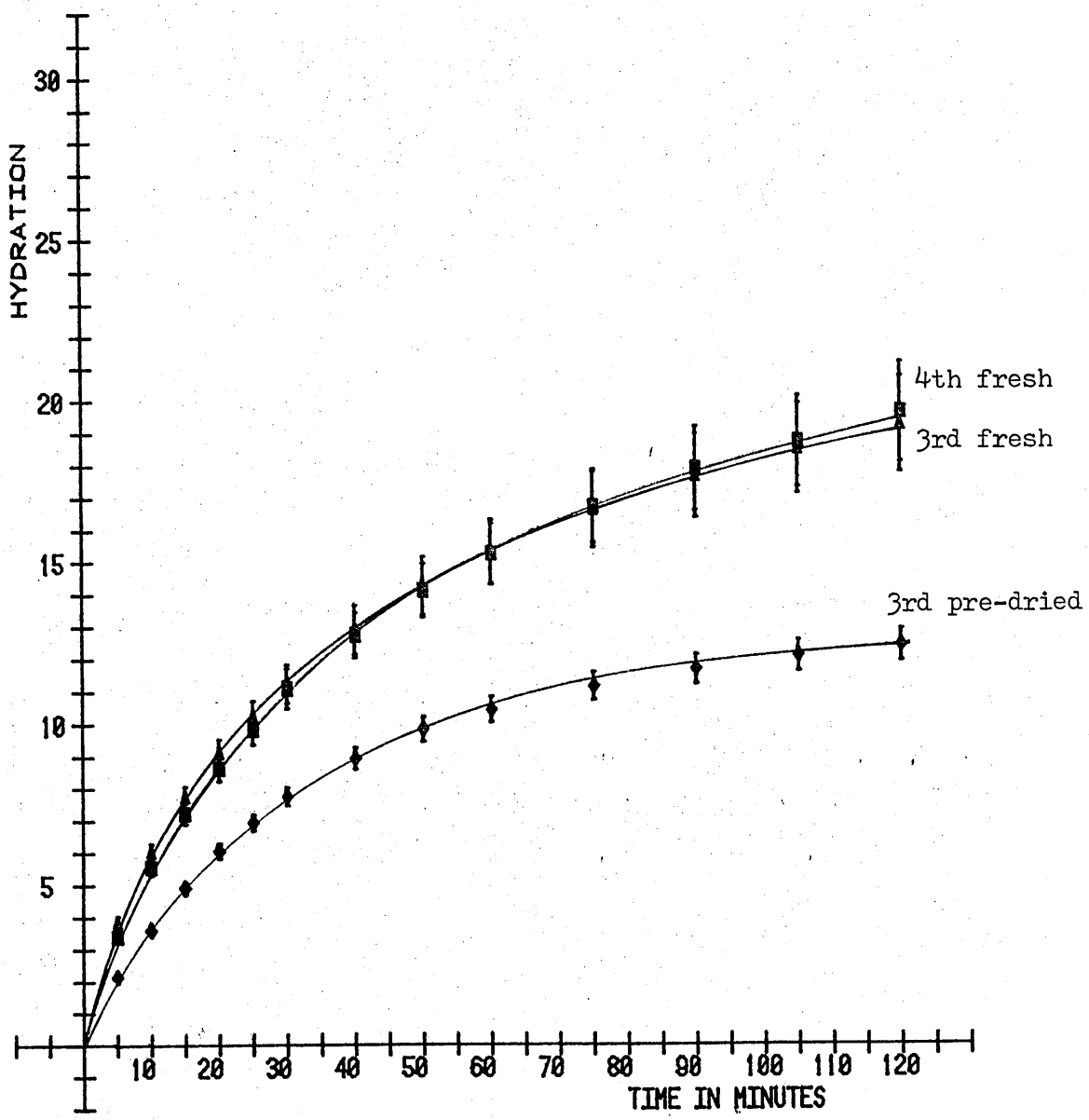

by this stage. A fourth swelling of fresh cornea produced a curve not significantly different from the third swelling curve.

4.1.4 General Observations.

Apart from the differences in swelling, fresh and pre-dried cornea differed in appearance and texture. The pre-dried cornea, when swollen, were firmer than the fresh at a similar hydration, and were less likely to disintegrate on handling. The swollen fresh cornea displayed a tendency to slip along the planes of the lammellae, and on drying did not always return to their original shape. This was not observed for the pre-dried specimens. This same problem was encountered with the extracted cornea discs (for which fresh cornea were used), but as this was also the case with the controls, any differences in swelling caused by mechanical damage would be about equal for both.

During extraction with sodium chloride and enzyme solutions, the specimens had the usual appearance of swollen cornea. However, the less gentle extractions effected with guanidine hydrochloride solution produced a contraction along the long axis of the fibrils, as demonstrated by the considerable reduction in diameter of the discs. This suggests that the collagen of the fibrils was being at least partly denatured. Washing in distilled water did not return the specimen to its original size. In cetyl pyridinium chloride solution the specimens did not become very swollen and the texture of the tissue was rather rubbery - as might be expected when the glycosaminoglycans become insoluble.

4.2 X-ray Diffraction.

4.2.1 First Order Interfibrillar Spacing.

Tables 4.7 and 4.8 give the data obtained for the first order interfibrillar spacing of fresh and pre-dried cornea respectively. These data include those obtained from the GX13 generator as well as those from the synchrotron X-ray beam; both from discs of cornea and from strips. Figures 4.7, 4.8 and 4.9 are examples of the films obtained using the synchrotron X-ray source. Figure 4.10 was obtained on the GX13 generator and figures 4.11 and 4.12 are examples of detector traces obtained using the synchrotron X-ray source and the position sensitive detector. Figures 4.7 and 4.8 demonstrate the effect of passing the X-rays at right-angles to the visual axis, to separate the collagen reflections and the interfibrillar reflections, (see section 3.2.2 and figure 3.1) and the different focusing of the beam in the horizontal and vertical directions. Figure 4.9 also shows an oriented pattern, and was obtained in the same way. To obtain the required reflection (interfibrillar) along the better-focused axis of the beam the specimen was mounted horizontally. Due to the short exposure time used to obtain the first order reflection, no collagen reflections are visible on this film, however, the shorter camera and longer exposure used for figures 4.7 and 4.8 produce both collagen reflections (sharp) and interfibrillar reflections (very diffuse). These weak interfibrillar reflections (most evident in the horizontally mounted specimen) arise from the packing of the fibrils rather than from the collagen structure, which gives sharper reflections along the other axis of the film.

The spread of the data makes it impossible to detect any difference in the interfibrillar spacing between strips viewed at right-angles to

Table 4.7 - interfibrillar spacing change for fresh cornea.

Hydration	d^2/nm^2
0.4	1911
0.7	1911
0.8	2107
1.0	2334
1.0	1729
1.3	2334
1.5	3292
1.6	2601
1.9	2601
1.9	2601
1.9	2302
1.9	2601
2.1	3118
2.4	2916
2.7	2601
2.9	3363

Hydration	d^2/nm^2
3.0	2916
3.1	2701
3.7	3839
4.3	3366
4.9	4424
5.6	5877
6.2	4802
6.6	5321
6.8	4842
7.1	5877
7.4	5154
7.5	6523
7.7	5498
8.2	4995
8.8	5877

Table 4.8 - interfibrillar spacing change for pre-dried cornea.

Hydration	d^2/nm^2
0.3	2141
0.5	1126
0.5	2141
0.5	1316
0.5	1558
0.6	2297
0.7	2001
0.9	1759
0.9	1654
1.1	2141
1.3	1654
1.4	2297
1.6	2141
1.6	1874
1.7	1874
1.9	2001
2.0	1874
2.5	1891
2.6	2141
2.7	2470
3.2	2141

Hydration	d^2/nm^2
3.4	1654
4.7	2583
6.3	3118
6.4	3404
6.5	3363
7.0	3542
7.7	3839
7.8	3278
8.4	3542
8.8	4297
9.2	4058
10.0	4424
10.3	4175
11.3	4424
11.3	4842
12.0	4842
12.3	4842
13.7	4995
14.4	5322
14.5	4084

Higher order interfibrillar and collagen reflections.

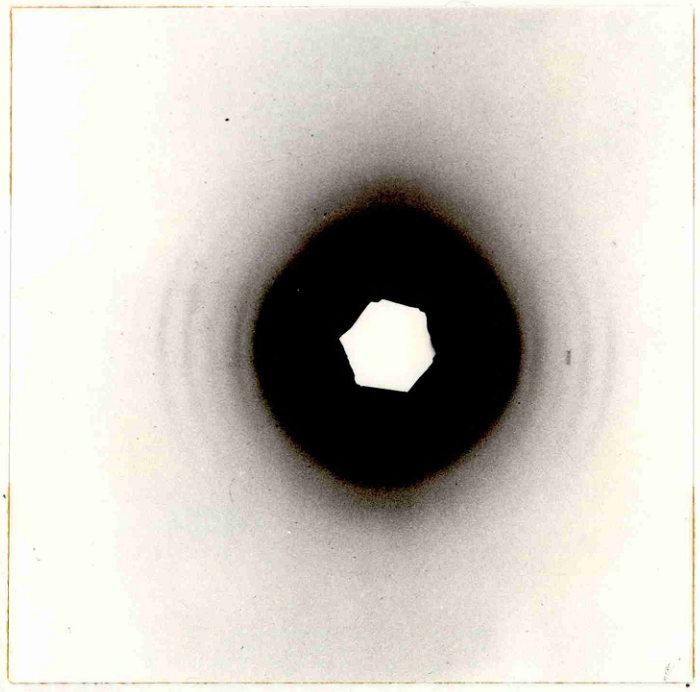

Figure 4.7 - Strip of fresh cornea mounted horizontally in the beam, with X-rays passing at right angles to the visual axis. Interfibrillar reflections appear in the vertical direction on the film.

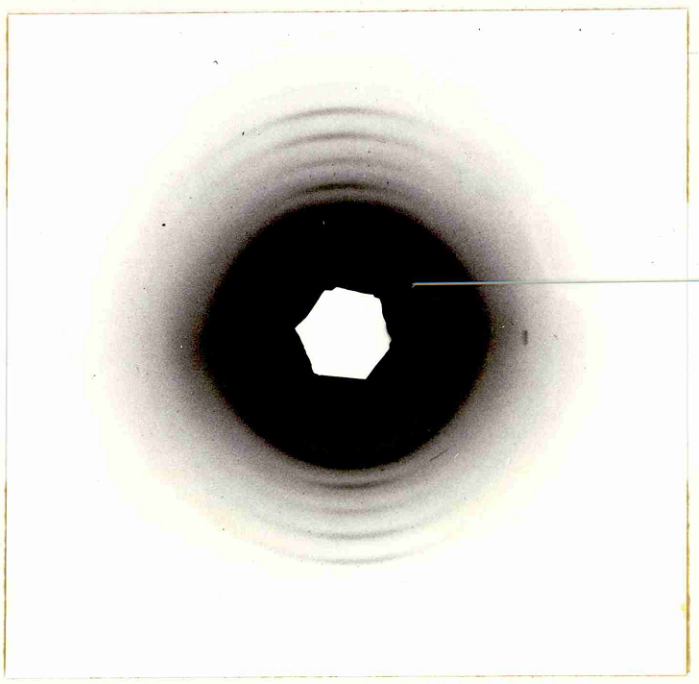

Figure 4.8 - same specimen as above, but mounted vertically in the beam so that the collagen reflections appear in the vertical direction on the film.

First order interfibrillar reflections.

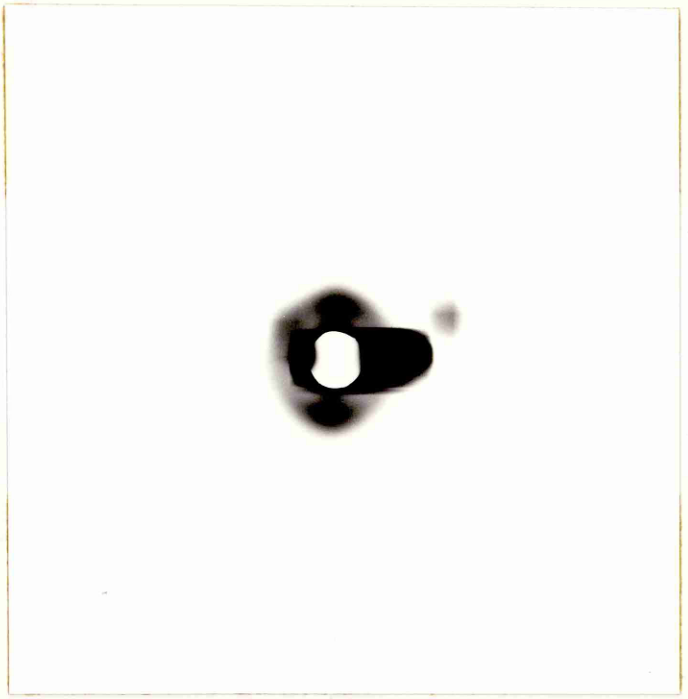

Figure 4.9 - Strip of fresh cornea mounted horizontally in the beam with X-rays passing at right angles to the visual axis. Interfibrillar reflection appears mainly in the vertical direction on the film.

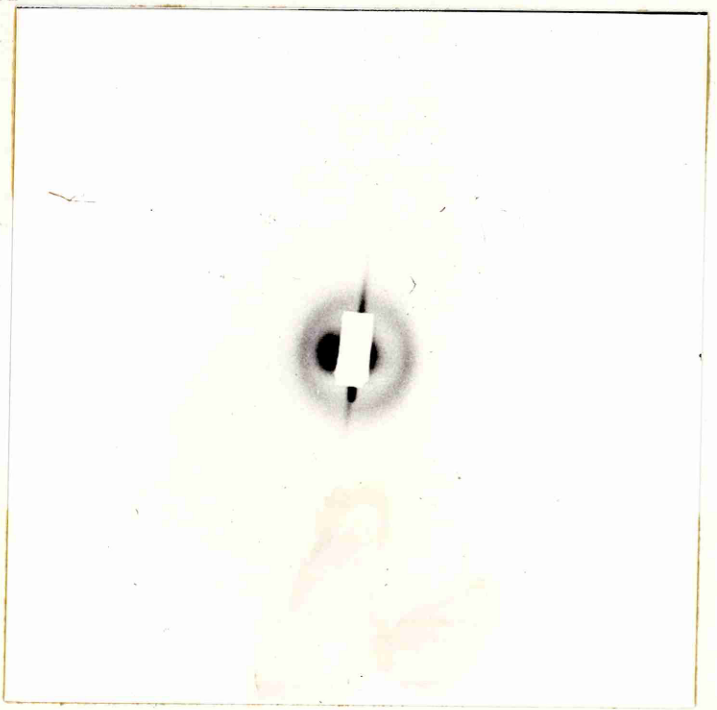

Figure 4.10 - Disc of cornea at hydration 4.3. Picture taken on the GX 13 monochromator camera, showing the first order interfibrillar spacing.

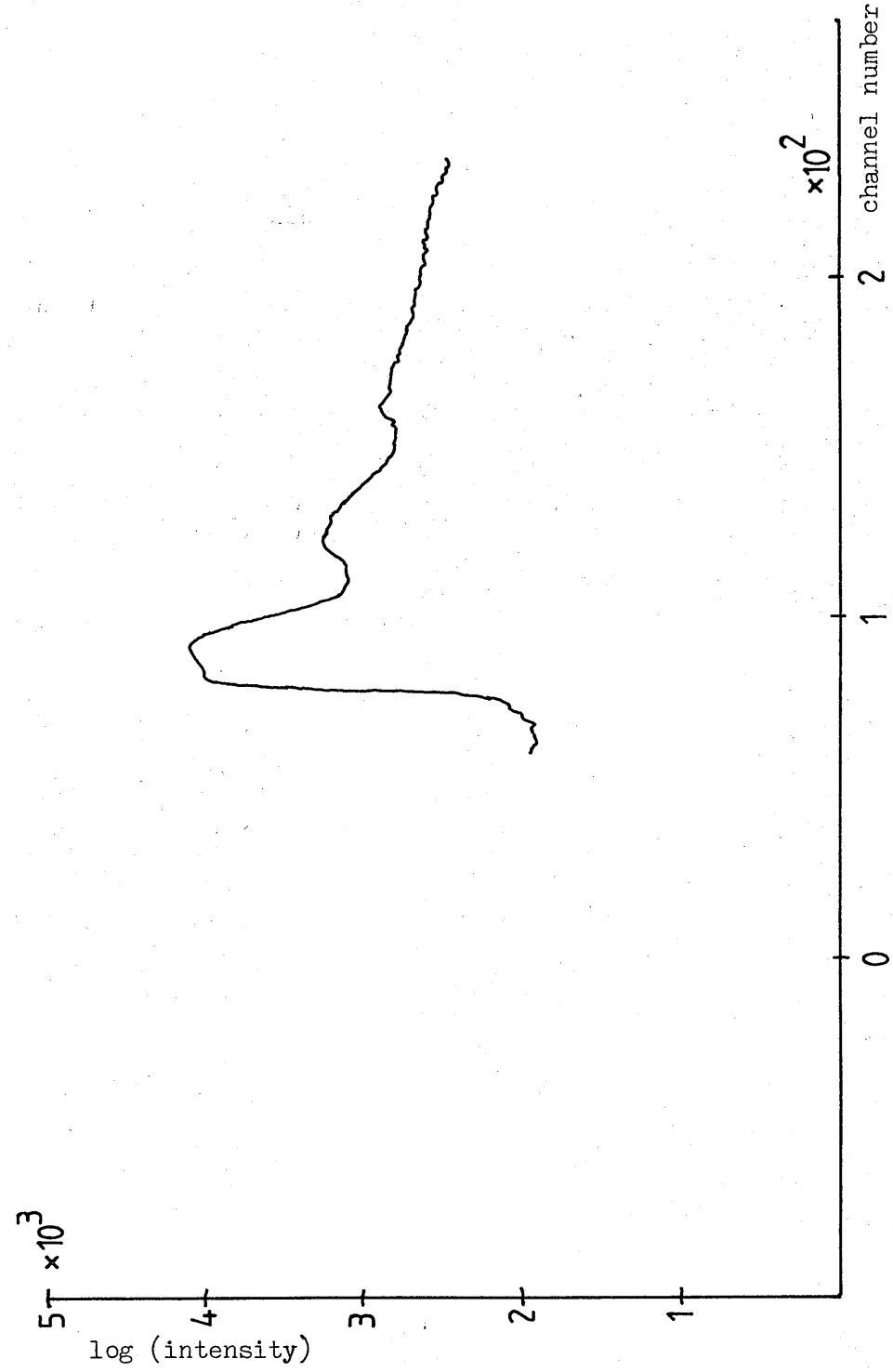

Figure 4·11 - Detector trace from pre-dried disc of cornea, rehydrated to H = 1.31

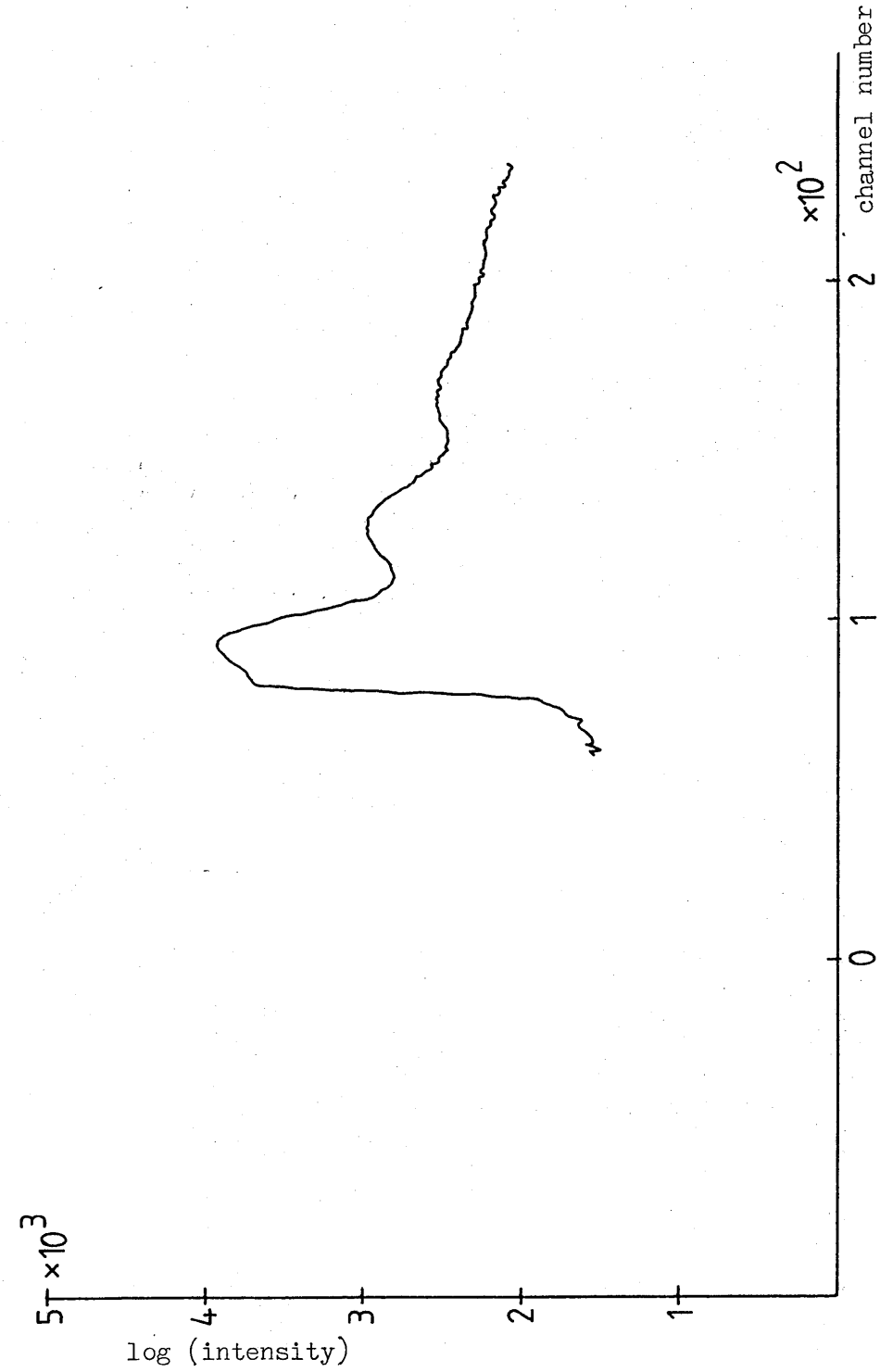

Figure 4·12 - Detector trace from fresh strip of cornea at hydration 0.8.
(X-rays parallel to visual axis)

Figure 4.13

Variation of (interfibrillar spacing)^2 with hydration for fresh and pre-dried cornea.

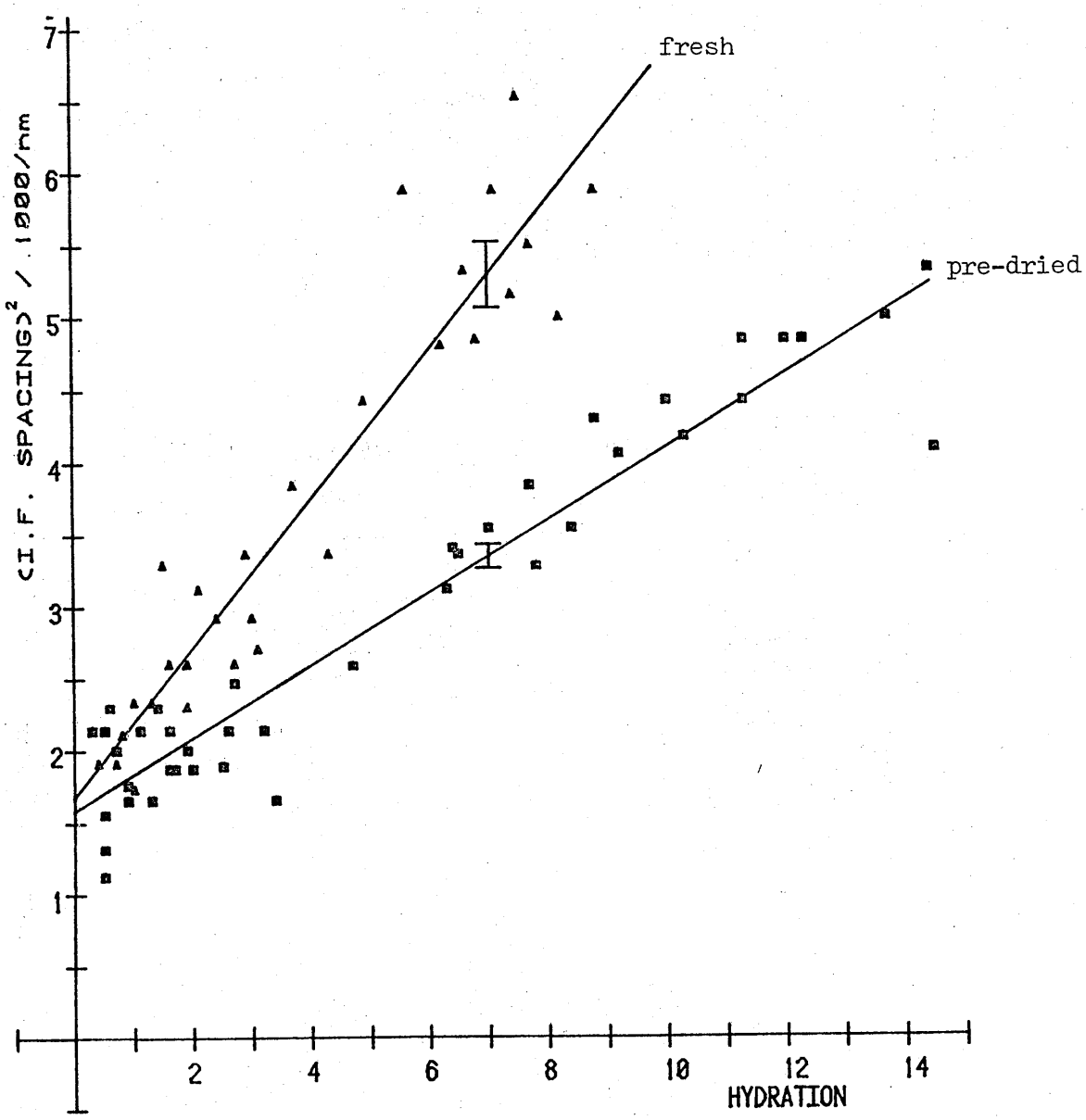

the visual axis and those viewed parallel to it. However, the difference between the spacings observed for fresh and pre-dried specimens is significant, as can be seen from the graph shown in figure 4.13. At hydrations greater than about 3.5 (physiological) the pre-dried cornea has a significantly smaller interfibrillar spacing than does the fresh, for any given hydration. The most obvious way to explain this is to assume the formation of 'lakes' (as proposed by Benedek,1971) - at least in pre-dried cornea.

4.2.2 Distribution of Water in the Corneal Stroma.

Goodfellow et al (1978) give a model for corneal hydration in terms of the interfibrillar spacings. They have assumed that the fibril radius is constant at all hydrations in excess of physiological, as appears to be the case in other collagenous tissue. However, more recent wide-angle X-ray diffraction studies indicate that the radii of the corneal fibrils continue to increase well beyond physiological hydration. (Cooke, 1980, unpublished results). In the model below, a constant fibril radius is not assumed, although certain assumptions have been made about the arrangement of fibrils in the dry cornea.

If we assume that, in the dry state, the collagen fibrils in the cornea are hexagonally close packed and the whole of the unit cell is filled with fibrils and other macromolecular material, then the cross-sectional area of one unit cell corresponds to the area of an equilateral parallelogram, where d_o is the length of one side of the parallelogram , and also the diameter of the fibril. We make no distinction between the collagen of the fibrils and the other dry material such as proteoglycan, and assume that this material has the same properties of hydration as does collagen.

We can now obtain an expression for the volume of the unit cell in terms of d_o (the 1,0 reflection at zero hydration), and equate it to the volume of dry material present in one unit cell at any hydration, in terms of R_o (the dry fibril radius):

$$\left.\begin{array}{l}\text{Volume of unit cell}\\ \text{in dry cornea}\end{array}\right\} = \frac{\sqrt{3}}{2} d_o^2 \, l$$

where l is the length of the fibril.

but $d_o = 2 R_o$, and $d_o^2 = 4 R_o^2$

$$\left.\begin{array}{l}\text{Volume of dry material}\\ \text{in one unit cell}\end{array}\right\} = 2\sqrt{3} \, R_o^2 \, l \qquad (1)$$

When water enters the cornea, it goes both into and between the fibrils. A certain volume of water will be taken up by the protein and other material without causing an increase in volume. (Goodfellow *et al*, 1978 and Maurice and Riley, 1970). We can define G as the volume of water absorbed by one volume of dry material before a total volume change takes place, following Goodfellow *et al*, 1978 . We then obtain an expression for the volume of water in one unit cell for any hydration, in terms of d (the 1,0 spacing as determined by X-ray diffraction) and R_o.

$$\left.\begin{array}{l}\text{Volume water taken up}\\ \text{by proteins etc.}\end{array}\right\} = 2\sqrt{3} \, R_o^2 \, l \, G$$

$$\left.\begin{array}{l}\text{Total volume of one}\\ \text{unit cell}\end{array}\right\} = \frac{\sqrt{3}}{2} d^2 \, l$$

$$\left.\begin{array}{l}\text{Volume water in one}\\ \text{unit cell}\end{array}\right\} = \frac{\sqrt{3}}{2} d^2 \, l + 2\sqrt{3} \, R_o^2 \, l \, G - 2\sqrt{3} \, R_o^2 \, l$$

$$= \frac{\sqrt{3}}{2} d^2 \, l + 2\sqrt{3} \, R_o^2 (G - 1) l \qquad (2)$$

But hydration is defined in terms of masses, (H = mass water/dry mass) therefore if we let ρ_w = density of water, and ρ_d = density of dry material (average), then:

$$\left.\begin{array}{l}\text{Mass water in one}\\ \text{unit cell}\end{array}\right\} = \rho_w \left[\frac{\sqrt{3}}{2} d^2 \, l + 2\sqrt{3} \, R_o^2 (G - 1) l\right] \qquad (3)$$

$$\left.\begin{array}{l}\text{Dry mass in one}\\ \text{unit cell}\end{array}\right\} = \rho_d\left[2\sqrt{3}\ R_o^2\ l\right] \qquad (4)$$

$$\text{Hydration} = \frac{\text{mass water}}{\text{dry mass}} = \frac{\text{equation (3)}}{\text{equation (4)}}$$

$$\text{Hydration} = \frac{\rho_w}{\rho_d}\left[\frac{d^2}{4R_o^2} + G - 1\right] \qquad (5)$$

Equation (5) assumes that all the water entering the cornea is distributed evenly in and between the fibrils. If, in fact, there are areas of the hydrated cornea devoid of fibrils, then there will be a discrepancy between this calculated hydration (H_c) and the experimentally determined hydration (H_m). The percentage water present as 'lakes' can be calculated as follows:

$$\left.\begin{array}{l}\text{Percentage lake}\\ \text{water}\end{array}\right\} = \left[\frac{H_m - H_c}{H_m}\right] \times 100 \qquad (6)$$

In order to calculate the percentage lakes predicted by this model, we need values for the densities of water (ρ_w) and dry material (ρ_d) and for the volume hydration (G) of the dry material.

We can assume the density of water to be 1, and use the value of 1.4 for the density of collagen (Hedbys and Mishima, 1966) as an estimate of the average density of the dry material. A value of 0.3 for the volume hydration of the fibrils was found by Maurice and Riley (1970) using birefringence and diffusion techniques, and we can use this value in our calculation. A range of values for the fibril radius have been obtained from electron microscopy work, however, it would seem that for our model, a more reasonable estimate of the dry fibril radius can be obtained from the graphs in figure 4.13. The intercepts and standard errors for the two lines were obtained from the curve fitting computer program, and the mean of these two values calculated:

for fresh cornea: intercept = 1677 ± 150 nm^2

for pre-dried cornea: intercept = 1585 ± 84 nm^2

mean intercept = 1607 ± 39 nm^2 (mean $\pm$ s.e.)

This represents the square of the interfibrillar spacing at hydration zero. Therefore, from this we can obtain a value of 20 ± 0.5 nm for the dry fibril radius.

Appendix I contains the results obtained from the interfibrillar spacings and hydrations already determined (figure 4.13). Because in the model we have assumed that the square of the interfibrillar spacing is directly proportional to the hydration, the values used in the calculations were those produced by fitting a straight line to the experimental data rather than the actual experimental values with their associated errors. Section A of the appendix contains the results for fresh cornea and section B those for pre-dried.

The first columns of the tables give the hydrations as measured by weighing (H_m) and the second the hydrations calculated from the model (H_c from equation (5)). The squares of the interfibrillar spacings (d^2) are given in the third columns and the percentage lake water, calculated from equation (6) in the fourth.

Using the most likely values for the density of collagen, the dry fibril radius and the volume hydration (G), as explained above, we find that, for fresh cornea 14.73% of the water is present as lakes at the lowest hydration measured (H = 0.4), and the percentage increases with increasing hydration. (table A1). Changing the parameters changes the magnitude of the lake water, but not the general trend. In fact, chang-

ing the dry fibril radius has most effect, and reducing it by 1 nm to 19 nm produces a negative value for percentage lake water at the lowest hydration (table A2). Even when the density is reduced to 1.2 the percentage lake water at the lowest hydration is still just positive (tables A3 and A4). A similar small change is observed for different values of G.

Using the same parameters for the pre-dried cornea data gives slightly larger values for the percentage lake water throughout than for fresh cornea. (tables B1 to B4).

4.2.3 Higher Orders of the Interfibrillar Spacing.

The use of the synchrotron x-ray source enabled the detection of weak reflections at greater angles than the first order. These were detected on film as can be seen in figure 4.7 and 4.8. However, they proved very difficult to measure either by eye or by densitometry from the film, but appear as quite distinct peaks on the detector plots. Figures 4.11 and 4.12 are two such detector traces of different specimens showing two outer weak reflections as well as the strong first order reflections. The change in spacing of these peaks is very small and rather irregular over the range of hydrations studied, as can be seen from the raw data given in tables 4.9 and 4.10. The error on these data is difficult to estimate, and is probably quite large, since often the higher order reflections from the collagen backbone were almost coincident with these broad reflections. (see section 3.2) However, even allowing for large errors, these reflections do not change enough with hydration to be higher order reflections of a regular lattice. It is most likely that the fibril transform is mainly responsible for them. Further discussion of this is to be found in Sayers et al (in preparation).

Table 4·9 - Change in position of 2nd and 3rd peaks of X-ray diffraction pattern with hydration. Strips of fresh cornea placed such that X-rays are directed parallel to (frontways) and at right angles to (sideways) the visual axis.

Hydration	2nd peak/channel no.		3rd peak/channel no.	
	sideways	frontways	sideways	frontways
0.1	126	129	166	171
0.8		127		166
1.0		138		177
2.0		113		159
2.2	119		161	
2.6	115	120	159	157
3.0	117	116	158	158
3.1	113	116	154	156
3.3	133		174	
3.7	114	117	156	157
4.4	118	119	157	158
12.7	118	116	155	158
13.6	110	116	155	149
25.9	115		158	

Table 4·10 - Change in position of 2nd and 3rd peaks of X-ray diffraction pattern with hydration. Strips of pre-dried cornea placed such that X-rays are directed parallel to (frontways) and at right angles to (sideways) the visual axis.

Hydration	2nd peak/channel no.		3rd peak/channel no.	
	sideways	frontways	sideways	frontways
0.5	125	135		175
0.9	127		168	
1.4	122	128	160	168
1.6	123	128	166	163
2.5	116		168	159
2.6	120	118	158	155
3.2	120	116	157	153
4.0	118	114	157	153
5.1	115	118	155	154
6.1	116	114	154	153

4.3 Inorganic Ion Analysis.

Tables 4.11 and 4.12 give the figures obtained for the quantities of sodium, potassium and chloride found in the corneal stroma. Table 4.11 gives the actual concentrations of the experimental solutions - both those obtained by swelling 10 cornea discs in $40cm^3$ distilled water, and those prepared by dissolving the residue of the hydrogen peroxide digestion of the swollen cornea in $40cm^3$ distilled water. Table 4.12 gives the concentrations of the ions as mmoles kg^{-1} dry tissue, and the percentage of each ion extracted by the distilled water.

The data given in table 4.12 shows that a large proportion of the total sodium, potassium and chloride is extracted by distilled water. Osmotic pressure measurements of the bathing solutions, taken at the end of the two-hour swelling period give a value of $4mOskg^{-1}$. Subsequent swelling of the same cornea in fresh distilled water gave a zero reading on the osmometer. However, even if all the residual ions were extracted at the second swelling, the resulting osmotic pressure would be too small to register on the instrument used. Both fresh and pre-dried specimens were used, but the results were not significantly different.

It seems likely that very little, if any, of the inorganic ions are immobilised by the macromolecular matrix of the corneal stroma.

Table 4·11 - Inorganic ions extracted from the corneal stroma by swelling ten 9mm discs in distilled water for 2 hours.

	Conc. ions in solutions prepared from 10 discs in 40 cm^3 distilled water/mM		
	$[Na^+]$	$[K^+]$	$[Cl^-]$
Extracted	2.27 ± 0.19	0.30 ± 0.03	2.35 ± 0.12
Residual	0.12 ± 0.01	0.01 ± 0.003	0.10 ± 0.01

Table 4·12 - Inorganic ions extractable by distilled water, expressed as mmoles per kg of dried tissue.

	Ions in corneal stroma, calculated as mmoles kg^{-1} dry tissue.		
	$[Na^+]$	$[K^+]$	$[Cl^-]$
Extractable	757 ± 64	100 ± 10	783 ± 40
Non-extractable	40 ± 3	3.3 ± 0.7	33 ± 3
percent extr'd.	95%	97%	96%

4.4 Change in pH of bathing solution.

Figure 4.14 shows the change in pH of $40cm^3$ of bathing solution when ten 9mm cornea discs are swollen for two hours. The lower curve gives a plot of pH against time for a bathing solution of distilled water, and the upper curve for a bathing solution of starting pH$\sim$8, (adjusted with sodium hydroxide solution). The data for these two graphs, together with the actual hydrogen ion concentrations, are given in tables 4.13 and 4.14.

At the end of the 2 hour swelling period the bathing solution from the distilled water experiment was found to have an osmotic pressure of 4 $mOskg^{-1}$. This value confirms that found for the bathing solutions obtained during the analysis of extractable inorganic ions (section 4.3), and also the 4 ± 1 $mOskg^{-1}$ found by measuring the osmotic pressure of the bathing solutions at the end of the swelling experiments on fresh and pre-dried cornea discs.(1 disc in $4cm^3$ distilled water). This value was found for first swellings only; second and subsequent swellings produced a bathing solution of zero osmotic pressure. (but see section 4.3).

From table 4.11 in the previous section, we see that the total ions extracted, measured by flame photometry, produce a bathing solution that is 4.9mM in concentration. At these very low concentrations we can approximate osmolality to molarity of total ions, and conclude that the osmotic pressure observed is due to extracted inorganic ions. The rise in pH observed when the cornea swells suggests that cations from the stroma are being exchanged for hydrogen ions from the bathing solution. However, a simple calculation shows that the proportion of cations involved in this ion exchange is very small compared with the total ions extracted:

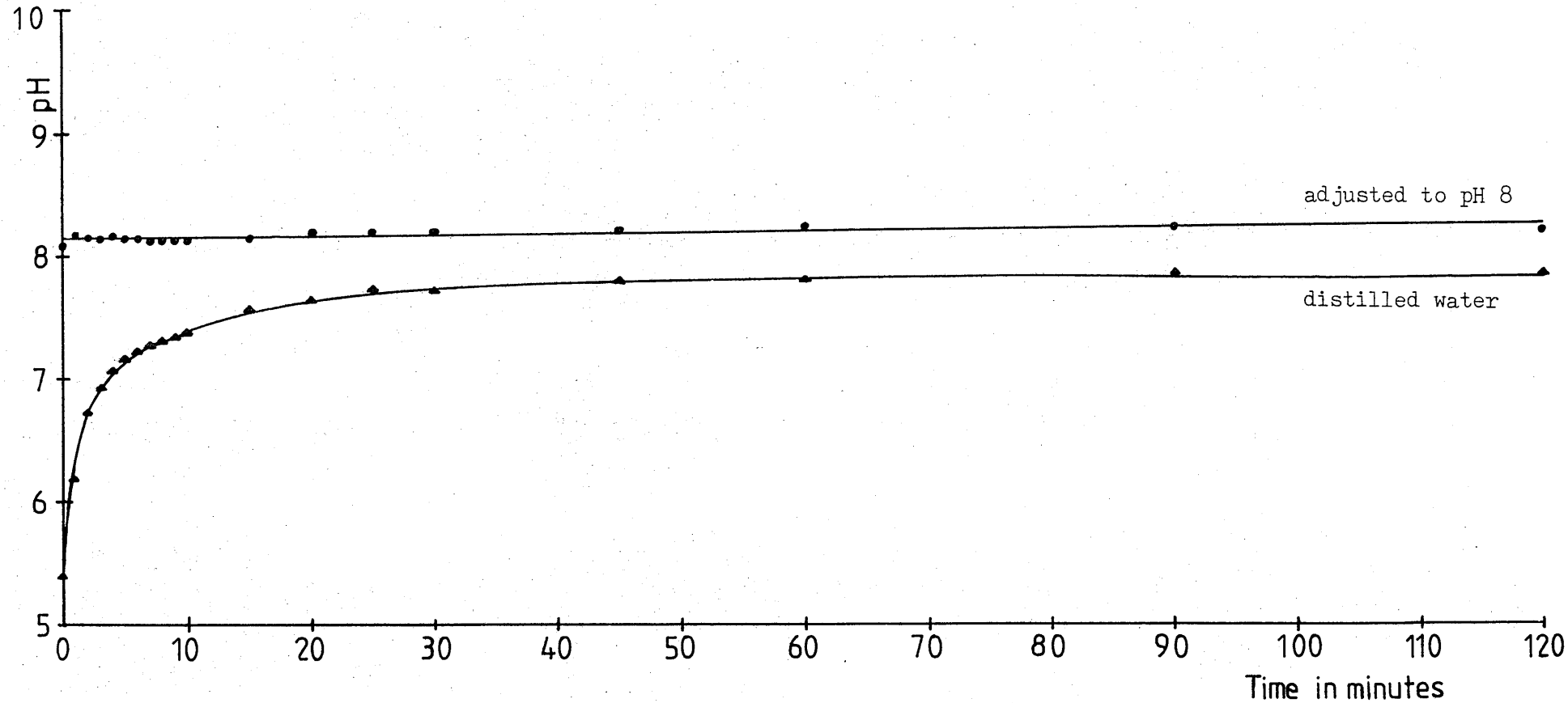

Figure 4·14 - Change of pH of bathing solution when cornea swells.

Change in pH of bathing solution when cornea swells.

Table 4·13 - bathing solution distilled water.

Time/ mins.	pH	$[H^+]$/mM
0	5.40	3.98×10^{-3}
1	6.20	6.31×10^{-4}
2	6.75	1.78×10^{-4}
3	6.95	1.12×10^{-4}
4	7.08	8.32×10^{-5}
5	7.17	6.76×10^{-5}
6	7.23	5.89×10^{-5}
7	7.26	5.50×10^{-5}
8	7.32	4.79×10^{-5}
9	7.34	4.57×10^{-5}
10	7.38	4.17×10^{-5}
15	7.59	2.57×10^{-5}
20	7.66	2.19×10^{-5}
25	7.73	1.86×10^{-5}
30	7.70	2.00×10^{-5}
45	7.79	1.62×10^{-5}
60	7.81	1.55×10^{-5}
90	7.84	1.45×10^{-5}
120	7.85	1.41×10^{-5}

Table 4·14 - bathing solution adjusted to pH 8 at start.

Time/ mins.	pH	$[H^+]$/mM
0	8.08	8.32×10^{-6}
1	8.18	6.61×10^{-6}
2	8.15	7.08×10^{-6}
3	8.15	7.08×10^{-6}
4	8.16	6.92×10^{-6}
5	8.15	7.08×10^{-6}
6	8.14	7.24×10^{-6}
7	8.13	7.41×10^{-6}
8	8.13	7.41×10^{-6}
9	8.12	7.59×10^{-6}
10	8.13	7.41×10^{-6}
15	8.15	7.08×10^{-6}
20	8.18	6.61×10^{-6}
25	8.18	6.61×10^{-6}
30	8.19	6.46×10^{-6}
45	8.20	6.31×10^{-6}
60	8.23	5.89×10^{-6}
90	8.23	5.89×10^{-6}
120	8.19	6.46×10^{-6}

The experiments to measure the change in pH of the bathing solution and those to determine the extractable inorganic ions both used 10 discs of cornea (9mm in diameter) in $40cm^3$ distilled water. Therefore we can make a direct comparison between the solutions.

For a pH change of 5.40 to 7.85, the change in hydrogen ion concentration is 3.97×10^{-3} mM. The total cations extracted from the cornea contribute 2.6mM to the molarity of the bathing solution. The cations extracted by distilled water are a factor of nearly 10^3 greater than the hydrogen ions taken up by the cornea.

When a bathing solution of starting pH~8 is used, there is effectively no hydrogen ion exchange, suggesting that the natural internal pH of the fluid in the corneal stroma is about 8. As the pH of the bathing solution is reduced, increasing amounts of hydrogen ions will be taken up, and consequently increasing numbers of negatively charged side chains on the macromolecular matrix will be neutralised. This means that the matrix fixed charge will decrease with pH - as the results of the microelectrode measurements in the next section indicate.

4.5 Microelectrode Measurements.

The potential difference that is observed between the inside of the corneal stroma and its bathing solution, arises because of the presence of an overall negative charge on the macromolecular matrix (matrix fixed charge), which is balanced by small diffusable cations. At equilibrium an electrochemical gradient is produced between the inside and the outside of the stroma. The internal concentration of diffusable ions can be calculated:

$$C_i = C_o \times \exp(-RT/ZF \times E) \quad \text{(Nernst equation)}$$

Where:

C_i = internal concentration of the ion.

Z = charge on the ion.

C_o = external concentration of the ion.

E = measured potential difference.

R = Gas constant.

T = absolute temperature.

F = Faraday constant.

A computer program based on the Perrin equation (Perrin and Sayce, 1967) was used to calculate the free external concentrations of each ion, and the internal concentrations calculated from the above equation using association constants given in Sillen and Martell (1964).

The matrix fixed charge can then be calculated as the sum of the internal ion concentrations (taking the charge into account):

$$[Pr^-] = \sum Z_i C_i$$

In applying this theory to cornea, it is necessary to make two basic assumptions. Firstly, since cornea swells almost indefinitely in aqueous solutions, no state of equilibrium can be attained. It is assum-

ed that this has no significant effect because the swelling rate is sufficiently slow that quasi-equilibrium conditions probably apply. Secondly, the measured matrix fixed charge is expected to vary inversely with hydration as the fixed charge is diluted at higher hydrations, and it is assumed that this variation is linear; at least over the range of hydrations encountered for fresh cornea. At very high hydrations the results indicate that this is not so.

The two computer programs used here calculated means and standard errors of matrix fixed charge ($[Pr^-]$) and $[Pr^-]$ x hydration (H) for each experiment, and the weighted mean of $[Pr^-]$ x H for each pH of buffer solution, and plotted this as a graph of $[Pr^-]$ x H against pH. Table 4.15 gives the results obtained for fresh cornea in all-phosphate bathing solutions of various pH's. Table 4.16 gives the results obtained for pre-dried cornea in a phosphate buffer of pH 7.75. Table 4.17 gives the results for sodium chloride extracted cornea and the control in pH 6.8 phosphate bathing solution. Table 4.18 gives the results obtained for fresh cornea in a chloride-containing bathing solution of pH 5.75.

Apart from the sodium chloride extracted and control specimens, all the cornea were at approximately physiological hydration. The variations in hydration were compensated for by multiplying the matrix fixed charge ($[Pr^-]$) by the hydration (H). The relevancy of these values of $[Pr^-]$ x H depend on the linearity of the inverse relationship between $[Pr^-]$ and hydration. If we assume a uniform hydration of the piece of cornea then matrix fixed charge should be inversely proportional to hydration as shown by Goodfellow (1975). However, other work presented in this thesis suggests that in fact the distribution of water in the swollen cornea is not uniform. The matrix fixed charge determinations performed on physiologically hydrated cornea show a large variation

Table 4.15 - Change in $[Pr^-]$ x H with pH of bathing solution for fresh cornea. All phosphate bathing solutions, ionic strength 0.02.

pH of bathing soln.	measured p.d./mV	$[Pr^-]$/mM	Hydration	$[Pr^-]$xH/ mM	mean $[Pr^-]$xH/ mM
2.95	-1.7 ± 0.2	1.7 ± 0.4	3.6 ± 1.0	6 ± 2	13 ± 8
	-5.9 ± 0.7	8.2 ± 1.1	2.4 ± 0.6	20 ± 6	
3.90	-4.0 ± 0.3	6.3 ± 0.5	3.2 ± 0.4	20 ± 3	75 ± 15
	-10.4 ± 0.2	17.1 ± 0.4	3.1 ± 0.7	53 ± 12	
	-12.3 ± 0.4	20.5 ± 0.7	3.5 ± 0.4	72 ± 9	
	-21.7 ± 0.5	39.1 ± 1.1	3.3 ± 0.4	129 ± 16	
	-21.1 ± 0.7	37.9 ± 1.5	2.0 ± 0.6	76 ± 23	
	-21.7 ± 0.8	39.1 ± 1.7	2.5 ± 0.4	98 ± 16	
4.93	-19.2 ± 0.5	34.8 ± 1.0	2.7 ± 0.2	94 ± 8	67 ± 6
	-14.8 ± 0.3	25.9 ± 0.6	2.2 ± 0.2	57 ± 5	
	-20.3 ± 0.3	37.2 ± 0.7	1.9 ± 0.3	71 ± 11	
	-17.9 ± 0.4	32.1 ± 0.9	2.1 ± 0.3	67 ± 10	
	-17.5 ± 0.3	31.2 ± 0.6	1.8 ± 0.3	56 ± 9	
	-17.5 ± 0.4	31.2 ± 0.8	1.7 ± 0.3	53 ± 9	

(± s.e.m, n=20)

Table 4·15 - continued.

pH of bathing soln.	measured p.d./mV	$[Pr^-]$/mM	Hydration	$[Pr^-]xH$/mM	mean $[Pr^-]xH$/mM
5.85	-25.1 ± 0.5	44.7 ± 1.2	2.3 ± 0.3	103 ± 14	97 ± 3
	-23.2 ± 0.4	40.4 ± 0.8	2.3 ± 0.2	93 ± 8	
	-24.5 ± 0.3	43.3 ± 0.7	2.5 ± 0.2	108 ± 9	
	-24.6 ± 0.4	43.5 ± 1.0	2.2 ± 0.2	96 ± 9	
	-23.0 ± 0.4	40.1 ± 0.8	2.3 ± 0.1	92 ± 4	
	-22.4 ± 0.5	38.7 ± 1.1	2.3 ± 0.2	89 ± 8	
6.80	-31.9 ± 0.8	51.9 ± 1.7	2.5 ± 0.4	130 ± 21	110 ± 10
	-32.3 ± 0.6	52.7 ± 1.3	2.6 ± 0.5	137 ± 27	
	-30.8 ± 0.4	49.5 ± 0.8	2.2 ± 0.3	109 ± 10	
	-32.2 ± 0.6	52.6 ± 1.4	2.2 ± 0.4	116 ± 16	
	-30.5 ± 0.4	48.7 ± 0.9	2.2 ± 0.5	107 ± 24	
	-29.6 ± 0.5	46.9 ± 1.2	3.3 ± 0.3	156 ± 15	
	-23.6 ± 0.7	35.4 ± 1.2	2.5 ± 1.0	88 ± 35	
	-19.1 ± 0.6	27.9 ± 1.0	2.8 ± 1.2	78 ± 34	
	-18.9 ± 0.8	27.6 ± 1.2	2.4 ± 0.8	66 ± 22	

(± s.e.m., n=20)

Table 4·15 - continued.

pH of bathing soln.	measured p.d./mV	$[Pr^-]$/mM	Hydration	$[Pr^-]$xH/ mM	mean $[Pr^-]$xH/ mM
	-32.1 ± 1.6	46.4 ± 3.3	2.3 ± 0.6	107 ± 29	
	-43.5 ± 1.0	74.7 ± 2.9	2.6 ± 0.4	194 ± 31	
	-37.8 ± 1.2	59.0 ± 2.9	2.7 ± 0.5	159 ± 36	
	-36.2 ± 0.6	55.2 ± 1.5	2.8 ± 0.5	154 ± 28	
	-29.5 ± 1.0	41.4 ± 1.8	2.9 ± 0.4	120 ± 17	
7.75	-26.7 ± 0.8	36.7 ± 1.4	2.8 ± 0.2	103 ± 8	116 ± 12
	-24.9 ± 1.4	36.1 ± 0.8	2.6 ± 0.7	94 ± 25	
	-22.0 ± 0.5	29.4 ± 0.7	3.0 ± 0.8	88 ± 24	
	-24.1 ± 0.6	32.4 ± 1.0	2.7 ± 0.8	88 ± 26	
	-19.7 ± 1.9	30.4 ± 0.8	2.6 ± 0.7	79 ± 21	
	-21.1 ± 0.8	28.1 ± 1.1	2.7 ± 0.9	76 ± 20	
	-39.9 ± 1.2	67.0 ± 3.4	2.3 ± 0.5	154 ± 34	
	-35.5 ± 0.8	55.8 ± 1.8	2.6 ± 0.4	145 ± 23	
	-37.8 ± 1.0	61.3 ± 2.6	3.0 ± 0.4	184 ± 26	
8.30	-38.9 ± 1.1	64.3 ± 3.0	2.8 ± 0.6	180 ± 39	166 ± 7
	-41.2 ± 1.5	70.6 ± 4.5	2.5 ± 0.5	177 ± 37	
	-37.3 ± 0.6	60.0 ± 1.6	2.6 ± 0.5	156 ± 24	

(± s.e.m., n=20)

Table 4.16 - Change in $[Pr^-]$ x H on pre-drying cornea. Specimens rehydrated in bathing solution to approximately physiological hydration. All phosphate buffer with ionic strength 0.02.

pH of bathing soln.	measured p.d./mV	$[Pr^-]$/mM	Hydration	$[Pr^-]$xH/ mM	mean $[Pr^-]$xH/ mM
7.75	-34.0 ± 0.5	50.3 ± 1.1	3.1 ± 0.7	156 ± 35	178 ± 18
	-34.7 ± 1.0	51.8 ± 2.2	2.6 ± 0.9	135 ± 47	
	-37.5 ± 0.8	58.2 ± 2.0	3.4 ± 0.3	198 ± 19	
	-46.7 ± 0.8	85.1 ± 2.7	2.6 ± 0.4	221 ± 35	

(± s.e.m., n=20)

Table 4·17 - Change in $[Pr^-]$ x H on extraction of fresh cornea with 0.15M sodium chloride solution.

	measured p.d./mV	$[Pr^-]$/mM	Hydration	$[Pr^-]$xH/mM	mean $[Pr^-]$xH/mM
NaCl extracted bathing soln: pH=6.80	-18.4 ± 0.8	26.8 ± 1.3	12.2 ± 1.2	327 ± 36	
	-13.9 ± 0.5	20.1 ± 0.7	12.8 ± 1.8	257 ± 37	219 ± 76
	-15.2 ± 0.8	22.0 ± 1.2	3.3 ± 1.2	73 ± 4	
control bathing soln: pH=6.80	-26.4 ± 0.7	40.4 ± 1.3	5.8 ± 0.3	234 ± 14	
	-13.6 ± 0.5	19.7 ± 0.7	4.3 ± 0.1	85 ± 3	131 ± 52
	-19.2 ± 0.6	28.0 ± 1.0	2.6 ± 0.5	73 ± 20	

(± s.e.m., n=20)

Table 4·18 - Change in $[Pr^-]$ x H on addition of chloride to the bathing solution, whilst maintaining the ionic strength at 0.02.

	measured p.d./mV	$[Pr^-]$/mM	Hydration	$[Pr^-]$xH/mM	mean $[Pr^-]$xH/mM
fresh cornea; bathing soln: pH=5.75, phosphate with 8 mM chloride, ionic strength=0.02.	-32.6 ± 0.6	65.2 ± 1.8	2.9 ± 0.1	189 ± 8	
	-31.4 ± 0.6	61.6 ± 1.7	2.7 ± 0.1	166 ± 8	
	-30.0 ± 0.5	57.6 ± 1.3	2.8 ± 0.2	161 ± 12	
	-31.7 ± 0.5	62.6 ± 1.6	3.1 ± 0.1	194 ± 8	179 ± 6
	-31.1 ± 0.3	60.7 ± 0.9	3.0 ± 0.1	182 ± 3	
	-32.3 ± 0.6	64.2 ± 1.7	2.8 ± 0.2	180 ± 14	

(± s.e.m., n=20)

in the results from different specimens, and this variation is large enough to mask any difference due to hydration. However, inspection of the results for sodium chloride extracted cornea (table 4.18), where two of the specimens were at very high hydrations (used straight after washing with water) and one was dried and rehydrated to physiological hydration, suggests that there is no simple relationship between $[Pr^-]$ and hydration. For simplicity, the mean of the $[Pr^-]$ x H of these results and of the control have been calculated and are plotted as a graph of $[Pr^-]$ x H against pH in figure 4.15. There does not seem to be any significant difference between these two values, suggesting that 0.15M sodium chloride solution does not extract any appreciable amount of charge-carrying molecules. In fact, both these values are rather lower than that obtained for fresh specimens in the same pH buffer (6.80), but the difference is not significant given the large standard errors involved.

Figure 4.16 is a graph of $[Pr^-]$ x H against pH for fresh cornea. There is considerable variation from one specimen to another, and at low pH's (5 and under) the cornea became very tough and great difficulty was experienced in inserting the microelectrode so that the time taken to make 20 measurements was rather longer than at higher pH's. However, the graph does show a steady increase in matrix fixed charge with pH, apart from the points around pH 7 and 8, which are not significantly different from each other.

In figure 4.17 a comparison is made between pre-dried and fresh tissue in bathing solutions of the same pH. The pre-dried specimens were rehydrated in the bathing solution to about the same hydration as the fresh tissue. The significantly higher matrix fixed charge found in the pre-dried cornea may be due to the fact that the interfibrillar spacing

Figure 4.15

Matrix fixed charge x hydration against pH for sodium chloride extracted cornea.

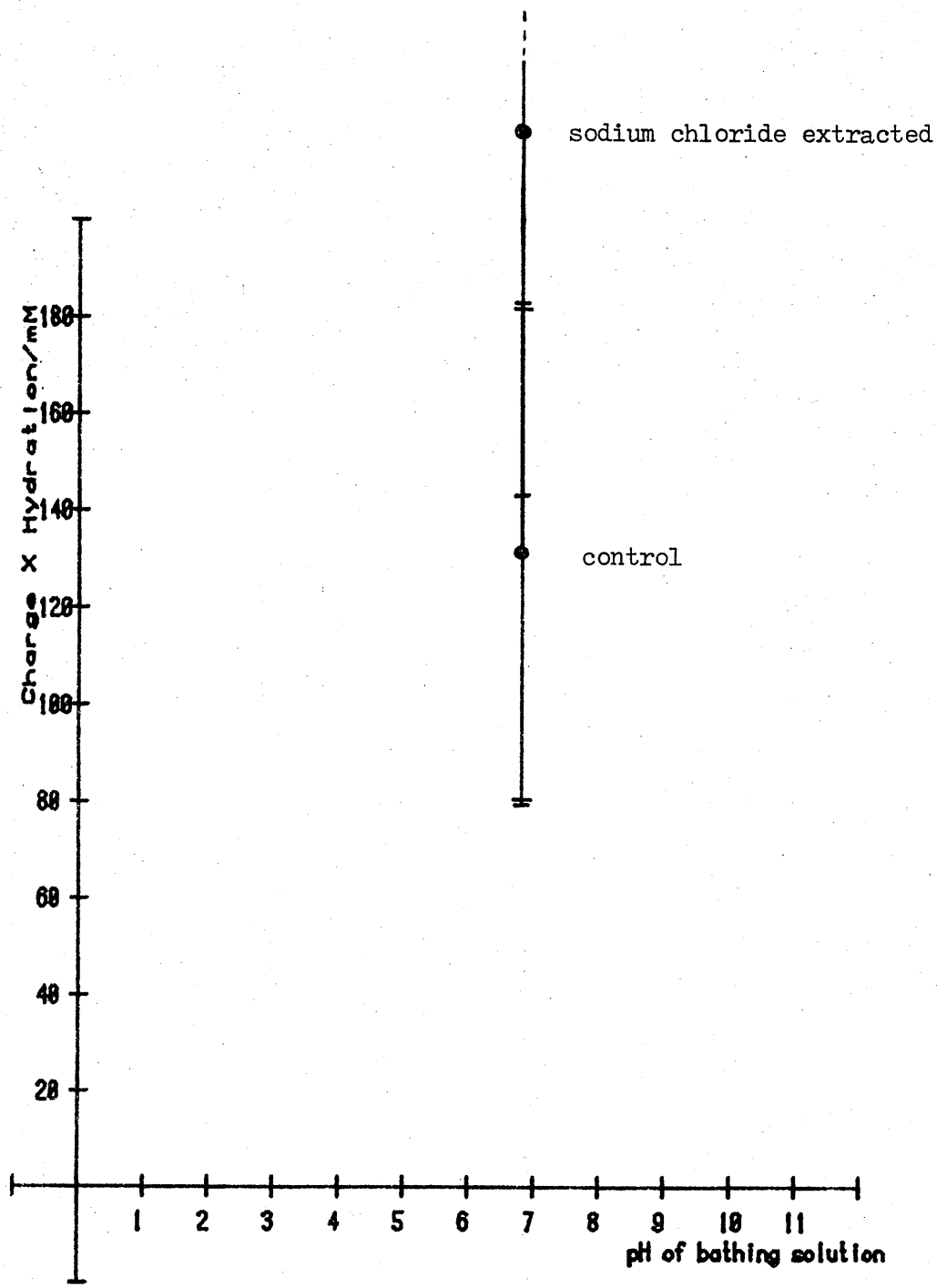

Figure 4.16

Variation in matrix fixed charge x hydration with pH for fresh cornea.

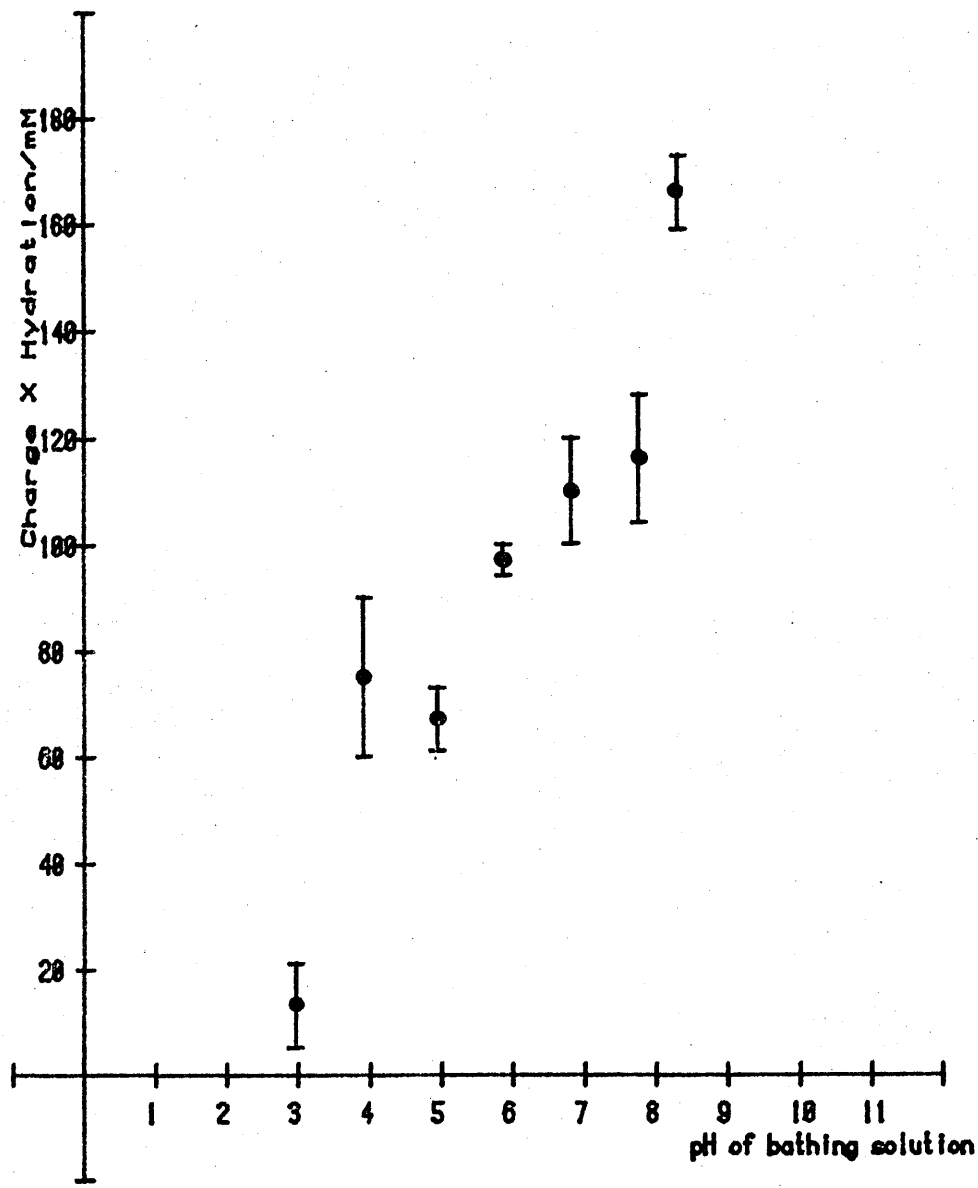

Figure 4.17

Matrix fixed charge x hydration against pH for fresh and pre-dried cornea.

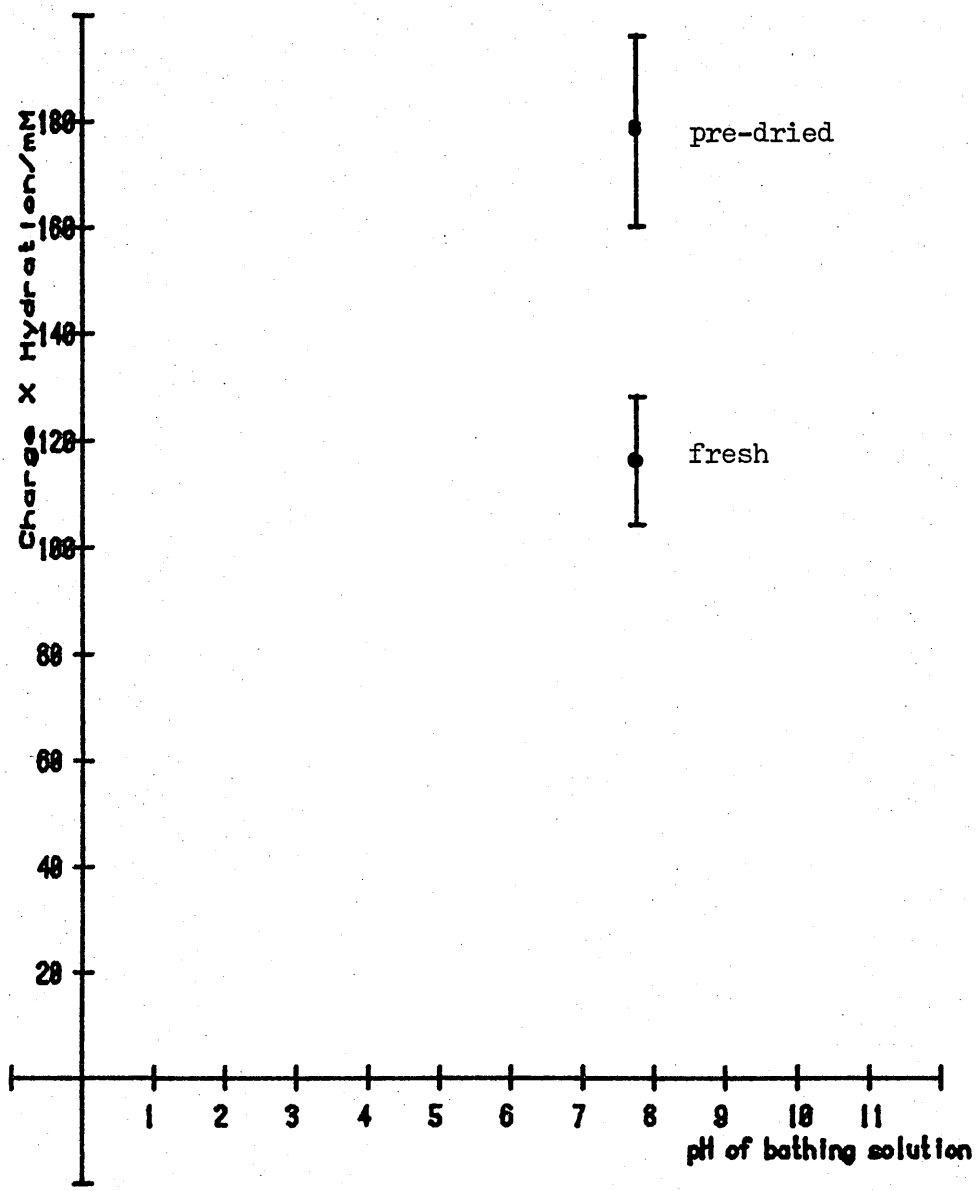

at a given hydration is smaller in pre-dried specimens than in fresh. (See figure 4.13 in previous section) This would mean that the volume of water between the fibrils is less than expected, and would have the effect of concentrating the matrix fixed charge.

Figure 4.18 shows the effect of adding chloride to the bathing solutions. Both results shown were from fresh specimens in bathing solutions of pH ~5.8. The very large difference in matrix fixed charge is most likely due to chloride ions becoming immobilised by and associated with the macromolecular matrix and thus effectively increasing the fixed charge.

Figure 4.18

Matrix fixed charge x hydration against pH for fresh cornea in an all phosphate bathing solution and in one containing 8mM chloride.

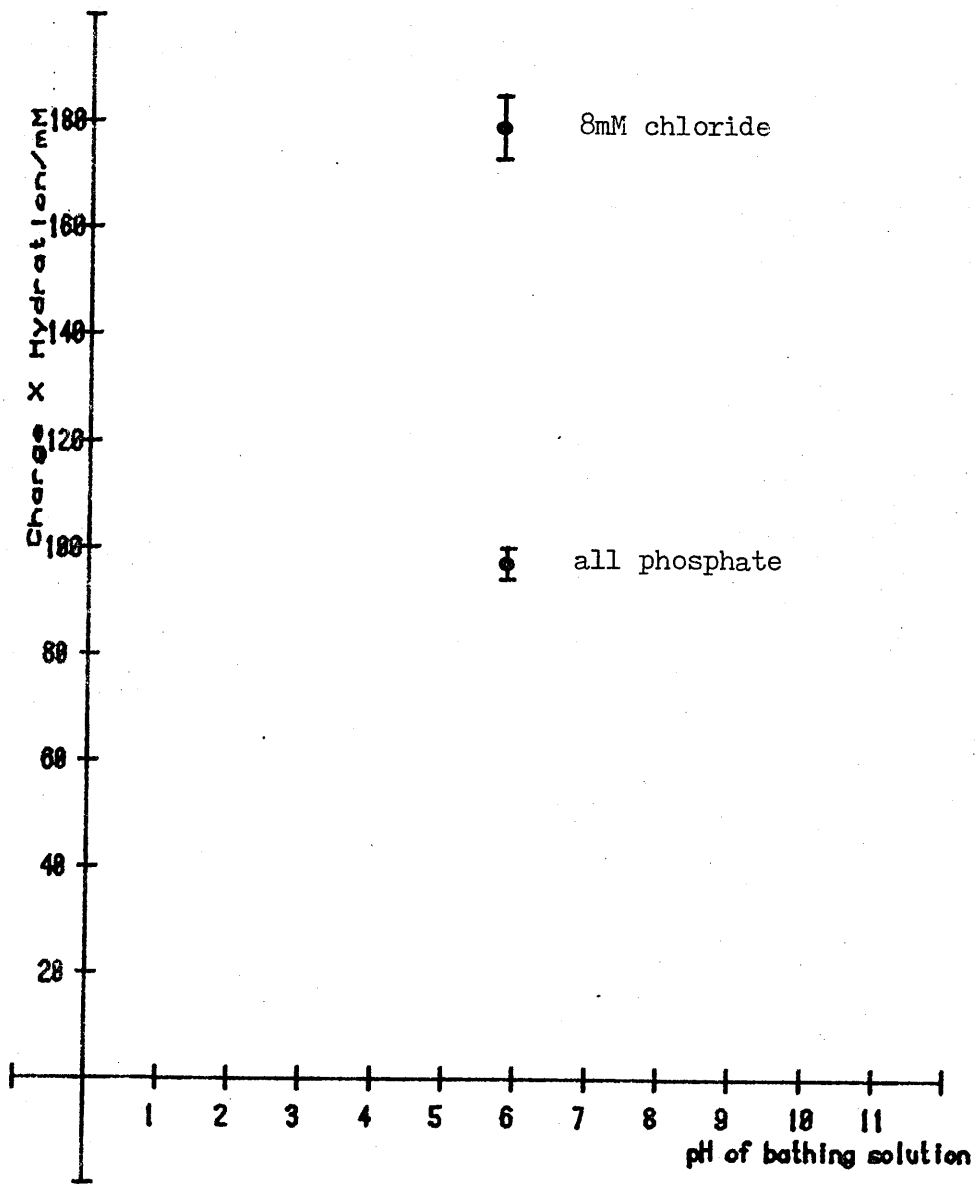

4.6 Microscopy.

4.6.1 Testing the Serum.

The Ouchterlony method (Ouchterlony and Nilsson, 1973) for checking the anti-serum obtained from the two rabbits showed that both contained at least two antibodies for the extract. Figure 4.19 is a photograph of one of the Ouchterlony plates which was stained with Coomassie Blue (Ouchterlony and Nilsson, 1973) to increase the contrast for the camera. The unstained precipitin lines were clearly visible to the eye when viewed against a dark background.

Similar tests performed on the pig invertebral disc anti-serum produced no precipitin lines at any of the dilutions used.

4.6.2 Immunofluorescence.

Figures 4.20 to 4.23 are photomicrographs of sections of fresh and pre-dried cornea at both physiological and higher hydrations. A low dilution of serum was used here and the sections are very overstained. However, although it is impossible to claim any specific binding of antibodies, the technique does produce some interesting pictures - particularly of very swollen specimens. Figure 4.20, a section of normal fresh cornea, is similar to pictures of mammalian corneal stroma obtained by other workers. (Payrau et al, 1967)

The section shown in figure 4.21 of very swollen fresh cornea shows a rather different structure to that seen in fresh tissue. The open-ness of the stained material suggests that large areas devoid of fibrils are being formed. If, as seems possible, these 'lakes' are tending to form

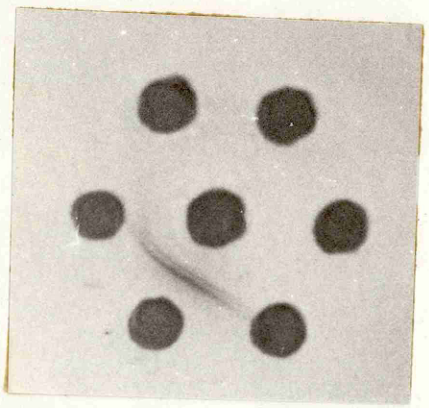

Figure 4·19 - Ouchterlony plate stained with Coomassie Blue, showing two precipitin lines between the centre well containing neat antigen and the outer well containing neat serum.

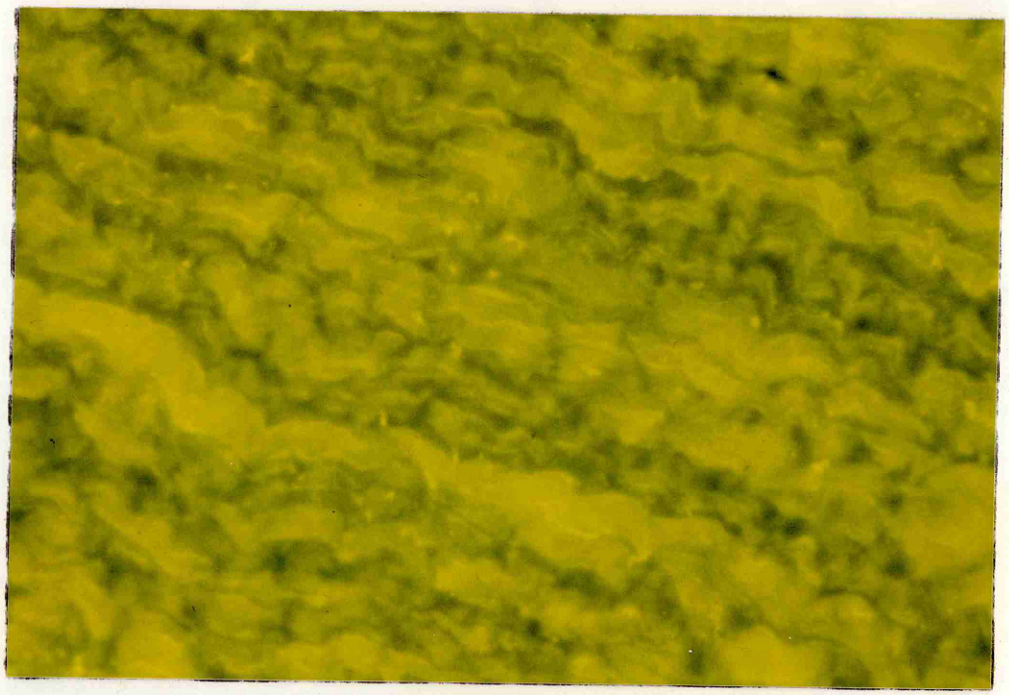

Figure 4·20 - Fresh cornea, hydration ~3.5.

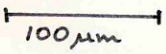

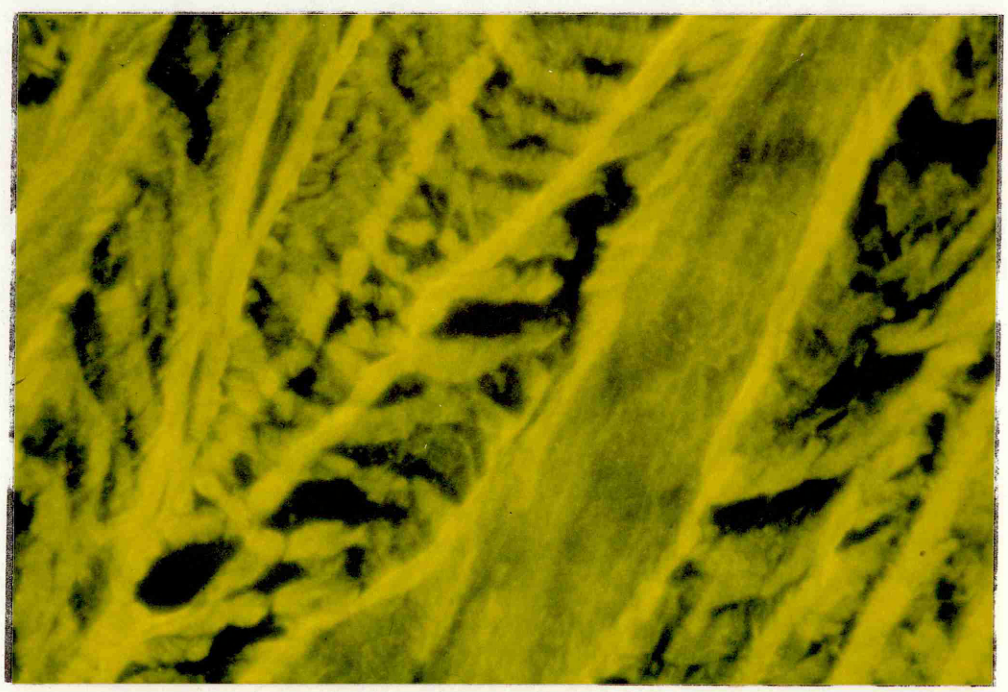

Figure 4·21 - Fresh cornea swollen for 4 hours in distilled water.

Hydration of specimen ~ 20.

(N.B. all photomicrographs - magnification is X 200.)

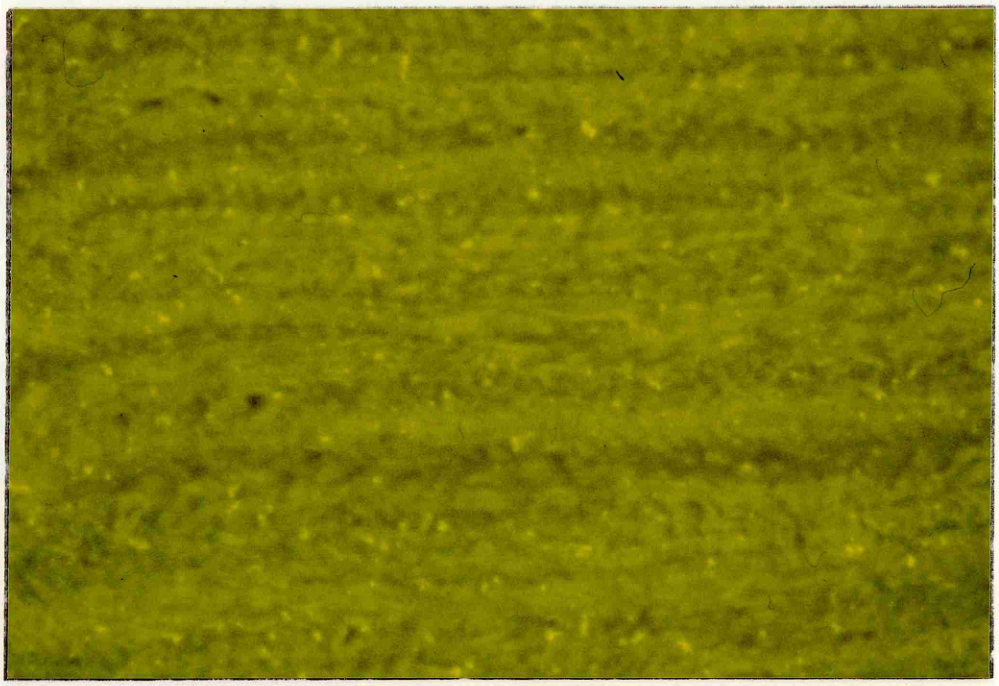

Figure 4·22 - Pre-dried cornea rehydrated in distilled water to a hydration of ~5.

100 μm

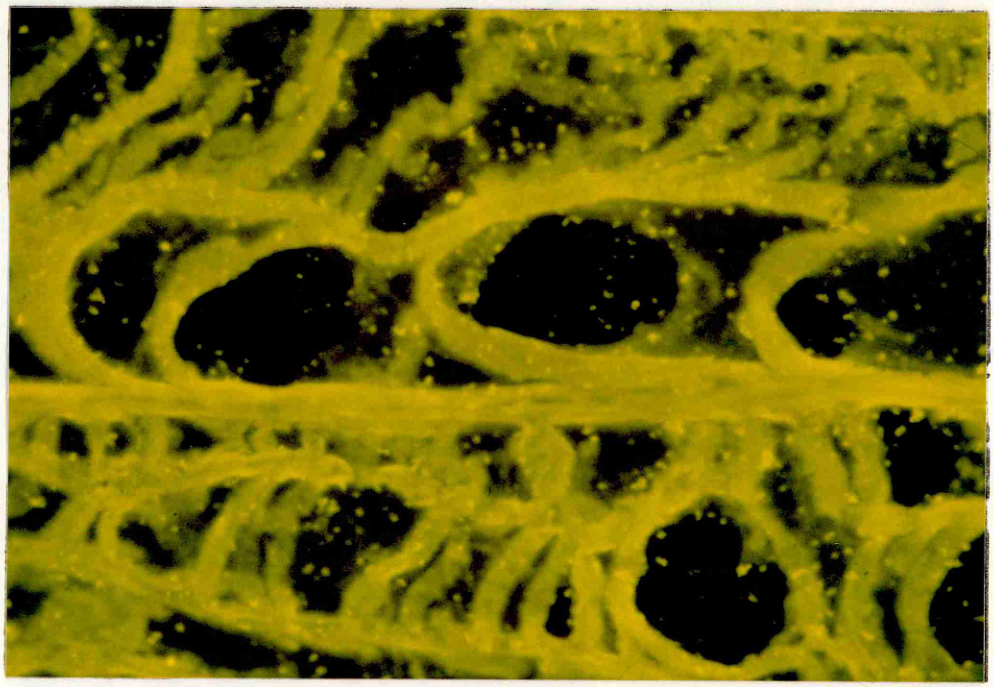

Figure 4·23 - Pre-dried cornea swollen for 4 hours in distilled water. Hydration of specimen ~ 20.

between the lammellae, it appears that the boundaries between lamellae are not well-defined; some interweaving of fibrils between neighbouring lammellae occurs.

The two figures 4.22 and 4.23 show sections of pre-dried cornea rehydrated to about physiological and very high hydrations. The picture for very swollen specimens is similar to that for fresh but with the stained material more condensed and lake areas larger. Figure 4.22 looks nothing like the section of fresh cornea in figure 4.20. The lammellae are less well-defined, but do not show the wavyness of those in the fresh section.

Figure 4.24, the sodium chloride extracted specimen, shows some disorder as might be expected after the extraction procedure, and the strips of very brightly stained material seen particularly in the very hydrated fresh and pre-dried specimens are absent from this section. The control specimen (figure 4.25) also appears disordered, but still retains some of the brightly staining material.

The specimens that were stained using higher dilutions of serum (1:30 and 1:300) produced only very weakly stained sections that were impossible to photograph successfully. The 1:30 dilution produced sections similar to those reproduced here, though less bright, and the 1:300 dilution produced sections with very little staining except for a few bright streaks that probably correspond to the brighter streaks seen on the other sections.

The pig invertebral disc antiserum produced similar though much weaker staining to the specifically prepared antiserum, (figure 4.26) even though no precipitin lines were visible on the Ouchterlony plates.

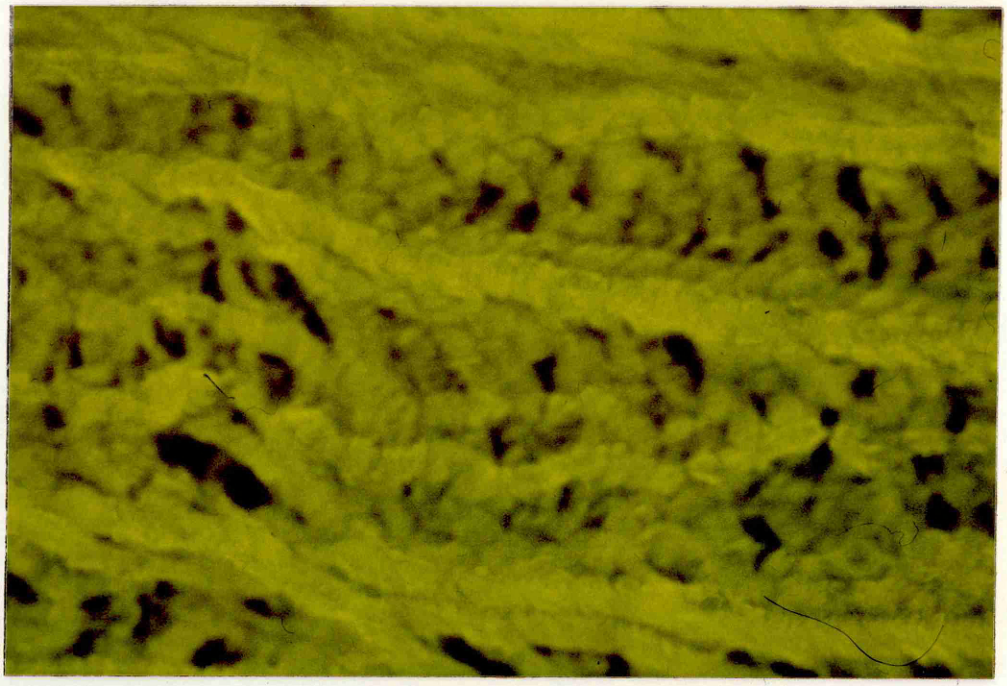

Figure 4·24 - Cornea extracted with 0.15M sodium chloride solution and washed in distilled water.

100 µm

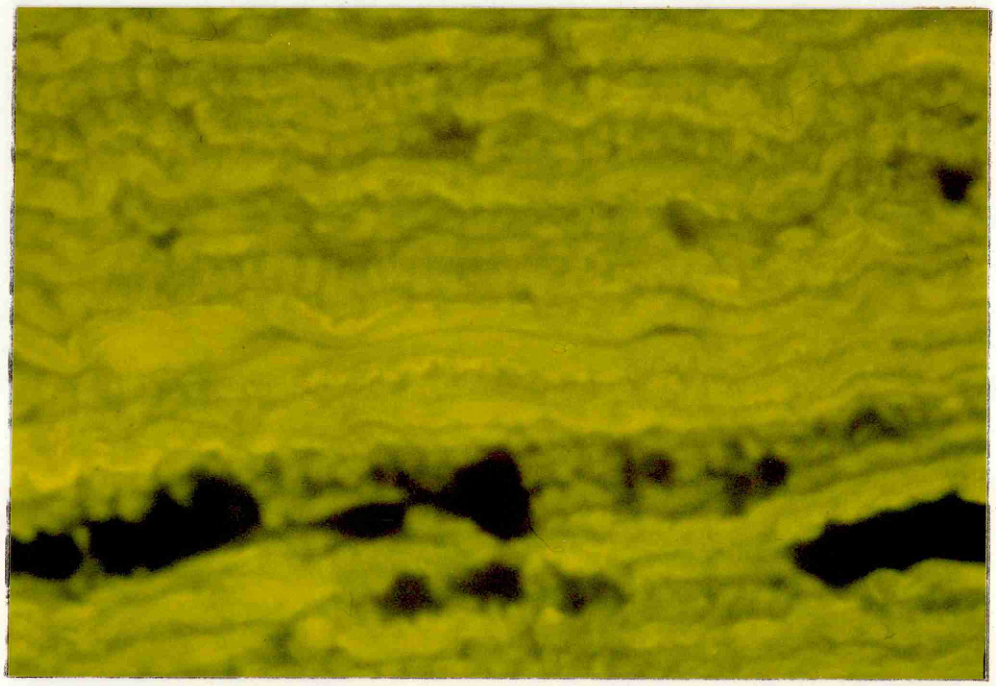

Figure 4·25 - Control specimen for sodium chloride extraction.

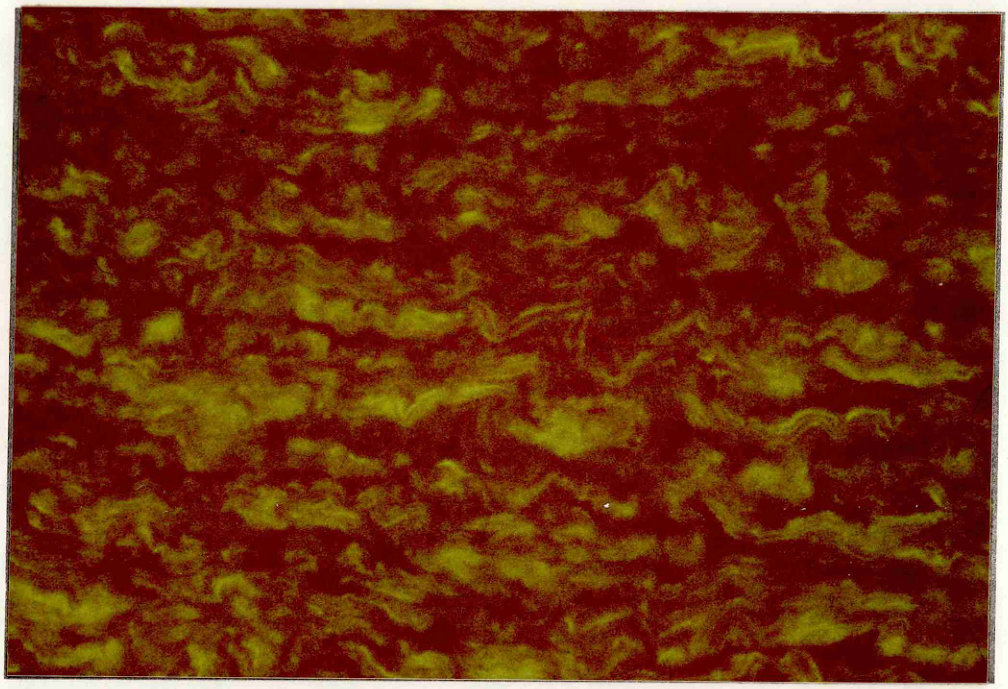

Figure 4.26 - Fresh cornea stained with pig invertebral disc proteoglycan antiserum.

100 µm

It is probable that the main antigens in the crude extract were proteins or glycoproteins and not proteoglycans, and even these were not completely removed during the extraction process. Silverman et al (1980) found an antigenic protein of molecular weight ~54 000, that was easily extracted from bovine corneal stroma with low ionic strength solutions.

4.6.3 Acridine Orange and Eosin and Haematoxylin Staining.

Figure 4.27 shows a section of fresh cornea stained with Acridine Orange, which is a stain that binds to acid mucopolysaccharides, producing an orange fluorescence on a green background. (Hicks and Matthaei, 1958). The orange areas shown in the photomicrograph are typical of the pattern seen for fresh cornea with this stain. However, swollen and extracted specimens showed no orange staining at all. Figure 4.28 is an eosin and haematoxylin stained section of fresh cornea. The nuclei of the keratocytes are visible as dark purple areas. It is possible that the orange areas of figure 4.27 correspond to the position of keratocytes which are producing the acid mucopolysaccharide-containing proteoglycans. Swelling and extraction would be likely to destroy these cells, which would account for the lack of acridine orange staining in such specimens.

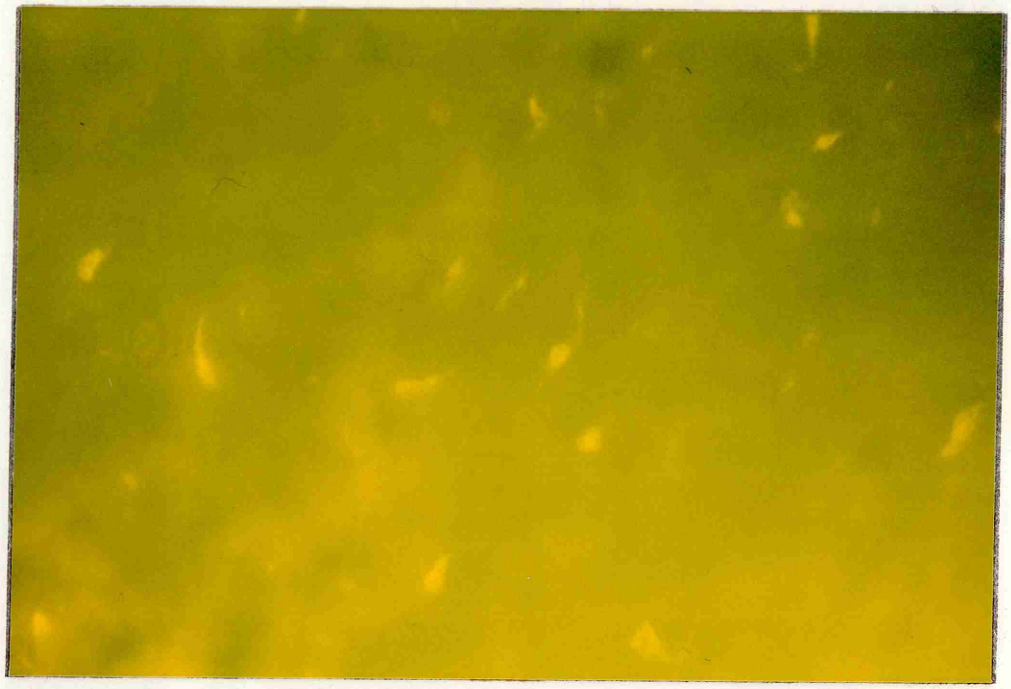

Figure 4.27 - Fresh cornea stained with Acridine Orange.

100 µm

Figure 4.28 - Fresh cornea stained with eosin and haemotoxylin.

CHAPTER 5

Discussion.

5.1 The effects of pre-drying corneal stroma.

The results presented in the previous chapter indicate that drying over silica gel has an effect on the rehydration properties of corneal stroma. The implications of the observed changes in swelling rate, interfibrillar spacing and microscopical appearance are discussed in detail here.

5.1.1 Swelling in distilled water.

Corneal stroma that has been pre-dried swells more slowly and to a lower final hydration than fresh tissue. Analysis of the actual swelling curves shows that the rate of swelling is not too different initially, but that it levels off much more quickly for pre-dried tissue than for fresh. This seems to suggest that some force is operating in pre-dried tissue that restricts the movement of water into the tissue at higher hydrations, but has little or no effect at low hydrations. Some sort of cross-linking between the fibrils and/or the lammellae is possible. These cross-links may be thought of as 'springs' which offer very little resistance to stretching in the initial stages and produce progressively more tension as the tissue swells.

The nature of these proposed structures is rather difficult to envisage. It seems unlikely that covalent bonding is involved, particularly as drying once-swelled tissue produces the reverse effect with a greater second swelling rate. The main difference between fresh and once-

swelled cornea appears to be the inorganic ion content. The effect of extracting nearly all the Na^+, K^+, and Cl^- during the first swelling indicates that these ions play some role in producing the restricted swelling. Biological macromolecules, existing as they do in an aqueous environment, have water molecules closely associated with them which are an integral part of their tertiary structure. The removal of water molecules can produce conformational changes with the formation of intra- and inter-molecular hydrogen and hydrophobic bonding, a thermodynamically controlled process where the entropy term is probably dominant, and the activation energy of the reverse reaction is relatively high. X-ray crystallography has been used to show that the structure of hydrated glycosaminoglycans in vitro depends to a certain extent on the cations present in solution, (Arnott, Guss and Winter, 1975). It seems likely, therefore, that the cations play a role in maintaining the conformation of the glycosaminoglycans in the corneal stroma, and it is these molecules that are responsible for the restricted swelling in pre-dried cornea. On drying, the close approach of glycosaminoglycan chains associated with neighbouring fibrils and the exclusion of water from between them may initiate the formation of intermolecular weak bonding interactions which would effectively form cross-links. To explain why this process does not happen in cornea depleted of inorganic ions, we assume that the conformational structure of the glycosaminoglycans is lost on removal of the ions and the polysaccharride chains are too open and amorphous to allow sufficient weak bonding interactions to occur.

5.1.2 Determination of interfibrillar spacing by X-ray diffraction.

Interfibrillar spacing determinations were carried out over a range of hydrations for both fresh and pre-dried corneal stroma. The results obtained showed that there were two distinct populations - the

values for fresh tissue and those for pre-dried. This very unexpected result indicates that the structure of the corneal stroma is not as simple as the swelling experiments suggested. In order to take account of the fact that, at a given hydration, the interfibrillar spacing is smaller in pre-dried tissue than in fresh, we must postulate a model that allows the water to be present in different environments. The increase in interfibrillar spacing with hydration shows that at least some of the water entering the cornea goes between or into the fibrils. To give the observed diffraction pattern, it is not necessary to have a very regular arrangement of fibrils throughout the cornea, but there must be regions where the fibrils are clumped together with a fairly constant interfibrillar spacing. Regions very much larger than the interfibrillar spacings, which are devoid of fibrils would not produce detectable X-ray reflections, although information about these may be present in the diffuse scattering. A structure where fibrils exist as bundles, like that shown in figure 5.1, separated by relatively large spaces, is not inconsistent with the results obtained from X-ray diffraction experiments.

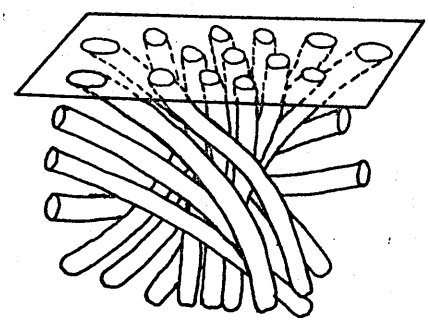

Figure 5.1 - two dimensional section of a region in which several chain molecules are approximately parallel.
(Vainshtein, 1966)

5.1.3 The structure from microscopy studies.

Immunofluorescence microscopy is a well established technique which allows the distribution of antigenic macromolecules in biological tissue to be determined. In this study, an attempt was made to use this technique to localise the proteoglycans in the corneal stroma. The sodium chloride extract used as an antigen, however, was not purified and was presumed to contain several antigenic species. Thus the serum obtained from the immunised rabbits contained more than one type of antibody (at least two were demonstrated by the appearance of precipitin lines on the Ouchterlony plates). The subsequent binding of serum antibodies to the sections of cornea proved to be non-specific, and not of much use for identifying the proteoglycans. However, this technique did produce micrographs that show some interesting structural features. Unlike electron microscopy and the more common types of light microscopy, the tissue was not fixed before sectioning and staining. This avoids artifacts due to the fixing process; a particular problem when the water content of the tissue is high as in swollen specimens. However, there are, of course, other problems associated with using frozen sections. Although fast-freezing should minimise the formation of large ice-crystals, there is still the possibility that this might happen, giving rise to equally troublesome artifacts. Also there may be some shrinkage and tearing of the tissue when the sections are dried onto the slides. Thus, several sections of different specimens were viewed, and very consistent results were obtained.

Fresh and pre-dried specimens showed significant differences, both at physiological and at higher hydrations. Both types of specimen showed evidence of large areas devoid of fibrils at high hydrations, but the pre-dried sections appeared to have their stained material in a more

closely packed form than the fresh, and larger unstained areas were evident. This closer packing was also seen in the sections of cornea at physiological hydration. The suggestion that the stained areas are collagen plus other macromolecules, and the unstained areas are spaces or 'lakes' is tentative, but this interpretation is very much in agreement with the results obtained from the swelling and X-ray studies. The arrangement of stained material as seen in the micrographs also suggests that there is considerable interweaving between lammellae. The bright specks, which become more concentrated in pre-dried tissue, may be the sites of the proteoglycan molecules, and the conformation and/or distribution of these molecules is different in pre-dried cornea.

5.1.4 Microelectrode measurements.

The use of this technique to determine the matrix fixed charge relies on measuring an 'average' potential difference between the inside of the tissue and its bathing solution. For a completely homogeneous material this potential is the same throughout the whole tissue. However, for a lattice of charged cylinders, the potential will vary across the lattice. This potential arises because the fibrils are negatively charged and there will be an uneven distribution of the ions between them, with the cations tending to move towards the fibrils and the anions away from them. Because of the relatively large size of the microelectrode tip ($\sim 1 \mu m$), what we measure is an average potential for the lattice, as demonstrated in figure 5.2. (see over page)

In this theoretical model, where the fibrils are evenly spaced and the water in the cornea is evenly distributed, the concentration of fixed negative charge will vary inversely with hydration. However, if some areas of the stroma are devoid of fibrils, this simple relationship

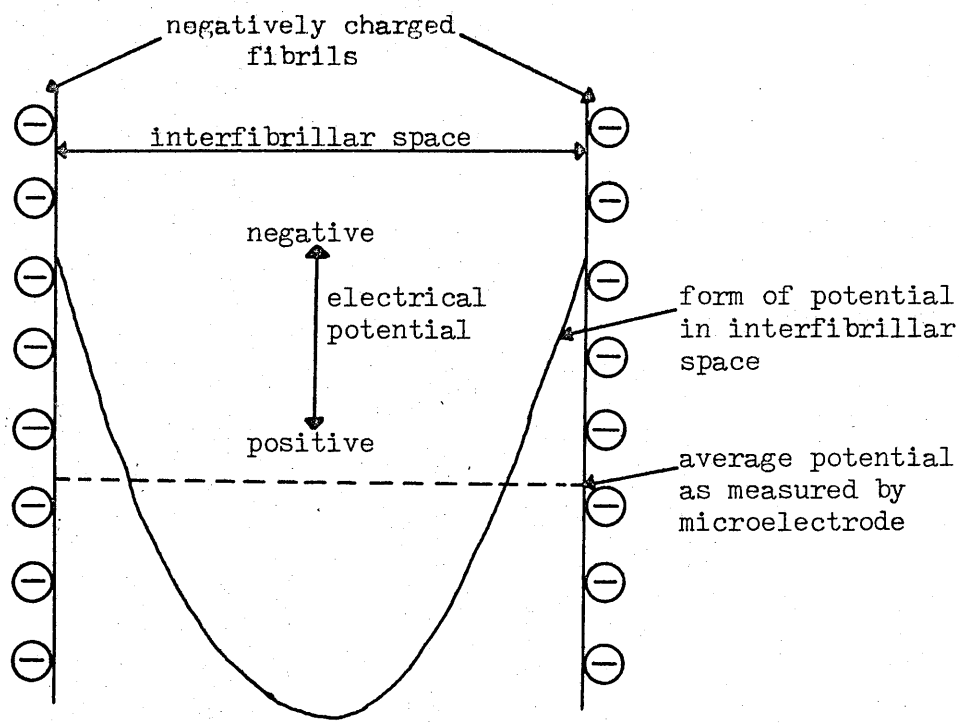

Figure 5.2 - Variation of potential across the interfibrillar space.

does not hold. A measurement taken with the microelectrode in a bundle of fibrils will give a potential difference rather higher than the average for the whole tissue. If the microelectrode enters a region containing no fibrils the measured potential would probably be close to zero. Since it is not possible to determine whether a near-zero reading arises from this or from incorrect penetration of the specimen, any such spurious readings were ignored. The result of this is that, for any specimen containing 'lakes', the calculated matrix fixed charge concentration will be higher than it should be. The size of the discrepancy will depend on the proportion of water present as lakes in the tissue. Other work presented here indicates that, at a given hydration, pre-dried tissue contains a larger volume of 'lakes' than fresh. Thus we would expect the measured matrix fixed charge concentration to be higher for pre-dried tissue than for fresh. The results do show that the fixed charge concentration for pre-dried cornea is larger than that for fresh by a factor

of nearly two.

5.1.5 The extraction of inorganic ions.

It is interesting to note that, although the inorganic ions are implicated in the formation of cross-links in pre-dried tissue, they are as easily extracted from this tissue by distilled water as they are from fresh cornea. No difference was found in analyses carried out using either type of specimen. Removal of these ions from the pre-dried tissue does not restore its swelling capacity. Therefore, although these ions seem necessary for producing the restrictive crosslinks, once formed, the ions do not appear to be necessary for their maintainance.

5.1.6 A model for corneal hydration.

In the previous chapter an equation (equation 6) is derived to describe the hydration of the corneal stroma in terms of the interfibrillar spacings. Appendix I contains the results of applying the model to the data. For all reasonable values of the constants, the results show that a significant amount of the water in the cornea is present as lakes. The proportion of lake water increases with increasing hydration. As indicated by the results of the X-ray diffraction studies, a larger proportion of the water exists as lakes in pre-dried cornea than in fresh. The implication of this is that pre-drying has the effect of either making the interfibrillar spaces less accessible to water or other areas (such as between lamellae) more accessible - or perhaps both. We can extend the cross-linked model to include these results by postulating that cross-linking occurs between the fibrils of one bundle, but not between different bundles. Thus there would be an increased resistance to water entering between the fibrils.

5.2 The effects of extraction.

Corneas treated with the various extraction media all showed a reduction in subsequent swelling. As expected, the reduction in swelling of the enzyme-extracted specimens was less than for those extracted with other solutions. If, as is suggested, the main contribution to the swelling pressure comes from the polysaccharide chains of the proteoglycans, then the reduction in swelling should be proportional to the fraction of the total glycosaminoglycans extracted. Sodium chloride and guanadine hydrochloride solutions were expected to extract both the proteoglycans (Axelsson and Heinegard, 1978, Dische *et al*, 1978, Hassel *et al*, 1979, Kaye *et al*, 1976), but the chondroitinase should only remove the chondroitin sulphate chains from one of them. The subsequent swelling properties confirm this hypothesis.

Whereas extraction with solutions designed to remove the proteoglycans causes a reduction in swelling, extraction with distilled water produces a small but significant increase. This increase was shown to occur mainly during the initial swelling period, and becomes insignificant at higher hydrations. These results suggest a force between the fibrils that is operative over short distances, becoming negligible at larger ones. The electrostatic force has these properties, and, as we are effectively dealing with negatively charged cylinders packed together, it would seem to be the most likely explanation. However, how do we explain an increase in the magnitude of this force after extraction with distilled water? We have already indicated the possible role of cations in the cornea, in maintaining the conformational structure of the glycosaminoglycans, and also suggested that these molecules are situated between the fibrils. These relatively large ions would then exert some screening effect on the electrostatic repulsion between the fibrils.

Removal of the ions would reduce this screening and thus increase the effective force.

5.3 The ionisation of the macromolecular matrix.

Microelectrode measurements of fresh cornea in various bathing solutions shows that the concentration of negative fixed charge in the macromolecular matrix is inversely proportional to the hydrogen ion concentration of the bathing solution. The hydrogen ion concentration of the bathing solution, and thus of the interfibrillar water, will determine the overall charge on the macromolecular matrix by affecting the protonation of the charged side chains. It is expected that the majority of the fixed negative charge arises from the highly charged chondroitin and keratan sulphates, therefore the extraction of these molecules should cause a measurable reduction in matrix fixed charge. For the simplest model for corneal structure, this should have been easy to demonstrate. The results obtained suggest that there is no difference between sodium chloride extracted cornea and those extracted with distilled water. However, if we compare the sodium chloride extracted specimens with fresh specimens in the same pH bathing solution, the results show that the extracted cornea do have a slightly lower matrix fixed charge. If we then take account of the problems mentioned earlier with respect to the method of correcting for hydration, we see that it is possible that the extraction process has had some effect on the fixed charge, but this is far from proven. The fact that the control specimens gave very similar results could indicate that a proportion of the proteoglycans were extracted by distilled water during the seven-day experiment.

It has been suggested earlier that the cations have a role in maintaining the conformation of the glycosaminoglycans in the cornea.

The inorganic ion analysis shows that apart from Na^+ and K^+ the corneal stroma contains a fairly high concentration of chloride ions. If these anions are freely diffusable, their concentration should have no effect on the measured matrix fixed charge. However, using a chloride-containing bathing solution to increase the internal concentration of Cl^- has the effect of doubling the measured matrix fixed charge. This suggests that these ions become in some way associated with the macromolecular matrix, and effectively increase its net negative charge. Although the net charge on the macromolecules is negative, there are still a number of side chains which will carry a positive charge. Electrostatic interaction between these positive groups and the negatively charged chloride ions could prevent free diffusion of Cl^- and cause an apparent increase in matrix fixed charge.

The values of fixed negative charge concentration obtained for fresh cornea show a steady increase with increasing pH, except at pH 7-8 where a plateau occurs. Measurement of the change in pH of the bathing solution whilst cornea swells suggests that there is a buffering effect in the swollen stroma which maintains the internal pH at about 8. By the time equilibrium has been established at this pH, the majority of the inorganic ions will have diffused out into the bathing solution, and many of the negatively charged side chains will have been protonated. The experimental results show that it is possible further to protonate the macromolecules but this requires a fairly large increase in the hydrogen ion concentration of the bathing solution.

5.4 Conclusion.

By using a variety of physical and chemical techniques to study the properties of bovine corneal stroma *in vitro*, we hoped to obtain suffic-

ient information to extrapolate from the *in vitro* to the *in vivo* situation. By obtaining data from a variety of techniques we are in a position to suggest an overall picture for the structure of corneal stroma.

In the past, experimental results mainly from electron microscopy have suggested a more ordered arrangement of the fibrils within the lamellae than appears to be the case from the results of this work. The experimental data reported here suggests that bovine corneal stroma has only a liquid-like structure with local order that extends over about two fibril diameters. (See also Sayers *et al*, in preparation). The ease with which lakes appear to form in swollen cornea suggests that in fresh cornea as well as in pre-dried specimens, the fibrils are arranged in 'bundles'. Although calculations (appendix I) do seem to indicate that lakes actually exist in fresh cornea, it seems that this result is a function of the 'approximate' nature of the suggested mathematical model, and that, although the potential for lake formation exists, actual lakes do not appear until the cornea is hydrated above the physiological state.

As regards the transparency of the cornea, the implications are that it is the formation of regions devoid of fibrils that are responsible for the scattering of visible light in swollen cornea. This is in agreement with the work of Hart and Farrell (1969), Benedek (1971), Goldman *et al* (1968) and others.

The results of this study also give some indication of the origin of the swelling pressure and the role of the proteoglycans and inorganic ions. This work indicates that the polysaccharide chains of the proteoglycans are the major contributors to the swelling pressure, and that it is their ability to alter their conformations that give them their high affinity for water. It would also appear that the inorganic ions play an

important part in maintaining the natural conformational structure of these molecules.

5.5 Suggestions for further work.

Shortage of time and, in some instances, lack of facilities and materials, have prevented some fairly obvious extensions of this work from being carried out.

The enzyme keratanase has recently become available commercially from Miles Laboratories Ltd. Extraction experiments using this enzyme, alone and with chondroitinase, are definitely indicated. Further investigation of the properties of all types of extracted cornea could be carried out using the X-ray diffraction, microelectrode and microscopy techniques.

Recent work using immunofluorescence microscopy to localise proteoglycans in invertebral disk (Beard et al, 1980) suggests that it would be worth following up this aspect of the work. Hassel et al (1979) have succeeded in separating corneal proteoglycans, and their published scheme would be a useful basis for preparing pure specimens of both corneal proteoglycans for use as antigens. The work could then probably be extended to the electron microscopy level by using the same anti-serum and staining with a conjugate having an electron dense label, such as ferritin.

APPENDIX I

Results of calculations using the mathematical model (equation 6) from chapter 4, section 4.2.2.

The values used were those obtained from the curve fitting program used to process the experimental data.

SECTION A

Computer print-out of results obtained from fresh cornea.

Table A1

DENSITY OF COLLAGEN = 1.4
RADIUS OF FIBRIL = 20
VALUE OF G = 0.3

HYDRN(wt.)	HYDRN(int.sp.)	INT.FIB.SP.	LAKE WATER
0.4	0.34	1884	14.73
0.7	0.41	2039	41.3[illegible]
0.8	0.43	2090	45.8[illegible]
1	0.47	2194	52.0[illegible]
1.3	0.54	2348	57.0[illegible]
1.5	0.59	2452	60.3[illegible]
1.6	0.61	2503	61.41
1.9	0.68	2658	63.8[illegible]
2.1	0.73	2761	65.11
2.4	0.8	2916	66.5[illegible]
2.7	0.87	3071	67.74
2.9	0.91	3174	68.3[illegible]
3	0.94	3226	68.66
3.1	0.96	3277	68.93
3.7	1.1	3587	70.23
4.3	1.23	3897	71.16
4.9	1.37	4206	71.83
5.6	1.53	4568	72.51
6.2	1.67	4877	72.94
6.6	1.76	5084	73.16
6.8	1.81	5187	73.29
7.1	1.88	5342	73.45
7.4	1.95	5497	73.59
7.5	1.97	5548	73.64
7.7	2.02	5652	73.72
8.2	2.13	5910	73.92
8.8	2.27	6219	74.13

Table A2

DENSITY OF COLLAGEN = 1.4
RADIUS OF FIBRIL = 19
VALUE OF G = 0.3

HYDRN(wt.)	HYDRN(int.sp.)	INT.FIB.SP.	LAKE WATER
0.4	0.43	1884	-7.99
0.7	0.5	2039	27.34
0.8	0.53	2090	33.27
1	0.58	2194	41.47
1.3	0.66	2348	49.11
1.5	0.71	2452	52.47
1.6	0.73	2503	53.86
1.9	0.81	2658	57.11
2.1	0.86	2761	58.77
2.4	0.94	2916	60.75
2.7	1.01	3071	62.23
2.9	1.07	3174	63.1
3	1.09	3226	63.47
3.1	1.12	3277	63.83
3.7	1.27	3587	65.55
4.3	1.42	3897	66.75
4.9	1.58	4206	67.74
5.6	1.75	4568	68.57
6.2	1.91	4877	69.15
6.6	2.01	5084	69.47
6.8	2.06	5187	69.62
7.1	2.14	5342	69.82
7.4	2.21	5497	70.01
7.5	2.24	5548	70.07
7.7	2.29	5652	70.18
8.2	2.42	5910	70.44
8.8	2.57	6219	70.72

Table A3

DENSITY OF COLLAGEN = 1.3
RADIUS OF FIBRIL = 20
VALUE OF G = 0.3

HYDRN(wt.)	HYDRN(int.sp.)	INT.FIB.SP.	LAKE WATER
0.4	0.36	1834	8.17
0.7	0.44	2039	36.88
0.8	0.46	2090	41.7
1	0.51	2194	48.34
1.3	0.59	2348	54.38
1.5	0.64	2452	57.3
1.6	0.66	2503	58.44
1.9	0.73	2658	61.08
2.1	0.78	2761	62.43
2.4	0.86	2916	64.02
2.7	0.93	3071	65.23
2.9	0.98	3174	65.94
3	1.01	3226	66.25
3.1	1.03	3277	66.54
3.7	1.18	3587	67.94
4.3	1.33	3897	68.96
4.9	1.48	4206	69.72
5.6	1.65	4568	70.32
6.2	1.8	4877	70.86
6.6	1.9	5084	71.12
6.8	1.95	5187	71.24
7.1	2.02	5342	71.41
7.4	2.1	5497	71.56
7.5	2.12	5548	71.62
7.7	2.17	5652	71.7
8.2	2.3	5910	71.94
8.8	2.45	6219	72.14

Table A4

DENSITY OF COLLAGEN = 1.2
RADIUS OF FIBRIL = 20
VALUE OF G = 0.3

HYDRN(wt.)	HYDRN(int.sp.)	INT.FIB.SP.	LAKE WATER
0.4	0.39	1884	0.52
0.7	0.47	2039	31.62
0.8	0.5	2090	36.84
1	0.55	2194	44.06
1.3	0.63	2348	50.8
1.5	0.69	2452	53.75
1.6	0.72	2503	54.98
1.9	0.8	2658	57.83
2.1	0.85	2761	59.3
2.4	0.93	2916	61.02
2.7	1.01	3071	62.36
2.9	1.06	3174	63.11
3	1.09	3226	63.43
3.1	1.12	3277	63.76
3.7	1.28	3587	65.27
4.3	1.44	3897	66.36
4.9	1.6	4206	67.19
5.6	1.79	4568	67.98
6.2	1.95	4877	68.43
6.6	2.06	5084	68.71
6.8	2.11	5187	68.84
7.1	2.19	5342	69.02
7.4	2.27	5497	69.19
7.5	2.3	5548	69.25
7.7	2.36	5652	69.34
8.2	2.49	5910	69.57
8.8	2.65	6219	69.82

SECTION B

Computer print-out of results obtained from pre-dried cornea.

Table B1

DENSITY OF COLLAGEN = 1.4
RADIUS OF FIBRIL = 20
VALUE OF G = 0.3

HYDRN(wt.)	HYDRN(int.sp.)	INT.FIB.SP.	LAT. WATER
0.3	0.24	1661	19.49
0.5	0.26	1711	47.23
0.6	0.27	1736	54.16
0.7	0.28	1761	59.11
0.9	0.3	1812	65.67
1.1	0.33	1862	69.80
1.3	0.35	1912	72.8
1.4	0.36	1938	73.91
1.6	0.38	1988	75.78
1.7	0.39	2013	76.54
1.9	0.42	2063	77.84
2	0.43	2089	78.37
2.5	0.48	2215	80.44
2.6	0.49	2240	80.76
2.7	0.51	2265	81.06
3.2	0.56	2391	82.26
3.4	0.58	2441	82.65
4.7	0.73	2768	84.38
6.3	0.91	3171	85.46
6.4	0.92	3196	85.51
6.5	0.93	3222	85.56
7	0.99	3347	85.79
7.7	1.07	3524	86.06
7.8	1.08	3549	86.09
8.4	1.15	3700	86.29
8.8	1.19	3801	86.39
9.2	1.24	3901	86.5
10	1.33	4103	86.68
10.3	1.36	4178	86.74
11.3	1.47	4430	86.92
12	1.55	4606	87.03
12.3	1.59	4682	87.07
13.7	1.74	5034	87.24
14.4	1.82	5211	87.31
14.5	1.83	5236	87.32

Table B2

DENSITY OF COLLAGEN = 1.4
RADIUS OF FIBRIL = 19
VALUE OF G = 0.3

HYDRN(wt.)	HYDRN(int.sp.)	INT.FIB.SP.	LAKE WATER
0.3	0.32	1661	-7.21
0.5	0.34	1711	30.72
0.6	0.35	1736	40.21
0.7	0.37	1761	46.98
0.9	0.39	1812	55.96
1.1	0.42	1862	61.72
1.3	0.44	1912	65.7
1.4	0.45	1938	67.23
1.6	0.48	1988	69.78
1.7	0.49	2013	70.83
1.9	0.52	2063	72.6
2	0.53	2089	73.33
2.5	0.59	2215	76.17
2.6	0.6	2240	76.61
2.7	0.62	2265	77.02
3.2	0.68	2391	78.66
3.4	0.7	2441	79.19
4.7	0.86	2768	81.5
6.3	1.06	3171	83.03
6.4	1.08	3196	83.11
6.5	1.09	3222	83.17
7	1.15	3347	83.42
7.7	1.24	3524	83.85
7.8	1.25	3549	83.9
8.4	1.33	3700	84.16
8.8	1.38	3801	84.31
9.2	1.42	3901	84.46
10	1.52	4103	84.7
10.3	1.56	4178	84.78
11.3	1.69	4430	85.03
12	1.77	4606	85.18
12.3	1.81	4682	85.23
13.7	1.99	5034	85.47
14.4	2.07	5211	85.57
14.5	2.09	5236	85.58

Table B3

DENSITY OF COLLAGEN = 1.3
RADIUS OF FIBRIL = 20
VALUE OF G = 0.3

HYDRN(wt.)	HYDRN(int.sp.)	INT.FIB.SP.	LAKE WATER
0.3	0.26	1661	13.3
0.5	0.28	1711	43.17
0.6	0.29	1736	50.64
0.7	0.3	1761	55.97
0.9	0.33	1812	63.03
1.1	0.35	1862	67.56
1.3	0.38	1912	70.71
1.4	0.39	1938	71.9
1.6	0.41	1988	73.91
1.7	0.42	2013	74.74
1.9	0.45	2063	76.13
2	0.46	2089	76.7
2.5	0.52	2215	78.94
2.6	0.53	2240	79.28
2.7	0.55	2265	79.61
3.2	0.61	2391	80.9
3.4	0.63	2441	81.32
4.7	0.79	2768	83.14
6.3	0.98	3171	84.34
6.4	0.99	3196	84.4
6.5	1.01	3222	84.45
7	1.07	3347	84.7
7.7	1.15	3524	84.99
7.8	1.16	3549	85.02
8.4	1.24	3700	85.23
8.8	1.28	3801	85.35
9.2	1.33	3901	85.46
10	1.43	4103	85.65
10.3	1.47	4178	85.72
11.3	1.59	4430	85.91
12	1.67	4606	86.03
12.3	1.71	4682	86.07
13.7	1.88	5034	86.26
14.4	1.96	5211	86.34
14.5	1.97	5236	86.35

Table B4

DENSITY OF COLLAGEN = 1.2
RADIUS OF FIBRIL = 20
VALUE OF G = 0.3

HYDRN(wt.)	HYDRN(int.sp.)	INT.FIB.SP.	LAKE WATER
0.3	0.28	1661	6.07
0.5	0.3	1711	38.43
0.6	0.32	1736	46.52
0.7	0.33	1761	53.3
0.9	0.36	1812	59.95
1.1	0.38	1862	64.86
1.3	0.41	1912	68.26
1.4	0.42	1938	69.56
1.6	0.45	1988	71.74
1.7	0.46	2013	72.64
1.9	0.49	2063	74.15
2	0.5	2089	74.78
2.5	0.57	2215	77.18
2.6	0.58	2240	77.56
2.7	0.59	2265	77.91
3.2	0.66	2391	79.31
3.4	0.68	2441	79.76
4.7	0.85	2768	81.73
6.3	1.06	3171	83.04
6.4	1.08	3196	83.1
6.5	1.09	3222	83.15
7	1.15	3347	83.43
7.7	1.25	3524	83.73
7.8	1.26	3549	83.78
8.4	1.34	3700	84
8.8	1.39	3801	84.13
9.2	1.44	3901	84.25
10	1.55	4103	84.46
10.3	1.59	4178	84.53
11.3	1.72	4430	84.74
12	1.81	4606	84.86
12.3	1.85	4682	84.91
13.7	2.03	5034	85.12
14.4	2.13	5211	85.2
14.5	2.14	5236	85.21

APPENDIX II

Print-outs of all the BASIC computer programs written for and used in this thesis.

Program 1.

Calculates hydrations from keyboard input of raw swelling data, and stores results on magnetic tape files.

```
100 PAGE
104 INIT
105 CALL "RATE",1200,0,2
110 PRINT "THIS PROGRAM WILL CALCULATE HYDRATIONS."
115 PRINT "IT WILL PROVIDE A HARD COPY OF THE RESULTS"
120 PRINT "ON THE LINE PRINTER IF YOU REQUIRE IT."
130 PRINT "MAKE SURE THE LINE PRINTER IS CONNECTED."
150 PRINT "IT WILL ALSO STORE THE RESULTS ON THE MAGNETIC"
155 PRINT "TAPE.THE SAFETY DEVICE ON THE CASSETTE"
160 PRINT "MUST BE TURNED AWAY FROM  SAFE  AND YOU MUST"
170 PRINT "SPECIFY THE NUMBER OF THE FILE TO BE USED."
180 PRINT
190 PRINT "CHECK ALL YOUR FILE NUMBERS BEFORE YOU START."
210 PRINT
220 PRINT "INPUT NO. OF DATA POINTS ";
230 INPUT Z
240 DIM H(Z)
250 L$=CHR(10)
260 DIM D(Z)
270 PRINT "INPUT EXPERIMENT NUMBER ";
280 INPUT I$
290 PRINT "INPUT WEIGHT OF HOOK ";
300 INPUT A
310 PRINT "INPUT WEIGHT OF HOOK PLUS CORNEA ";
320 INPUT B
330 LET C=B-A
340 PRINT "INPUT EACH WET WEIGHT FOLLOWED BY RETURN"
350 FOR J=1 TO Z
360 INPUT D(J)
370 LET H(J)=(D(J)-B)/C
380 LET H(J)=INT(H(J)*1000)/1000
390 NEXT J
400 PRINT "CHECK VALUES AND PRESS RETURN WHEN READY";
410 INPUT M$
420 PAGE
430 PRINT "EXPERIMENT NUMBER IS ";I$
440 PRINT
450 PRINT "DRY WEIGHT OF CORNEA IS ";C
460 PRINT
470 FOR J=1 TO Z
480 PRINT "J=";J;"     HYDRATION =";H(J)
490 NEXT J
500 PRINT
510 PRINT "IS OUTPUT TO BE PRINTED ON LINEPRINTER?";
520 INPUT P$
530 IF P$<>"YES" THEN 670
540 PRINT "CHECK LINE PRINTER IS O.K.                "
550 PRINT "PRESS RETURN WHEN READY.";
560 INPUT M$
570 PRINT @40:L$
```

```
580 PRINT @40:"EXPERIMENT NUMBER IS ";I$,L$
590 PRINT @40:L$
600 PRINT @40:"DRY WEIGHT OF CORNEA IS ";C,L$
610 PRINT @40:L$
620 FOR J=1 TO 6
622 PRINT @40:"TIME IS ";J/2*10;" MINS.       ";
623 PRINT @40:"HYDRATION IS ";H(J),L$
624 NEXT J
626 FOR J=7 TO 9
628 PRINT @40:"TIME IS ";(J-3)*10;" MINS.       ";
629 PRINT @40:"HYDRATION IS ";H(J),L$
630 NEXT J
632 FOR J=10 TO Z
634 PRINT @40:"TIME IS ";(J-5)*15;" MINS.       ";
635 PRINT @40:"HYDRATION IS ";H(J),L$
636 NEXT J
660 PRINT @40:L$
670 PRINT "DO YOU WANT THE RESULTS STORED ON FILE?";
680 INPUT N$
690 IF N$<>"YES" THEN 780
700 PRINT "INPUT FILE NUMBER REQUIRED.";
720 INPUT F
750 FIND F
760 WRITE I$,C,H
770 PRINT @40:"THIS DATA STORED ON MAGNETIC ";
771 PRINT @40:"TAPE FILE NUMBER ";F,L$
780 PRINT @40:L$
790 PRINT @40:L$
800 PRINT @40:L$
810 PRINT @40:L$
820 PRINT @40:L$
830 PRINT @40:L$
840 PRINT @40:L$
850 PRINT @40:L$
860 PRINT @40:L$
870 PRINT @40:L$
880 PRINT @40:L$
890 PRINT @40:L$
895 PRINT @40:L$
900 PRINT "DO YOU WANT TO PROCESS ANOTHER SET OF DATA?";
910 INPUT S$
915 PAGE
920 IF S$="YES" THEN 220
950 END
```

Program 2.

Reads hydration data from magnetic tape (ref. program 1), calculates mean and standard error for each point and plots graph of hydration against time.

```
100 REM GRAPH PLOTTING PROGRAM WITH MEANS AND S.E.
110 INIT
120 CALL "RATE",1200,0,2
130 L$=CHR(10)
140 PRINT "INPUT FIRST AND LAST FILES TO BE ACCESSED. ";
150 INPUT B,C
160 DIM M(13)
170 DIM S(13)
180 DIM E(13)
190 DIM D(13)
200 DIM Y$(72)
210 DIM Q$(72)
220 DIM F$(72)
230 FOR I=1 TO 13
240 LET Z=0
250 LET Y=0
260 LET X=0
270 FOR J=1 TO C-B+1
280 FIND J+B-1
290 READ @33:P$,P
300 FOR T=1 TO I
310 READ @33:A
320 NEXT T
330 LET X=X+A^2
340 LET Y=Y+A
350 NEXT J
360 LET M(I)=Y/(C-B+1)
370 LET S(I)=((X/(C-B+1)-M(I)^2)/(C-B))^0.5
380 NEXT I
390 PAGE
400 PRINT "WHAT IS THE TITLE OF YOUR GRAPH?"
410 INPUT Y$
420 INPUT Q$
430 INPUT F$
440 PRINT @40:Y$,L$
450 PRINT @40:Q$,L$
460 PRINT @40:F$,L$
470 PRINT @40:L$
480 FOR I=1 TO 13
490 PRINT M(I);S(I)
500 LET E(I)=INT(M(I)*1000+0.5)/1000
510 LET D(I)=INT(S(I)*1000+0.5)/1000
520 PRINT @40:"MEAN IS ";E(I),"STANDARD ERROR IS ";D(I),L$
530 NEXT I
540 PRINT "WHICH SYMBOL DO YOU WANT?"
550 PRINT "TRIANGLE = 1, SQUARE = 2, DIAMOND = 3";
555 PRINT "NO SYMBOL = 4. ";
```

```
560 INPUT Q
570 WINDOW -10,130,-2,32
580 PRINT "DO YOU WANT TO PUT GRAPH ON GRAPH PLOTTER? ";
590 INPUT R$
600 IF R$<>"YES" THEN 630
610 LET N=1
620 GO TO 640
630 LET N=32
640 PRINT "DO YOU WANT TO DRAW NEW AXES? ";
650 INPUT T$
660 PAGE
670 IF T$<>"YES" THEN 850
680 AXIS @N:5,1
690 MOVE @N:-5,-1
700 FOR U=10 TO 120 STEP 10
710 RMOVE @N:10,0
720 PRINT @N:U
730 NEXT U
740 RMOVE @N:-35,-1
750 PRINT @N:"TIME IN MINUTES";
760 MOVE @N:-8,-0.3
770 FOR V=5 TO 30 STEP 5
780 RMOVE @N:0,5
790 PRINT @N:V
800 NEXT V
810 RMOVE @N:0,-7
820 PRINT @N,25:90
830 PRINT @N:"HYDRATION";
840 PRINT @N,25:0
850 MOVE @N:0,0
860 FOR I=1 TO 6
870 RMOVE @N:5,M(I)
880 RDRAW @N:0,S(I)
890 RDRAW @N:0.2,0
900 RDRAW @N:-0.4,0
910 RMOVE @N:0.2,-S(I)
920 RDRAW @N:0,-S(I)
930 RDRAW @N:0.2,0
940 RDRAW @N:-0.4,0
950 RMOVE @N:0.2,S(I)
960 GOSUB Q OF 1410,1480,1570,1650
970 RMOVE @N:0,-M(I)
980 NEXT I
990 FOR I=7 TO 9
1000 RMOVE @N:10,M(I)
1010 RDRAW @N:0,S(I)
1020 RDRAW @N:0.2,0
1030 RDRAW @N:-0.4,0
1040 RMOVE @N:0.2,-S(I)
1050 RDRAW @N:0,-S(I)
1060 RDRAW @N:0.2,0
1070 RDRAW @N:-0.4,0
1080 RMOVE @N:0.2,S(I)
1090 GOSUB Q OF 1410,1480,1570,1650
1100 RMOVE @N:0,-M(I)
1110 NEXT I
1120 FOR I=10 TO 13
1130 RMOVE @N:15,M(I)
1140 RDRAW @N:0,S(I)
1150 RDRAW @N:0.2,0
```

```
1160 RDRAW @N:-0.4,0
1170 RMOVE @N:0.2,-S(I)
1180 RDRAW @N:0,-S(I)
1190 RDRAW @N:0.2,0
1200 RDRAW @N:-0.4,0
1210 RMOVE @N:0.2,S(I)
1220 GOSUB Q OF 1410,1480,1570,1650
1230 RMOVE @N:0,-M(I)
1240 NEXT I
1250 MOVE @N:10,31
1260 PRINT @N:Y$
1270 MOVE @N:10,30
1280 PRINT @N:Q$
1290 MOVE @N:10,29
1300 PRINT @N:F$
1310 RMOVE -120,0
1320 PRINT "PLOT THIS DATA AGAIN WITH A NEW TITLE? ";
1330 INPUT Z$
1340 PAGE
1350 IF Z$="YES" THEN 400
1360 PRINT "PLOT THIS DATA AGAIN WITH THE SAME TITLE? ";
1370 INPUT Z$
1380 PAGE
1390 IF Z$="YES" THEN 480
1400 GO TO 1660
1410 REM DRAW TRIANGLE.
1420 RMOVE @N:0,0.2
1430 RDRAW @N:-0.5,-0.36
1440 RDRAW @N:1,0
1450 RDRAW @N:-0.5,0.36
1460 RMOVE @N:0,-0.2
1470 RETURN
1480 REM DRAW SQUARE.
1490 RMOVE @N:0,0.2
1500 RDRAW @N:-0.6,0
1510 RDRAW @N:0,-0.4
1520 RDRAW @N:1.2,0
1530 RDRAW @N:0,0.4
1540 RDRAW @N:-0.6,0
1550 RMOVE @N:0,-0.2
1560 RETURN
1570 REM DRAW DIAMOND.
1580 RMOVE @N:0,0.2
1590 RDRAW @N:-0.6,-0.2
1600 RDRAW @N:0.6,-0.2
1610 RDRAW @N:0.6,0.2
1620 RDRAW @N:-0.6,0.2
1630 RMOVE @N:0,-0.2
1640 RETURN
1650 RETURN
1660 END
```

Program 3.

Calculates matrix fixed charge ([Pr^-]) and standard error from keyboard input of raw microelectrode data. Accepts keyboard input of mean hydration and standard error and stores them with the corresponding [Pr^-] on magnetic tape files.

```
100 PAGE
105 INIT
110 CALL "RATE",1200,0,2
115 L$=CHR(10)
120 DIM C(3),D(3),F(3),G(3),A(20),Z(20)
121 DIM A$(72),S(20),E(20),B$(3)
125 PRINT "INPUT TITLE"
130 INPUT A$
135 PRINT "Input pH of buffer."
140 INPUT H
145 PRINT @40:A$,L$
150 PRINT @40:L$
155 PRINT "Input number of ion species.";
160 INPUT N
165 PRINT "Input ion concentration + charge at each'?'."
170 FOR P=1 TO N
175 PRINT "?";
180 INPUT A(P),Z(P)
185 PRINT @40:"Concentration is ";
186 PRINT @40:A(P),"Charge is ";Z(P),L$
190 NEXT P
195 PRINT @40:L$
200 PRINT "Are the the concentrations correct?"
205 INPUT B$
210 IF B$="NO" THEN 125
215 PRINT "Input number of experiments. ";
220 INPUT X
225 FOR J=1 TO X
230 PAGE
235 PRINT "Input number of data points. ";
240 INPUT Y
245 PRINT "Input potentials as positive values at each'?'"
250 LET U=0
255 LET T=0
260 FOR I=1 TO Y
265 PRINT "? ";
270 INPUT W
275 PRINT @40:W;"  ";
280 LET U=U+W^2
285 LET T=T+W
290 NEXT I
295 PRINT "Have you entered the potentials correctly?"
300 INPUT B$
305 IF B$="NO" THEN 235
310 PRINT @40:L$
315 PRINT @40:L$
320 PRINT @40:L$
325 LET E(J)=-T/Y
```

```
330 LET S(J)=((U/Y-E(J)^2)/(Y-1))^0.5
335 NEXT J
340 PRINT "Input file number."
345 INPUT R
350 FIND R
355 WRITE "No. Expts. at pH ",H," is ",X
360 FOR J=1 TO X
365 PRINT @40:L$
370 PRINT @40:L$
371 PRINT @40:"Experiment number is ";J,L$
372 PRINT @40:L$
373 PRINT @40:"Mean Pot. is ";E(J);"      ";
374 PRINT @40:"Stand. Error is ";S(J),L$
375 FOR Q=1 TO 3
380 C(Q)=0
385 D(Q)=0
390 F(Q)=0
395 NEXT Q
400 K=0
405 FOR Q=1 TO 3
410 FOR P=1 TO N
415 B=A(P)*EXP(-0.03999996*Z(P)*E(J))
420 C(Q)=C(Q)+B
425 D(Q)=D(Q)+B*Z(P)
430 F(Q)=F(Q)+A(P)
435 NEXT P
440 G(Q)=C(Q)-F(Q)
445 K=K+1
450 IF K=2 THEN 465
455 E(J)=E(J)+S(J)
460 GO TO 470
465 E(J)=E(J)-2*S(J)
470 NEXT Q
500 A1=D(1)-D(2)
505 B1=D(3)-D(1)
510 IF A1=>B1 THEN 535
520 E1=B1
525 GO TO 545
535 E1=A1
540 PAGE
545 PRINT "Input H and s.e. for expt. no. ";J
550 INPUT A2,B2
555 PRINT "Have you entered these correctly?"
560 INPUT B$
565 IF B$="NO" THEN 540
570 WRITE D(1),E1,A2,B2
575 PRINT @40:L$
580 PRINT @40:"Swelling Pressure is ";G(1),L$
585 A3=G(1)-G(2)
590 B3=G(3)-G(1)
595 IF A3=>B3 THEN 610
600 PRINT @40:"Standard error is ";B3,L$
605 GO TO 615
610 PRINT @40:"Standard error is ";A3,L$
615 NEXT J
620 PAGE
625 PRINT "Loading next program."
630 FIND 5
635 OLD
999 END
```

Program 4.

Reads microelectrode data from magnetic tape (ref. program 3), calculates $[Pr^-]$ x H for each experiment and mean $[Pr^-]$ x H with standard error. Plots a graph of $[Pr^-]$ x H against pH.

```
2000 PAGE
2010 INIT
2020 CALL "RATE",1200,0,2
2030 L$=CHR(10)
2040 DIM E(20),F(20),A$(72),Z$(22),C$(20),D$(5)
2045 DIM A(20),B(20),C(20),D(20)
2060 PRINT
2070 PRINT "Do you want to put graph on plotter?"
2080 INPUT B$
2090 IF B$="YES" THEN 2120
2100 V=32
2110 GO TO 2130
2120 V=1
2130 PRINT "Input title."
2140 INPUT A$
2150 PRINT "Input data file number."
2160 INPUT R
2170 PRINT @40:A$,L$
2180 PRINT @40:L$
2190 W=0
2200 M=0
2210 S=0
2220 FIND R
2230 READ @33:C$,P,D$,N
2235 PRINT @40:C$;P;D$;N,L$
2240 FOR I=1 TO N
2250 READ @33:A(I),B(I),C(I),D(I)
2258 PRINT @40:L$
2260 PRINT @40:"Charge conc. and error is ";A(I),B(I),L$
2270 PRINT @40:"Hydration and error is ";C(I),D(I),L$
2280 PRINT @40:L$
2290 E(I)=A(I)*C(I)
2300 F(I)=((B(I)/A(I))^2+(D(I)/C(I))^2)^0.5*E(I)
2310 K=F(I)^2
2320 W=W+1/K
2330 NEXT I
2340 FOR I=1 TO N
2350 M=M+E(I)/F(I)^2
2360 NEXT I
2370 M=M/W
2380 PRINT @40:"pH of buffer is ";P,L$
2390 PRINT @40:L$
2400 FOR I=1 TO N
2405 PRINT @40:L$
2410 PRINT @40:"(ChargeXHydration) for expt. ";I;
2415 PRINT @40:" is ";E(I),L$
2420 PRINT @40:"Error for expt. ";I;" is ";F(I),L$
2425 PRINT @40:L$
```

```
2430 S=S+(E(I)-M)^2/F(I)^2
2440 NEXT I
2450 S=(S/((N-1)*W))^0.5
2460 PRINT @40:L$
2470 PRINT @40:L$
2480 PRINT @40:"Mean of charge X hydration is ";M,L$
2490 PRINT @40:"Standard error is ";S,L$
2520 PAGE
2530 PRINT "Do you want to draw new axes?"
2535 WINDOW -1,12,-20,200
2540 INPUT B$
2550 IF B$="NO" THEN 2730
2560 PAGE
2565 PRINT @V:A$
2570 Z$="Charge X Hydration/mM"
2590 AXIS @V:1,20
2600 FOR J=1 TO 11
2610 MOVE @V:J-0.3,-9
2620 PRINT @V:J
2630 NEXT J
2640 MOVE @V:8.5,-15
2650 PRINT @V:"mH";
2660 FOR J=20 TO 180 STEP 20
2670 MOVE @V:-0.8,J-2
2680 PRINT @V:J
2690 NEXT J
2700 MOVE @V:-0.7,100
2709 PRINT @V,25:90
2710 PRINT @V:Z$
2711 PRINT @V,25:0
2720 MOVE @V:0,0
2730 MOVE @V:P,M
2740 RDRAW @V:0,S
2750 RDRAW @V:0.1,0
2760 RDRAW @V:-0.2,0
2770 RMOVE @V:0.1,0
2780 RDRAW @V:0,-2*S
2790 RDRAW @V:0.1,0
2800 RDRAW @V:-0.2,0
2810 PRINT "DONE"
2840 END
```

Program 5.

Accepts keyboard input of hydration and (interfibrillar spacing)^2 and plots a graph. Accepts keyboard input of slope and intercept (obtained from curve fitting program) and draws appropriate line.

```
100 REM PLOTS GRAPH OF D^2 AGAINST H
110 INIT
120 CALL "RATE",1200,0,2
130 L$=CHR(10)
140 PRINT "HOW MANY POINTS ARE THERE?"
150 INPUT Z
160 DIM D(Z)
170 DIM H(Z)
180 PRINT "INPUT VALUES OF D^2 AND H FOLLOWED BY RETURN."
190 FOR I=1 TO Z
200 INPUT D(I),H(I)
210 NEXT I
220 PRINT "WHICH SYMBOL DO YOU WANT?"
230 PRINT "TRIANGLE = 1, SQUARE = 2, DIAMOND = 3  ";
235 PRINT "NO SYMBOL = 4. ";
240 INPUT Q
250 WINDOW -1,15,-500,7100
260 PRINT "DO YOU WANT TO PUT GRAPH ON GRAPH PLOTTER? ";
270 INPUT R$
280 IF R$<>"YES" THEN 310
290 LET N=1
300 GO TO 320
310 LET N=32
320 PRINT "DO YOU WANT TO DRAW NEW AXES? ";
330 INPUT T$
340 PAGE
350 IF T$<>"YES" THEN 510
360 AXIS @N:1,500
370 FOR I=2 TO 15 STEP 2
380 MOVE @N:I-0.3,-300
390 PRINT @N:I;
400 NEXT I
410 MOVE @N:11,-500
420 PRINT @N:"HYDRATION";
430 FOR I=1000 TO 8000 STEP 1000
440 MOVE @N:-0.6,I-100
450 PRINT @N:I/1000
460 NEXT I
470 MOVE @N:-0.7,3200
480 PRINT @N,25:90
490 PRINT @N:"(I.F. SPACING) / 1000/nm"
500 PRINT @N,25:0
510 MOVE @N:0,0
520 FOR I=1 TO Z
530 MOVE @N:H(I),D(I)
540 GOSUB Q OF 1000,1070,1160,1240
550 NEXT I
```

```
560 PRINT "INPUT SLOPE AND INTERCEPT OF LINE."
570 INPUT S,T
580 MOVE @N:0,0
590 MOVE @N:0,T
600 DRAW @N:H(Z)+1,S*(H(Z)+1)+T
660 PRINT "INPUT ERROR ON SLOPE"
670 INPUT E
680 H1=7
690 D1=S*H1+T
700 MOVE @N:H1,D1
710 RDRAW @N:0,E*H1
720 RDRAW @N:-0.2,0
730 RDRAW @N:0.4,0
740 MOVE @N:H1,D1
750 RDRAW @N:0,-E*H1
760 RDRAW @N:-0.2,0
770 RDRAW @N:0.4,0
780 PRINT "DO YOU WANT TO PLOT THIS DATA AGAIN?"
790 INPUT A$
800 IF A$="YES" THEN 220
810 PRINT "DO YOU WANT TO PLOT NEW DATA?"
820 INPUT B$
830 IF B$="YES" THEN 140
840 GO TO 9999
1000 REM DRAW TRIANGLE.
1010 RMOVE @N:0,24
1020 RDRAW @N:-0.05,-44
1030 RDRAW @N:0.1,0
1040 RDRAW @N:-0.05,44
1050 RMOVE @N:0,-24
1060 RETURN
1070 REM DRAW SQUARE.
1080 RMOVE @N:0,24
1090 RDRAW @N:-0.06,0
1100 RDRAW @N:0,-48
1110 RDRAW @N:0.12,0
1120 RDRAW @N:0,48
1130 RDRAW @N:-0.06,0
1140 RMOVE @N:0,-24
1150 RETURN
1160 REM DRAW DIAMOND.
1170 RMOVE @N:0,24
1180 RDRAW @N:-0.06,-24
1190 RDRAW @N:0.06,-24
1200 RDRAW @N:0.06,24
1210 RDRAW @N:-0.06,24
1220 RMOVE @N:0,-24
1230 RETURN
1240 RETURN
9999 END
```

Program 6.

Accepts keyboard input of hydration, (interfibrillar spacing)^2, and constants:- dry fibril radius (R_o), density of collagen (ρ_m) and value of G. Calculates the percentage water apparently present as lakes using the model derived in chapter 4.

```
100 INIT
110 CALL "RATE",1200,0,2
120 L$=CHR(10)
130 PRINT "INPUT NUMBER OF VALUES OF H AND D^2."
140 INPUT N
150 DIM H(N),D(N),A(N),H1(N)
160 PRINT "INPUT VALUES OF H AND D^2."
170 FOR I=1 TO N
180 INPUT H(I),D(I)
190 NEXT I
200 PRINT "INPUT DENSITY OF COLLAGEN."
210 INPUT C
220 PRINT "INPUT VALUE OF G."
230 INPUT G
240 PRINT "INPUT RADIUS OF FIBRIL."
250 INPUT R
270 FOR I=1 TO N
280 H1(I)=(D(I)/(4*R*R)+G-1)/C
290 A(I)=(H(I)-H1(I))*100/H(I)
300 NEXT I
310 PRINT "DO YOU WANT TO USE LINEPRINTER?"
320 INPUT A$
330 IF A$="YES" THEN 360
340 Z=32
350 GO TO 370
360 Z=40
370 PAGE
380 PRINT @Z:"DENSITY OF COLLAGEN = ";C,L$
390 PRINT @Z:"RADIUS OF FIBRIL = ";R,L$
400 PRINT @Z:"VALUE OF G = ";G,L$
410 PRINT @Z:L$
420 PRINT @Z:"HYDRN(wt.)","HYDRN(int.sp.)","INT.FIB.SP.    ";
425 PRINT @Z:"LAKE WATER",L$
430 FOR I=1 TO N
440 PRINT @Z:H(I),INT(H1(I)*100)/100,D(I);"              ";
445 PRINT @Z:INT(A(I)*100)/100,L$
450 NEXT I
460 PRINT "DO YOU WANT TO CHANGE THE FIBRIL RADIUS?"
470 INPUT B$
480 IF B$="YES" THEN 240
490 PRINT "DO YOU WANT TO CHANGE VALUE OF G?"
500 INPUT C$
510 IF C$="YES" THEN 220
520 PRINT "DO YOU WANT TO CHANGE VALUE OF DENSITY?"
530 INPUT D$
540 IF D$="YES" THEN 200
999 END
```

REFERENCES

Alexander,R.J., Silverman,B. and Henley,W.L. (1980) ARVO meeting, Suppl. Invest.Ophth.Vis.Sci. p.186.

Arnott,S., Guss,J.M. and Winter,W.T. (1975) In 'Extracellular Influences on Gene Expression', Eds. Slanhoh,H.C. and Grenlich,R.C., Academic Press.

Axelsson,I. and Heinegard,D. (1978) Biochem. J., 169, 517-530.

Beard,H.K., Ryvar,R., Brown,R. and Muir,H. (1980) Immunology, 41, 491-501.

Benedek,G.B. (1971) Appl. Opt., 10, 459-473.

Borcherding,M.S., Blacik,L.J., Sittig,R.A., Bizzell,J.W., Breen,M. and Weinstein,H.G. (1975) Exp. Eye Res., 21, 59-70.

Davson,H. (1980) 'Physiology of the Eye', 4th Ed., Churchill Livingstone, Edinburgh.

Dische,Z., Cremer-Bartels,G. and Kaye,G.I. (1978) referred to in Kaye et al (1976) and pre-print of intended publication kindly supplied by Dr. Kaye.

Elliott,G.F., Goodfellow,J.M. and Woolgar,A.E. (1978) J. Appl. Cryst., 11, 496.

Elliott,G.F., Goodfellow,J.M. and Woolgar,A.E. (1980) J. Physiol., 298, 453-470.

Francois,J., Rabaey,M. and Vandermeersche,G. (1954) Ophthalmologica, Basel, 127, 74.

Friedman,M.H. and Green,K. (1971) Am. J. Physiol., 221, 356-362.

Friedman,M.H., Kearns,J.P., Michenfelder,C.J. and Green,K. (1972) Am. J. Physiol., 222, 1565-1570.

Goldman,J.N. and Benedek,G.B. (1967) Invest. Ophthalmol., 6, 574-599.

Goldman,J.N., Benedek,G.B., Dohlman,C.H. and Kravitt,B. (1968) Invest. Ophthalmol., 7, 501-519.

Goodfellow,J.M. (1975) PhD. Thesis, The Open University.

Goodfellow,J.M., Elliott,G.F. and Woolgar,A.E. (1978) J. Mol. Biol., 119, 237-252.

Green,K., Hastings,B. and Friedman,M.H. (1971) Am. J. Physiol., 220, 520-525.

Haber,A. and Runyan,R.P. (1973) 'General Statistics', 2nd. Ed., Addison-Wesley, London.

Harding,J.J. and Crabbe,M.J.C. (1979) FEBS LETTERS, 100, 351-356.

Hart,R.W. and Farrell,R.A. (1969) J. Opt. Soc. Am., 59, 766.

Hart,R.W. and Farrell,R.A. (1971) Bull. Math. Biophys., 33, 165-186.

Hascall,V.C. (1977) J. Supramol. Struct., 7, 101-120.

Hassel,J.R., Newsome,D.A. and Hascall,V.C. (1979) J. Biol. Chem., 254, 2346-2354.

Hedbys,B.O. (1961) Expl. Eye Res., 1, 81-91.

Hedbys,B.O. and Mishima,S. (1962) Expl. Eye Res., 1, 262-275.

Hedbys,B.O. (1963) Exp. Eye Res., 2, 112-121.

Hedbys,B.O., Mishima,S. and Maurice,D.M. (1963) Exp. Eye Res., 2, 99-111.

Hedbys,B.O. and Mishima,S. (1966) Expl. Eye Res., 5, 221-228.

Hicks and Matthaei (1958) J. Path. Bact., 75, 473.

Hodson,S.A. (1971) J. Theor. Biol., 33, 419-427.

Hogan,M.J., Alvarado,J.A. and Weddell,J.E. (1971) In 'Histology of the Human Eye', W.B. Saunders Co., Philadelphia and London.

Kaye,G.I., Cremer-Bartels,G., Buddecke,E. and Dische,Z. (1976) In 'The Structure of the Eye', III, Eds. Yamada,E. and Mishima,S.,63-76.

Leydhecker,W., Akiyama,K. and Neumann,H.G. (1958) Klin. Mbl. Augenheilk, 133, 662-670.

Maurice,D.M. (1957) J. Physiol. (Lond), 136, 263-286.

Maurice,D.M. (1969) In 'The Eye', Ed. Davson,H., 2nd. ed. London, Academic Press.

Maurice,D.M. and Riley (1970) In 'Biochemistry of the Eye', Ed. Graymore, C.N., London, Academic Press.

Mathews,M.B. (1967) In 'The Connective Tissue', Eds. Wagner,B.M. and Smith,D.E., p.304, Baltimore: Williams and Wilkins.

Meek,K.M., Elliott,G.F., Sayers,Z., Whitburn,S.B. and Koch,M. (1981) J. Mol. Biol., In Press.

Mishima,S. and Kudo,T. (1967) Invest. Ophthalmol., N.Y., 6, 329.

Naylor,G.R.S. (1978) Pflugers Arch., 378, 107-110.

Otori,I. (1967) Expl. Eye Res., 6, 356-367.

Ouchterlony,O. and Nilsson,L.A. (1973) In 'Handbook of Experimental Immunology', Ed. Weir,D.M., chapter 19, 2nd. ed.

Payrau,P., Pouliquin,Y., Faure,J.P. and Offret,G. (Eds.) (1967) 'La transparence de la cornée, les méchanismes de ses altérations.', Masson et cie editeurs, Paris, Ch. 2, 38-148.

Perrin,D.D. and Sayce,I.G. (1967) Talanta, 14, 833-842.

Pirie,A. (1947) Biochem. J., 41, 185-190.

Plöem,J.S. (1967) Z. wiss. Mikr., 68, 129.

Sillen,L.G. and Martell,A.E. (1964) Chem. Soc. Spec. Publ. 17, 'Stability Constants'.

Silverman,B., Alexander,R.J. and Henley,W.L. (1980a) ARVO meeting, Suppl. Invest. Ophth. Vis. Sci. p.27.

Silverman,B., Alexander,R.J. and Henley,W.L. (1980b) I.S.E.R. congress, New York, P. Int. Soc. Eye Res., 1, 98.

Suzuki,S., Saito,H., Yamagata,T., Anno,K., Seno,N., Kawai,Y. and Furuhashi,T. (1968) J. Biol. Chem., 213, 1543-1550.

Vainshtein,B.K. (1966)'Diffraction of X-rays by Chain Molecules', Elsevier, Amsterdam, London, New York.

Yamagata,T., Saito,H., Habuchi,O. and Suzuki,S. (1968) J. Biol. Chem., 243, 1523-1535.